

KNOCK RATING OF GASEOUS FUELS IN A MODIFIED COOPERATIVE  
FUEL RESEARCH (CFR) ENGINE

A THESIS SUBMITTED TO  
THE GRADUATE SCHOOL OF NATURAL AND APPLIED SCIENCES  
OF  
MIDDLE EAST TECHNICAL UNIVERSITY

BY  
İLTER İMRAN BODUR

IN PARTIAL FULFILLMENT OF THE REQUIREMENTS  
FOR  
THE DEGREE OF MASTER OF SCIENCE  
IN  
MECHANICAL ENGINEERING

JULY 2015



Approval of the thesis:

**KNOCK RATING OF GASEOUS FUELS IN A MODIFIED COOPERATIVE  
FUEL RESEARCH (CFR) ENGINE**

submitted by **İLTER İMRAN BODUR** in partial fulfillment of the requirements  
for the degree of **Master of Science in Mechanical Engineering Department,**  
**Middle East Technical University** by,

Prof. Dr. Mevlüde Gülbin Dural ÜNVER

\_\_\_\_\_

Dean, Graduate School of **Natural and Applied Sciences**

Prof. Dr. Raif Tuna BALKAN

\_\_\_\_\_

Head of Department, **Mechanical Engineering**

Assoc. Prof. Dr. Ahmet YOZGATLIGİL

\_\_\_\_\_

Supervisor, **Mechanical Engineering Dept., METU**

**Examining Committee Members:**

Prof. Dr. Ahmet Demir BAYKA

Automotive Engineering Dept., Atılım University

\_\_\_\_\_

Assoc. Prof. Dr. Ahmet YOZGATLIGİL

Mechanical Engineering Dept., METU

\_\_\_\_\_

Assoc. Prof. Dr. Yiğit YAZICIOĞLU

Mechanical Engineering Dept., METU

\_\_\_\_\_

Asst. Prof. Dr. Ahmet Buğra KOKU

Mechanical Engineering Dept., METU

\_\_\_\_\_

Asst. Prof. Dr. Ali Emre TURGUT

Mechanical Engineering Dept., METU

\_\_\_\_\_

**Date:** 15.07.2015

I hereby declare that all information in this document has been obtained and presented in accordance with academic rules and ethical conduct. I also declare that, as required by these rules and conduct, I have fully cited and referenced all material and results that are not original to this work.

Name, Last Name: İLTER İ. BODUR

Signature :

## ABSTRACT

### KNOCK RATING OF GASEOUS FUELS IN A MODIFIED COOPERATIVE FUEL RESEARCH (CFR) ENGINE

Bodur, İlder İmran

M.S., Department of Mechanical Engineering

Supervisor: Assoc. Prof. Dr. Ahmet Yozgatlıgil

July 2015, 98 pages

The objective of this study is to determine the Research Octane Number (RON) of Liquefied Petroleum Gas (LPG) using a Cooperative Fuel Research (CFR) engine. In order to do this, a series of modifications were carried out on the engine components including piston and fuel feeding system prior to the experiments. The experiments were conducted on a wide range of LPG fuel compositions, consisting of various volumetric ratios of propane, iso-butane, n-butane, and trace amount of olefins to determine the RON of LPG using the well-documented *bracketing* method accepted by the American Society for Testing and Materials (ASTM). A mathematical model for variation of LPG research octane number with the volumetric ratios of consisting gaseous fuels was also developed.

Keywords: Gaseous fuels, Liquefied petroleum gas, LPG composition, Cooperative fuel research engines, Octane number of LPG

## ÖZ

### MODİFİYE EDİLMİŞ DEĞİŞKEN SIKIŞTIRMA ORANLI MOTOR KULLANARAK GAZ YAKITLARIN OKTAN SAYILARININ BELİRLENMESİ

Bodur, İlter İmran

Yüksek Lisans, Makine Mühendisliği Bölümü

Tez Yöneticisi: Doç.Dr. Ahmet Yozgatlıgil

Temmuz 2015, 98 sayfa

Bu çalışmanın amacı, Sıvılaştırılmış Petrol Gazının (LPG) CFR motoru aracılığıyla Araştırma Oktan Sayısının (RON) belirlenmesidir. Bu amaçla, motor üzerinde piston ve yakıt besleme sistemi de dahil olmak üzere bir takım değişiklikler uygulanmıştır. Değişken volümetrik oranlarda propan, izo-bütan, n-bütan ve eser miktarlarda olefin içeren LPG kompozisyonları üzerinde deneyler yapılarak, ASTM tarafından belirlenmiş olan hesaplama prosedürü kullanılarak RON değerleri elde edilmiştir. Ek olarak LPG içeriğinde bulunan gaz yakıtların volumetrik oranlarının değişiminin, LPG oktan sayısı değişimine olan etkileri matematiksel olarak modellenmiştir.

Anahtar Kelimeler: Gaz yakıtlar, Sıvılaştırılmış petrol gazı, LPG kompozisyonu, CFR motoru, LPG'nin oktan sayısı

*To My Family,*

*In Loving Memory of Ilter BODUR*

## ACKNOWLEDGEMENTS

First and above all, I would like to express my deepest gratitude to my supervisor Professor Ahmet YOZGATLIGİL for his endless patience, encouragement and reassurance during my research and education. I would also like to thank to Professor A. Demir BAYKA and Professor A. Buğra KOKU for their endless supports and lifesaving comments during all dead-end situations during my research.

I would like to express my sincere thanks to my friends Çağdaş AKSU, Sina SHAFEE, T.Uluç YAMALI and Ramin BARZEGAR for their personal supports as friends and professional supports as laboratory colleagues. They all willingly supported with the smaller and bigger problems both in this study and personal life.

I would like to appreciate AYGAZ for their continuous contributions this research study. The generosity of their staff in providing continuous progression during the study has been appreciated.

I would like to express my gratitude to the administrative and technical staff of Mechanical Engineering Department of Middle East Technical University.

The last but not the least, I would like to express my sincerest appreciation to my family, for their endless love and support, and their encouragement for achieving my ambitious goals. There is no way for me to repay them for their perseverance.



## TABLE OF CONTENTS

ABSTRACT .....	v
ÖZ .....	vi
ACKNOWLEDGEMENTS .....	viii
TABLE OF CONTENTS .....	ix
LIST of TABLES .....	xiii
LIST of FIGURES .....	xiv
LIST of SYMBOLS .....	xvi
CHAPTERS	
1. INTRODUCTION .....	1
1.1. Motivation .....	1
1.2. Engine Knock (Detonation).....	2
1.2.1. Definition of Knock .....	2
1.2.2. Effects of Knock .....	4
1.2.3. Parameters Affecting Knock .....	5
1.2.3.1. Engine Parameters .....	6
1.2.3.2. Operation Parameters.....	7
1.2.3.3. Fuel Parameters.....	8
1.2.4. Methods of Knock Prevention .....	10
1.3. Octane Testing.....	13
1.3.1. Definition of Octane Rating .....	13
1.3.2. Octane Testing Methods .....	14
1.3.2.1. Research Octane Number (RON) Testing .....	16

1.3.2.2.	Motor Octane Number (MON) Testing .....	17
1.3.3.	Reference Fuels and Additives .....	17
1.3.3.1.	Iso-Octane.....	18
1.3.3.2.	N-Heptane.....	18
1.3.3.3.	Tetra Ethyl Lead (TEL) .....	19
1.4.	Liquified Petroleum Gas as a Fuel in Internal Combustion Engines .....	20
1.4.1.	Liquified Petroleum Gas .....	20
1.4.1.1.	LPG Use as an Alternative Fuel .....	21
1.4.1.2.	Composition of LPG.....	23
1.4.1.3.	The Pros and Cons of LPG .....	23
1.5.	Octane Testing of LPG.....	25
1.5.1.	Near Infrared Regression (NIR) Spectroscopy Method .....	25
1.5.2.	Gas Chromatography (GC) Method .....	25
2.	LITERATURE SURVEY .....	27
2.1.	LPG Combustion.....	27
2.1.1.	Effects of Higher Hydrocarbons on LPG Combustion .....	28
2.1.2.	Experimental Studies on LPG Flame Characteristics.....	29
2.1.3.	Experimental Studies on Syngas Flame Characteristics.....	40
2.2.	LPG Octane Number Measurement .....	48
2.3.	Aim of the Study .....	50
3.	EXPERIMENTAL SETUP .....	51
3.1.	Octane Testing System.....	51
3.1.1.	Cooperative Fuel Research (CFR) Engine.....	51
3.1.2.	Detonation Pick-up .....	59
3.1.3.	Compression Ratio Control Mechanism.....	59
3.1.4.	Fuel Tanks and Fuel Selector.....	60

3.1.5.	Air – Fuel Ratio Control Mechanism.....	61
3.1.6.	Air Heating System.....	62
3.2.	Gaseous Fuel System.....	63
3.2.1.	Fuel Tanks.....	64
3.2.2.	LPG Evaporator .....	64
3.2.3.	Air-Fuel Ratio Control Mechanism .....	66
3.2.4.	Gaseous Fuel Mixer .....	66
3.3.	Data Acquisition System .....	67
3.3.1.	Oscilloscope .....	68
3.3.2.	Data Acquisition Card.....	68
3.3.3.	Software .....	68
4.	EXPERIMENTAL METHOD.....	69
4.1.	Composition of Test Fuels .....	69
4.2.	Reference Fuels .....	73
4.3.	Test Procedure.....	74
4.4.	Calculation Procedure .....	77
4.4.1.	Data Processing .....	77
4.4.2.	Peak Value Selection-Elimination.....	77
4.4.3.	Detonation Voltage Determination .....	78
4.4.4.	Octane Value Calculation.....	78
5.	RESULTS and CONCLUSION .....	79
5.1	Regression Analysis: Octane Number vs. Propanest, P2, nbutanest, OlefinC3st. .....	82
	BIBLIOGRAPHY.....	91
	APPENDICES .....	97
A-1	Technical Drawing of Original Piston .....	97

A-2 Technical Drawing of Modified Piston.....	98
---	----

## LIST of TABLES

Table 1.1: Data on fuel properties.....	10
Table 1.2: Oxygenate properties .....	13
Table 1.3: Standard conditions for RON test.....	16
Table 1.4: Standard conditions for MON test .....	17
Table 1.5: Basic properties of iso-octane.....	18
Table 1.6: Basic properties of n-heptane.....	19
Table 1.7: Octane numbers for blends of tetraethyl lead in iso-octane.....	20
Table 1.8: Composition of LPG components and their higher heating values .....	21
Table 1.9: Typical properties of commercial LPG gas components.....	23
Table 3.1: Diameters of pulleys for RON and MON tests.....	51
Table 3.2 : Specifications of a standard Waukesha CFR engine .....	53
Table 3.3: Specifications of a standard BASF CFR engine .....	54
Table 4.1: Compositions of test fuels provided by AYGAZ Company.....	70
Table 4.2: Compositions of Olefins Samples Provided by AYGAZ Company.....	72
Table 5.1: Research octane numbers for the fuel samples prepared by AYGAZ Company .....	80
Table 5.2: Descriptive statistics of all variables.....	81
Table 5.3: Calculation parameters.....	83
Table 5.4: Research octane numbers for LPG samples including various amounts of olefins prepared by AYGAZ Company .....	84
Table 5.5: Descriptive statistics of all variables.....	87
Table 5.6: Calculation parameters.....	88

## LIST of FIGURES

Figure 1.1: Cylinder pressure versus crank angle traces of cycles .....	2
Figure 1.2: Difference between normal/abnormal combustion and pre-ignition.....	3
Figure 1.3: Examples of component damage from abnormal engine combustion. ....	5
Figure 1.4: Gasoline octane number increase .....	12
Figure 1.5: Molecular structure of iso-octane.....	18
Figure 1.6: Molecular structure of n-heptane .....	19
Figure 2.1: Experimental setup of Huzayyin et al .....	31
Figure 2.2: Samples of the preheat temperature effect on the pressure record and pressure rise rate for LPG–air mixtures at the specified conditions .....	32
Figure 2.3: Optical setup for Schlieren system.....	33
Figure 2.4: Bunsen burner experimental setup .....	34
Figure 2.5: Effect of mixture composition on laminar flame speed.....	35
Figure 2.6: Schematic diagram of experimental setup .....	36
Figure 2.7: Variation of laminar flame speed with N <sub>2</sub> dilution .....	36
Figure 2.8: Air/fuel pre-mixer.....	37
Figure 2.9: Schematic diagram of flame propagation speed detection system.....	38
Figure 2.10: Position and signal of photodiode .....	38
Figure 2.11: Comparison of flame propagation speed obtained by LDM method and the high speed camera method.....	39
Figure 2.12: Diagram of experimental apparatus .....	41
Figure 2.13: Comparison of experimental traces with model results for flames .....	41
Figure 2.14: Experimental setup [43] .....	42
Figure 2.15: Pressure dependence of the mass burning rate.....	43
Figure 2.16: Experimental setup [44, 45] .....	45
Figure 2.17: Diagnostics setup [44, 45].....	45
Figure 2.18: The straight burner setup .....	46
Figure 2.19: Experimental setup [46] .....	47
Figure 2.20: Experimental and predicted laminar flame speed variation .....	48
Figure 3.1: Pulleys for RON setup and MON setup .....	52
Figure 3.2: Comparison of piston height before and after reconditioning.....	55
Figure 3.3: New designed piston head.....	56

Figure 3.4: New head gasket.....	56
Figure 3.5: Scale Disc, Dial Indicator.....	57
Figure 3.6: Pressure gauge .....	58
Figure 3.7: Graphical representation of cylinder height vs. in-cylinder pressure.....	58
Figure 3.8: Detonation pickup, Cross section of detonation pickup.....	59
Figure 3.9: Worm gear .....	60
Figure 3.10: Fuel tanks and fuel selector .....	61
Figure 3.11: Fuel tank and screw spindle.....	62
Figure 3.12: Air heater, Cross section of air heater .....	63
Figure 3.13: LPG tank.....	64
Figure 3.14: LPG evaporator.....	65
Figure 3.15: LPG on-off switch, Solenoid control unit .....	65
Figure 3.16: LPG fuel flow control valve .....	66
Figure 3.17: LPG Mixer.....	67
Figure 3.18: LPG nozzle .....	67
Figure 4.1: 99.9% pure olefins.....	71
Figure 4.2: Transfer of LPG and olefins into tanks .....	71
Figure 4.3: Reference fuels prepared by Tübitak MAM.....	73
Figure 5.1: Matrix Plot of octane number.....	82
Figure 5.2: Comparison of actual octane numbers vs. predicted octane number .....	83
Figure 5.3: Octane numbers of pure olefins.....	85
Figure 5.4: Octane number comparison of samples containing 15% of each olefins .....	85
Figure 5.5: Octane number comparison of samples having equal amount of olefins .....	86
Figure 5.6: The plot of actual olefin and predicted olefin for each experiment.....	89

## LIST of SYMBOLS

### *Abbreviations*

<i>(A/F)</i>	Air Fuel Ratio	<i>NTC</i>	Negative Temperature
<i>BTC</i>	Before Top Dead Center		Coefficient
<i>°CA</i>	Crank Angle Degree	<i>ON</i>	Octane Number
<i>CCD</i>	Charge-Coupled Device	<i>P</i>	Pressure
<i>CFR</i>	Cooperative Fuel Research	<i>PIV</i>	Particle Image Velocimetry
<i>CVCC</i>	Constant Volume Combustion	<i>RON</i>	Research Octane Number
	Chamber	<i>RPM</i>	Revolutions per Minute
<i>GC</i>	Gas Chromatography	<i>SE</i>	Standard Error
<i>ICCD</i>	Intensified Charge-Coupled	<i>SI</i>	Spark Ignition
	Device	<i>TBA</i>	Tertiary Butyl Alcohol
<i>HHV</i>	Higher Heating Value, MJ/kg	<i>TDC</i>	Top Dead Center
<i>LDM</i>	Laser Deflection Method	<i>TEL</i>	Tetra Ethyl Lead
<i>LHV</i>	Lower Heating Value, MJ/kg	<i>UV</i>	Ultraviolet
<i>LNG</i>	Liquefied Natural Gas		
<i>LPG</i>	Liquefied Petroleum Gas		
<i>LPLi</i>	Liquid Port Injection	<i>(g)</i>	Gaseous State
<i>MMT</i>	Methylcyclopentadienyl	<i>(l)</i>	Liquid Phase
	Manganese Tricarbonyl	<i>(s)</i>	Solid State
<i>MON</i>	Motor Octane Number	<i>st</i>	standardized
<i>MTBE</i>	Methyl Teriary Butyl Ether	<i>s</i>	stoichiometric
<i>NIR</i>	Near Infrared Spectroscopy	§	Typical Values

### *Nomenclature*



# **CHAPTER 1**

## **INTRODUCTION**

### **1.1. Motivation**

Internal combustion engines have been an indispensable part of transportation and industrial usage in recent years. However, persistent problems such as engine knock, fuel autoignition and emissions have increased demand for better understanding of the combustion phenomenon, the burning characteristics of the fuel, flow field and turbulence interaction inside the combustion chamber.

Also nowadays, besides conventional fuels such as diesel and gasoline, new fuels are being utilized in the internal combustion engines such as liquefied petroleum gas (LPG), natural gas, biodiesel, hydrogen etc. Among these fuels, LPG serves as a clean and one of the most important alternative fossil fuel in the world having a considerable advantage in terms of combustion pollution, easier transportation and maintenance.

Nowadays, LPG is known to be used in over 17 million vehicles in many countries [1] including Turkey, where its application was legalized in 1995 [2]. Another important aspect of the LPG fuel is its high octane rating which shows the fuel's resistance to detonation or knocking. The LPG fuel can withstand higher compression ratios without knocking which makes it favorable for engine use.

However, there are currently very few studies on determination of the LPG octane number based on rating tests using research engines which was the main motivation behind doing this thesis. In this work, a modified research engine is then used in order to specify octane number of LPG with different compositions.

## 1.2. Engine Knock (Detonation)

### 1.2.1. Definition of Knock

Engine knock, a name which comes from the pinging noise emitted from an internal combustion engine due to the generation of shockwaves produced in the combustion chamber, is known as the most damaging abnormal combustion phenomenon. The shockwaves occur because of the auto-ignition of the unburned air-fuel-residual gas mixture ahead from the flame front.

The pressure, temperature and density of the air fuel mixture ahead from the flame, also known as “end gas”, increase due to the compression caused by the propagation of flame through combustion chamber. Due to these increments, ingredients of end gas mixture may undergo chemical reactions before normal combustion causing auto ignition which leads to spontaneous and rapid release of their chemical energy.

In this situation, end gas burns very quickly, releasing its energy at a rate 5 to 25 times faster than that of characteristic normal combustion, causing high frequency pressure oscillations in combustion chamber as shown in figure 1.1 [7].

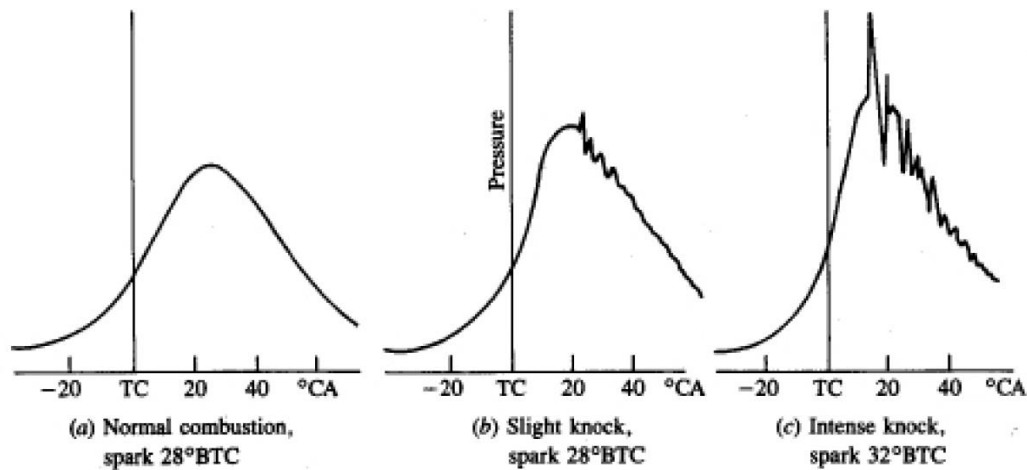


*Figure 1.1: Cylinder pressure versus crank angle traces of cycles with (a) normal combustion, (b) light knock, and (c) heavy knock. 4000 rev/min, wide open throttle, 381-cm<sup>3</sup> displacement single cylinder engine [7]*

Engine knock is sometimes confused with surface ignition, which is ignition of the air-fuel mixture by a hot spot in the combustion chamber, and may lead to detonation. Surface ignition may occur before spark ignition (pre-ignition) or after normal ignition (post-ignition), and may produce one or more flames at the same time in combustion chamber. The difference between engine knock and post ignition is shown in the figure 1.2.

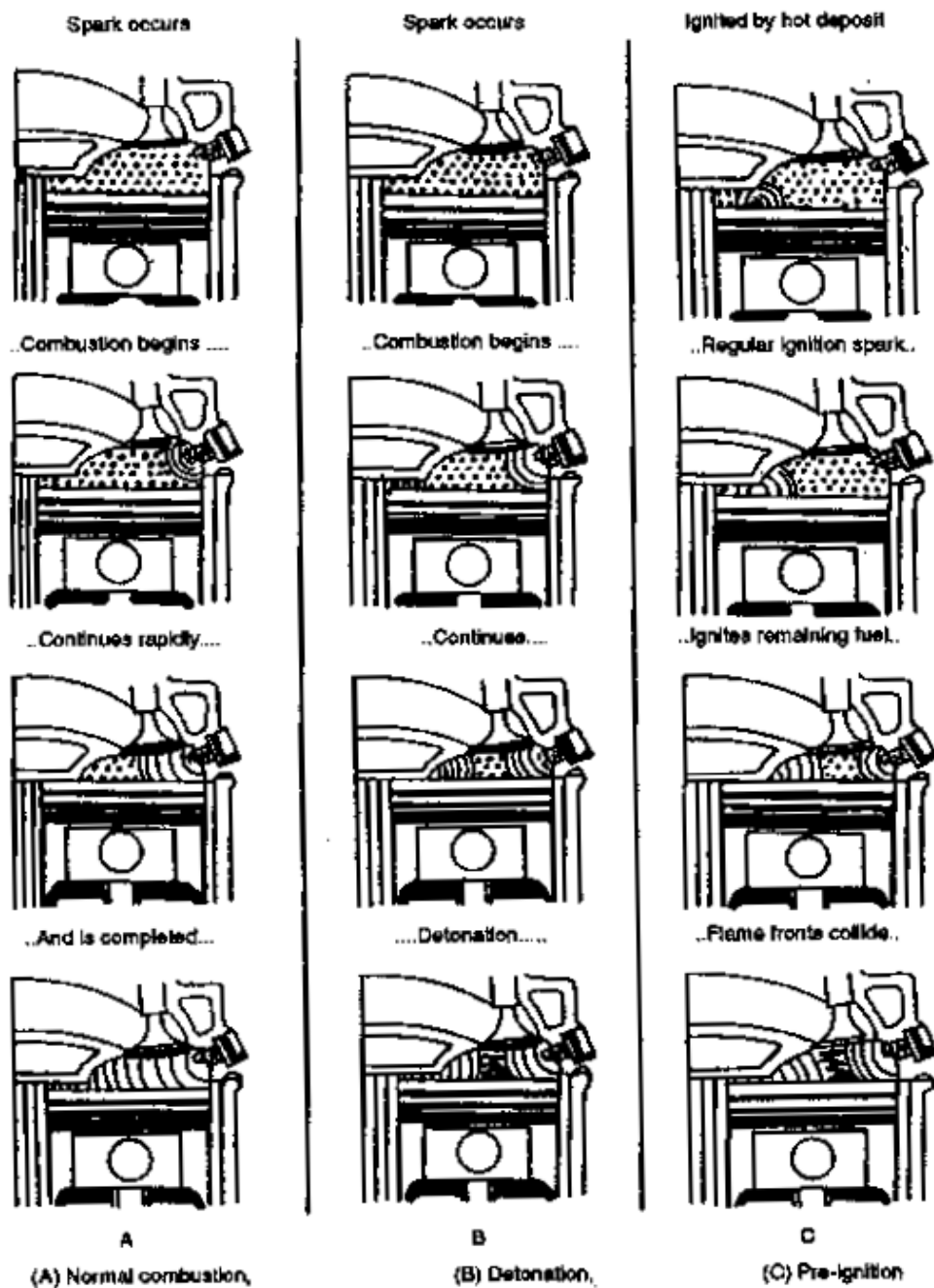


Figure 1.2: Difference between normal/abnormal combustion and pre-ignition [9]

### **1.2.2. Effects of Knock**

Due to the sudden increase in pressure and temperature during engine detonation, the engine performance and lifespan are affected in an undesirable way; such as, increase in engine emissions, decrease in engine thermal efficiency, considerable increase in specific fuel consumption and possibility of structural harms to engine block [8].

Because of the direct relation between the compression ratio of an internal combustion engine and the knocking phenomena, detonation limits the compression ratio and thus the performance and efficiency of engine. In addition, the amount of carbon deposits increases while an engine is working under knocking conditions.

Under knocking conditions, the engine works roughly due to movement and vibrations of pressure waves creating loud pulsating noises as a result of detonation. The pressure oscillations can increase the rate of wear of combustion chamber of the engine.

As it can be seen in figure 1.3, erosion of piston crown, pitting of inlet and outlet valves and cylinder head, may result heavy damage and furthermore complete wreckage of the engine. Also, at engines with higher level of noise, detonation becomes more dangerous since it is easier to detect the engine knock in smaller engines.

The considerable amount of damage to engine during detonation is caused by the increased amount of rate of heat transfer from combustion chamber to engine block. A temperature difference as high as 150°C between a non-detonating and detonating engine could occur due to rapid completion of combustion which fundamentally reduces the thickness of inactive stagnant gas on cylinder walls decreasing the heat transfer rate, due to produced shock waves during engine knock.

Under knocking conditions, the power output and the efficiency of the engine decreases due to the increased heat transfer rate through cylinder walls. In addition, the other effect of increased heat transfer rate to the cylinder walls is the possibility of increased local heating, especially of spark plug, which may lead to an increase of the tip temperature resulting in ignition of the air-fuel mixture before spark (pre-ignition).

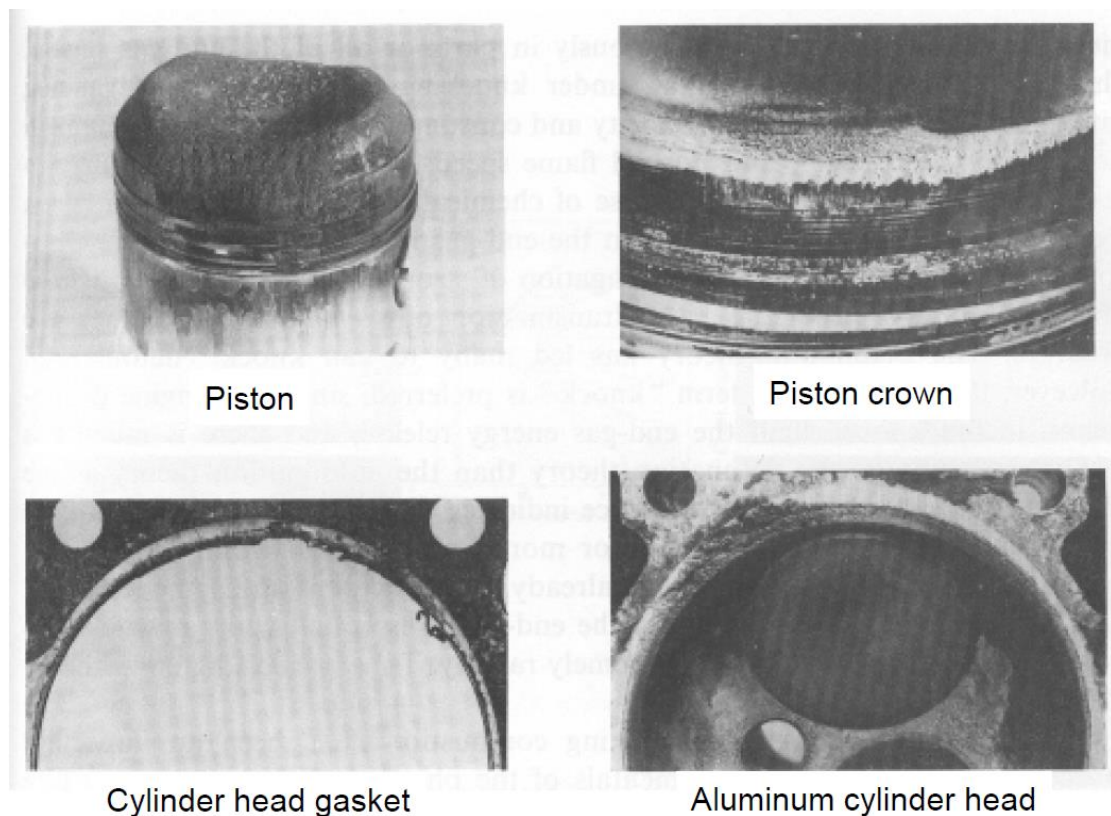


*Figure 1.3: Examples of component damage from abnormal engine combustion [7].*

In summary, the magnitude of harm given to engine by knocking depends on detonation intensity and duration. Trace amount of knock does not have a significant effect on engine performance and durability. On the other hand, heavy knock can lead to engine damage, such as piston ring sticking or breakage, cylinder head gasket failure, cylinder head-piston crown-top land erosions piston melting or holing etc., as discussed above.

### **1.2.3. Parameters Affecting Knock**

Even though the fundamentals of knocking phenomena is not completely understood, the reasons for an engine to work under knocking conditions can be categorized under three main groups; engine parameters, operation parameters, and fuel parameters which will be briefly discussed in the following two sections.

### **1.2.3.1. Engine Parameters**

Engine parameters affecting the possibility and intensity of knock are based on the design of the engine. Those design parameters have a great effect on the pressure, temperature, density, and the local temperature concentration points inside the combustion chamber, leading to detonation.

The most important engine parameter affecting knock is the compression ratio, since increasing the compression ratio increases both the temperature and pressure in combustion chamber and the density of the unburned air-fuel mixture. The delay period of the end gas reduces as the temperature increases making the engine becomes more knock prone.

The induction of the engine also has an effect on knock tendency, since it directly affects the density and pressure of the mixture inside combustion chamber. For instance, using a forced induction such as turbocharger or supercharger, increases pressure and density resulting in increasing knocking tendency.

Large engines, have a greater knocking tendency, since the time required for the flame to propagate across combustion chamber is longer. It can be said that flame travel distance across the combustion chamber and flame speed affects the knock tendency. Due to this reason, location of the spark plug is of great importance in engine design. If the spark plug is placed in a centric position, the flame travel distance becomes minimized and the engine becomes more resistant to detonation. For reducing the flame travel distance, two or more spark plugs are normally used on certain engines that are available on market. In addition, exhaust valves are usually placed close to spark plug in order to mitigate possibility of end gas detonation. Thus the tendency of knock and the pre-ignition possibility reduces.

On the other hand, turbulence of the air-fuel mixture, which depends on the design and speed of engine is another factor affecting the flame speed. So increasing the turbulence of mixture, increases the flame speed resulting in the reduction of the knock tendency.

The design of the combustion chamber also has an effect on the end gas temperature which influences the detonation by means of pre-ignition caused by spark plug and exhaust valve. In addition, the delay period depends on the coolant temperature. As the temperature of coolant increases, delay period decreases, which results in an increased knock tendency.

Finally, the engines octane number requirement increases due to the build-up of deposits in the combustion chamber. The requirement for octane number increase may vary between 1-13 octane number according to amount of deposits. As the engine is completely cleaned, the octane number requirement reverts to original value.

#### **1.2.3.2. Operation Parameters**

The operation parameters affecting knock tendency can be classified as, engine load, engine speed, air-fuel ratio, and throttle position.

The power produced by a spark ignition engine is controlled by the throttle position. When the engine runs under low load and high throttle condition, the initial and final pressure of the mixture compression decreases and the increased amount of residual gases dilutes the air-fuel mixture. The dilution of the mixture reduces the flame speed and prolongs the ignition lag. As the flame speed decreases, the possibility of knock increases, as explained in section 1.2.3.1.

As mentioned, the air-fuel mixture turbulence directly affects the flame speed and the turbulence of the mixture increases as the speed of engine increases. The flame speed and engine speed are nearly linearly proportional, in other words as the engine speed is doubled, the duration of flame to traverse combustion chamber is halved. For the reasons explained in section 1.2.3.1, as the engine speed is increased, knock tendency decreases, since the turbulence and speed of flame is increased.

The effect of air-fuel ratio on knocking tendency of an engine varies according to the ratio. Since the flame speed reduces for both lean and very rich mixture, the knock tendency increases at very lean and very rich ratios of air and fuel.

In lean combustion, the amount of heat released is lower, resulting in reduced flame temperature and flame speed. As the flame speed decreases, time needed for flame propagation increases, as a result possibility of knocking increases.

On the other hand, in very rich mixture condition, combustion becomes incomplete resulting production of more C and CO species leading to a decrease in heat and flame speed, thus increasing the possibility of knock.

The effect of air-fuel ratio on knock tendency is used in octane number verification of fuels. At constant compression ratio, the air-fuel ratio is arranged to obtain the maximum knock intensity during experiment. More information about air-fuel ratio arrangements will be given in chapter 2.

### 1.2.3.3. Fuel Parameters

Engine knock, is a phenomenon that is affected by both engine and fuel factors [7]. Up to this point, the engine design and operation parameters were discussed, however, knock occurrence depends majorly on the fuels' anti-knock quality.

Petroleum fuels usually include many types of hydrocarbons having different molecular size and structure. The different molecular size and structures enables hydrocarbons to have a wide variation of resistance to knock. The knock tendency increases as the carbon-chain length increases and decreases as the carbon atoms are centralizing. In addition, saturated hydrocarbons are more prone to knock than the unsaturated hydrocarbons.

The relation between knock tendency and molecular structure is discussed below [7]:

*Paraffins:* Increase in the length of carbon chain, decreases the knock resistance. As the carbon atoms are compacted by incorporating side chains, knock resistance increases. Also, addition of methyl groups ( $\text{CH}_3$ ) near to basic carbon chain, increases knock resistance.

*Olefins:* Introducing double bonds, increases the knock resistance. For instance, while introducing one double bond has a little antiknock effect, two or three double bonds increases knock resistance more. On the other hand, acetylene ( $\text{C}_2\text{H}_2$ ) and propylene ( $\text{C}_2\text{H}_4$ ) are exceptions to this rule.

*Napthenes and aromatics:* Napthenes, which generally tend to knock more than corresponding size aromatics, also reduce knocking tendency when double bonds are introduced. Similar to olefins, they tend to decrease knock when one double bond and when two or three double bonds are introduced, the knocking tendency decreases more. Both group of fuels become more knock tendentious when side chain attached



to basic ring structure is lengthened whereas branching of side chains decreases the knock tendency.

Commercial fuels are usually blends of a number of individual hydrocarbon compounds from all the hydrocarbon series of classes: alkanes (paraffins), cyclanes (naphthenes) alkenes (olefins) and aromatics, and they contain various chemical additives in order to improve fuel quality [7]. The additives present in modern fuels are used for improving the knock quality but also;

- ⇒ Controlling surface ignition
- ⇒ Reducing spark plug fouling
- ⇒ Resisting gum formation
- ⇒ Resisting rust formation
- ⇒ Reducing carburetor icing
- ⇒ Removing carburetor or injector deposits
- ⇒ Minimizing the deposits in the intake system
- ⇒ Preventing valve sticking.

With the help of antiknock agents, the octane number of fuels can be increased without modifying the fuel's hydrocarbon composition by refinery processing which is an expensive method. The table below shows the octane ratings of common blended fuels and several individual hydrocarbon compounds.

Lead alkyls are the most effective antiknock agents. It is stable and fuel-soluble in the form of lead-alkyls. Tetraethyl lead (TEL)  $(C_2H_5)_4Pb$  which was first introduced in 1923 and Tetramethyl lead (TML)  $(CH_3)_4Pb$  since 1960, had been primarily used in the past as gasoline additives [7, 10]. However, their usage has been prohibited due to environmental concerns and damage to catalytic devices used for emission control. The manganese antiknock compound, which is also known as MMT (methylcyclopentadienyl manganese tricarbonyl) was also used as a supplementary antiknock agent for TEL. Nowadays, MMT is sometimes used as an antiknock additive for unleaded gasoline; however, its concentration is limited due to exhaust catalytic convertor plugging.

Table 1.1: Data on fuel properties [7]

Fuel	Formula (phase)	Molecular weight	Specific gravity: (density,† kg/m³)	Heat of vaporization, kJ/kg‡	Specific heat		Higher heating value, MJ/kg	Lower heating value, MJ/kg	LHV of stoich. mixture, MJ/kg	(A/F) <sub>s</sub>	(F/A) <sub>s</sub>	Fuel octane rating	
					Liquid, kJ/kg · K	Vapor c <sub>p</sub> , kJ/kg · K						RON	MON
Practical fuels													
Gasoline	C <sub>8</sub> H <sub>18.76</sub> (l)	~110	0.72–0.78	305	2.4	~1.7	47.3	44.0	2.83	14.6	0.0685	92–98	80–90
Light diesel	C <sub>12</sub> H <sub>24.6</sub> (l)	~170	0.84–0.88	270	2.2	~1.7	44.8	42.5	2.74	14.5	0.0690	—	—
Heavy diesel	C <sub>16</sub> H <sub>34.4</sub> (l)	~200	0.82–0.95	230	1.9	~1.7	43.8	41.4	2.76	14.4	0.0697	—	—
Natural gas§	C <sub>4</sub> H <sub>10</sub> N <sub>0.11</sub> (g)	~18	(~0.79†)	—	—	~2	50	45	2.9	14.5	0.069	—	—
Pure hydrocarbons													
Methane	CH <sub>4</sub> (g)	16.04	(0.72†)	509	0.63	2.2	55.5	50.0	2.72	17.23	0.0580	120	120
Propane	C <sub>3</sub> H <sub>8</sub> (g)	44.10	0.51 (2.0†)	426	2.5	1.6	50.4	46.4	2.75	15.67	0.0638	112	97
Isooctane	C <sub>8</sub> H <sub>18</sub> (l)	114.23	0.692	308	2.1	1.63	47.8	44.3	2.75	15.13	0.0661	100	100
Cetane	C <sub>18</sub> H <sub>38</sub> (l)	226.44	0.773	358	1.6	1.6	47.3	44.0	2.78	14.82	0.0675	—	—
Benzene	C <sub>6</sub> H <sub>6</sub> (l)	78.11	0.879	433	1.72	1.1	41.9	40.2	2.82	13.27	0.0753	115	115
Toluene	C <sub>7</sub> H <sub>8</sub> (l)	92.14	0.867	412	1.68	1.1	42.5	40.6	2.79	13.50	0.0741	120	109
Alcohols													
Methanol	CH <sub>4</sub> O(l)	32.04	0.792	1103	2.6	1.72	22.7	20.0	2.68	6.47	0.155	106	92
Ethanol	C <sub>2</sub> H <sub>6</sub> O(l)	46.07	0.785	840	2.5	1.93	29.7	26.9	2.69	9.00	0.111	107	89
Other fuels													
Carbon	C(s)	12.01	~2§	—	—	—	33.8	33.8	2.70	11.51	0.0869	—	—
Carbon monoxide	CO(g)	28.01	(1.25†)	—	—	1.05	10.1	10.1	2.91	2.467	0.405	—	—
Hydrogen	H <sub>2</sub> (g)	2.015	(0.090†)	—	—	1.44	142.0	120.0	3.40	34.3	0.0292	—	—

(l) liquid phase; (g) gaseous phase; (s) solid phase.

† Density in kg/m³ at 0°C and 1 atm.

‡ At 1 atm and 25°C for liquid fuels; at 1 atm and boiling temperature for gaseous fuels.

§ Typical values.

RON, research octane number; MON, motor octane number.

#### 1.2.4. Methods of Knock Prevention

Preventing or reducing the knock tendency of an internal combustion engine is an issue regarding engine design and working conditions as well as the fuel which is entering combustion chamber.

By far the most important parameter regarding engine design concerning detonation is the compression ratio. Reducing the piston diameter will prevent knock from occurrence due to the short distance flame has to travel. Coating the piston head, combustion chamber and quench area with thermal barrier coatings will make the flame travel smoother and keep the piston and cylinder head surface under the coating cooler.

The temperature of the coating will inherently be hotter however, the heat produced during combustion will be forced to remain inside combustion chamber to produce more power. Coating combustion chamber parts reduces the timing needed for all energy to release, limiting the spark advance at maximum brake torque and reducing the chance of detonation [11].

Another design parameter which is used for reducing the possibility of knock is called “Reverse Flow Cooling”. In this method, the coolant is first directed to the cylinder head instead of engine block, thus, more heat is absorbed from combustion area. This

system, indeed, slightly reduces the thermal efficiency, on the other hand, power acquired increases by permitting higher compression ratio without detonation.

Knock sensor, which is usually an accelerometer mounted on cylinder block, which senses the vibration levels above a prescribed normal value, is used for controlling knock during engine operation.

Knock sensor automatically adjusts the ignition timing, with the help of ignition timing system, spark without any unnecessary retard to avoid knocking as the fuel octane rating and sensitivity and ambient conditions change [7]. In addition, by retarding the spark timing, the maximum pressure can be reached during power stroke with a lower magnitude.

Another method for preventing knock is controlling the air-fuel ratio. However using lean and rich mixture conditions decreases the flame speed and thus increase the knocking tendency. By using extremely rich or lean air-fuel mixtures, the flame temperature can be kept low since insufficient burning occurs and thus the tendency of knock decreases considerably. In contrast, the air-fuel ratio is used for obtaining the maximum knock intensity while conducting octane measuring tests [4, 5].

Injecting water to intake manifold is another option for decreasing the possibility of knock since, as water is injected into intake manifold or directly into combustion chamber, the end gas temperature and therefore the delay period decreases. Increasing the octane number of fuel entering in combustion chamber is another effective way of preventing detonation.

As it was mentioned in section 1.2.3.3, the most effective way to increase the octane number of spark ignition engine fuel is adding lead alkyls since lead in the form of lead alkyls is stable and fuel soluble. However, because of the damage to catalytic devices for emission control and the toxicological aspects of lead in the urban environment, usage of lead as an anti-knock agent is prohibited. The average effect of various amounts of tetraethyl lead to regular gasoline is showed in the figure 1.4.

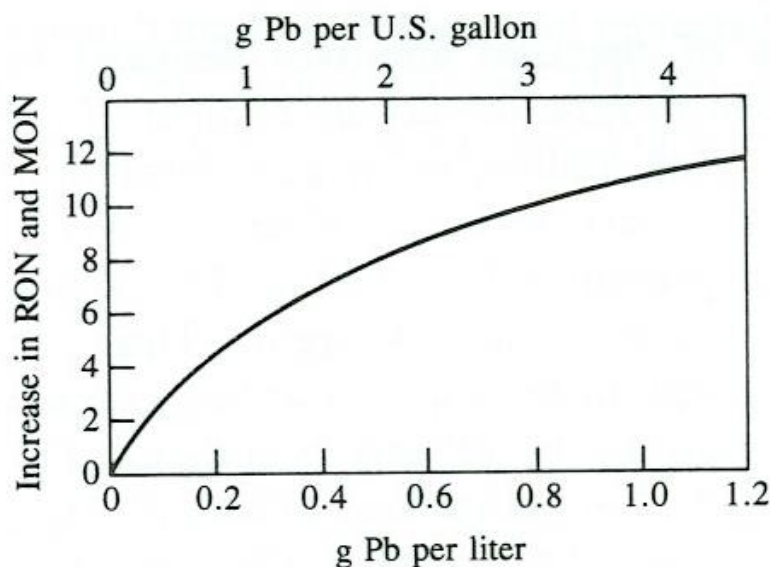


Figure 1.4: Gasoline octane number increase resulting from use of antiknock additive tetraethyl lead. Varies with fuel composition: average values shown [7]

Using alcohols and ethers as an antiknock additive is becoming more common nowadays due to their excellent antiknock quality. Methylcyclopentadienyl manganese tricarbonyl (MMT) which is used as an octane promoter especially with paraffinic gasolines. MMT is also used as a supplement to TEL and, it is about twice as effective as TEL in terms of research octane number gain and nearly equally effective in terms of motor octane number gain on a weight of metal basis.

Nowadays, the use of oxygen containing organic compounds, also known as oxygenates, instead of gasoline is continuously increasing. This is because oxygenates can be produced from non-petroleum sources making them economically viable, and also their good antiknock quality. The strict emission regulations make oxygenates important for providing octane quality of fuels with restricted lead alkyl usage.

In addition several oxygenates such as methanol, ethanol, tertiary butyl alcohol and methyl tertiary butyl ether are used directly as automotive fuels. Table 1.2 indicates the antiknock characteristics of oxygenates with respect to gasoline.

Table 1.2: Oxygenate properties [7]

	Methanol	Ethanol	TBA	MTBE	Gasoline
Typical (R+M)/2 blending value	112	110	98	105	87-93
Weight percent oxygen	50	35	22	18	0
Stoichiometric (A/F)	6.5	9.0	11.2	11.7	14.5
Specific gravity	0.796	0.794	0.791	0.746	0.74
Lower heating value, MJ/kg	20.0	26.8	32.5	35.2	44.0
Latent heat of vaporization, MJ/kg	1.16	0.84	0.57	0.34	0.35
Boiling temperature, °C	65	78	83	55	27-227

TBA, tertiary butyl alcohol; MTBE, methyl tertiary butyl ether

### 1.3. Octane Testing

Octane testing is a comparison of knock resistance of a sample fuel with that of reference fuels. There are different types of octane number determination methods among which the ASTM 2699 Research method and ASTM 2700 Motor method are approved as the standard octane number measurement methods for liquid fuels using standardized Cooperative Fuel Research – CFR engine. The detailed information regarding research method, motor method and standard CFR engine will be given in sections 1.3.2.1, 1.3.2.2 and 3.1.1, respectively.

In addition, for defining the anti-knock quality of fuels used in cars which are operated on chassis dynamometer or on road, road octane rating methods are developed.

#### 1.3.1. Definition of Octane Rating

Octane number for a spark ignition engine fuel is defined as “*any one of several numerical indicators of resistance to knock obtained by comparison with reference fuels in standardized engine or vehicle tests*” [4, 5]. In other words, the octane number of a fuel gives us information about the fuel’s resistance to detonation or knocking and determines if the fuel will detonate under given operating conditions, however, it does not give any information about the energy content of fuel. A fuel with high octane number can withstand higher compression ratios without knocking.

As mentioned before, octane number of a fuel has a direct effect on knocking characteristics and it is not a single quantity. The parameters affecting octane number of fuel can be listed as;

- ⇒ Engine design
- ⇒ Operating conditions during test
- ⇒ Ambient conditions during test
- ⇒ Mechanical condition of the engine
- ⇒ Type of fuel and oil used in the engine in past operation

The octane number scale of a fuel is based on a mixture of two hydrocarbons, also known as reference fuels, which are iso-octane and n-heptane having octane numbers of 100 and 0, respectively. A sample fuel's octane number is determined by comparing its knocking characteristics with that of blends of reference fuels. For instance, a fuel having octane number of 95 has similar knock resistance to a fuel blend of 95% iso-octane and 5% n-heptane on a volumetric basis.

### **1.3.2. Octane Testing Methods**

Although there are several methods for octane number determination of fuels, ASTM introduces two different types of octane number and their corresponding tests. These test are known as research octane number (RON) and motor octane number (MON) and which are conducted using ASTM 2699 and ASTM 2700 tests respectively [12]. The detailed information about these testing methods will be given in sections 1.3.2.1 and 1.3.2.2. Both methods use the same test engines with different operating settings for testing parameters.

In general, the RON test simulates;

- ⇒ Mild conditions of operation
- ⇒ Low engine speeds
- ⇒ No-load conditions
- ⇒ City driving

In contrast, the MON test represents,

- ⇒ Severe conditions of operation
- ⇒ High engine speeds
- ⇒ High load conditions
- ⇒ Performance of high-way driving.

Because of the difference between two methods, research octane number is generally higher than the motor octane number. The difference between these two octane numbers gives the fuel sensitivity, i.e.

$$\text{Fuel Sensitivity} = RON - MON \quad (1.1)$$

Which is a parameter that varies with the source of crude petroleum and the processes used during petroleum refinery. The octane numbers of reference fuels are accepted to be the same for both RON and MON by definition. Due to this reason, paraffins are expected to have no or a little fuel sensitivity since the reference fuels are also paraffins.

Internal combustion engines work under a variety of speeds, loads and weather conditions. For this reason, research and motor octane testing methods do not generally give the exact prediction about a fuel's behavior in an automobile since the standardized test are conducted in a single cylinder engine with wide open throttle and fixed spark timings.

Thus there are several methods to determine the fuels Road Octane Number on actual vehicles on chassis dynamometers or on the road. However, a fuel's road octane number differs from research and motor octane numbers, generally ranging between the two.

The road ON can thus be related with eq. (1.2);

$$\text{Road ON} = a(RON) + b(MON) + c \quad (1.2)$$

Where; a, b, and c are experimentally predefined constants and studies show that  $a \approx 0.5$  and  $b \approx 0.5$  give acceptable results [4, 5].

The antiknock index, which is derived from the mean value of RON and MON, is now used for characterizing the antiknock quality of a fuel in United States as in eq. (1.3).

$$\text{Antiknock index} = \frac{RON + MON}{2} \quad (1.3)$$

The ASTM RON and ASTM MON tests are conducted on a standardized, single cylinder, variable compression ratio Cooperative Fuel Research – CFR engine. The specifications of the engine are given in section 3.1.1. Although both tests are

conducted on the same engine, there are a number of differences in the operating conditions of the engine and the main differences are;

- ⇒ Engine speed
- ⇒ Inlet air temperature
- ⇒ Inlet air-fuel mixture temperature
- ⇒ Ignition advance.

The detailed information and operating parameters for both tests will be given in the following two sections.

#### 1.3.2.1. Research Octane Number (RON) Testing

Research octane number, for a spark ignition engine fuel, is defined as “*the numerical rating of knock resistance obtained by comparison of its knock intensity with that of primary reference fuel blends when both are tested in a standardized CFR engine*” operating under the conditions specified in ASTM D 2699 [4].

RON gives information about the quality of fuel under mild conditions of operation [13]. Mild operation is identified by low engine speeds and no-load conditions, similar to urban driving. The operating conditions of RON method is shown in table 1.3.

Table 1.3: Standard conditions for RON test [4]

Research Octane Number - RON Test	
Test Method	ASTM D 2699
Engine	Cooperative Fuel Research
Engine Speed	600 ± 6 RPM
Intake Air Temperature	52 ± 1°C
Intake Air Humidity	3,56-7,12 gH <sub>2</sub> O/kg dry air
Intake Mixture Temperature	n/a
Coolant Temperature	100 ± 1,5°C
Oil Temperature	57 ± 8°C
Ignition Advance	13 CAD BTC



### 1.3.2.2. Motor Octane Number (MON) Testing

Motor octane number, for a spark ignition engine fuel is defined as “*the numerical rating of knock resistance obtained by comparison of its knock intensity with that of primary reference fuels when both are tested in a standardized CFR engine*” operating under the conditions specified in ASTM D 2700 [5].

MON gives information about the quality of fuel under severe conditions of operation [14]. Severe operation is identified by high engine speeds and high-load conditions, similar to performance or high-way driving conditions.

In addition, motor octane number also gives information about knock characteristics of aviation fuels in aviation piston engines, with aid of an equation correlating to “aviation-method octane number or performance number” [14]. The operating conditions of MON method is given in the table 1.4;

Table 1.4: Standard conditions for MON test [5]

Motor Octane Number - MON Test	
Test Method	ASTM D 2700
Engine	Cooperative Fuel Research
Engine Speed	900 ± 9 RPM
Intake Air Temperature	38 ± 2,8°C
Intake Air Humidity	3,56-7,12 gH <sub>2</sub> O/kg dry air
Intake Mixture Temperature	149 ± 1°C
Coolant Temperature	100 ± 1,5°C
Oil Temperature	57 ± 8°C
Ignition Advance	14-26 CAD BTC

### 1.3.3. Reference Fuels and Additives

During octane tests, knock intensities of sample fuels are compared with that of reference fuels containing different volumetric ratios of iso-octane and n-heptane. Iso-octane and n-heptane are used for sample fuels having octane number lower than 100. For samples having an octane number higher than 100, tetraethyl lead is added to iso-octane according to an empirical formula.

### 1.3.3.1. Iso-Octane

Iso-octane, also known as 2,2,4-trimethylpentane, is an organic compound used as reference fuel in RON and MON tests having an octane number of 100. It is also an important component of gasoline which can be used as an octane number enhancer.

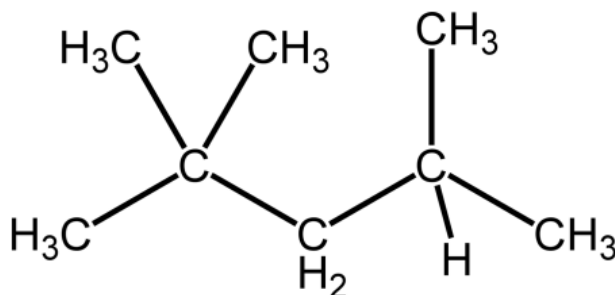


Figure 1.5: Molecular structure of iso-octane [19]

Iso-octane which is used in RON and MON tests must have a minimum of 99.75% purity [4, 5]. The basic properties of iso-octane are given in the table 1.5.

Table 1.5: Basic properties of iso-octane [19]

<b>Molecular Formula</b>	$C_8H_{18}$
<b>Molar Mass</b>	$114.2 \text{ g/mol}^{-1}$
<b>Appearance</b>	Colorless liquid
<b>Density</b>	$688.0 \text{ kg/m}^3$ , liquid
<b>Melting point</b>	$-107.4^\circ\text{C}$ , $166.0 \text{ K}$
<b>Boiling point</b>	$99.3^\circ\text{C}$ , $372.0 \text{ K}$

### 1.3.3.2. N-Heptane

N-heptane, is a straight chain alkene used in RON and MON test with an octane rating of zero. Because of its zero octane rating, n-heptane is not desired in automotive fuels, since it burns explosively causing engine knocking.

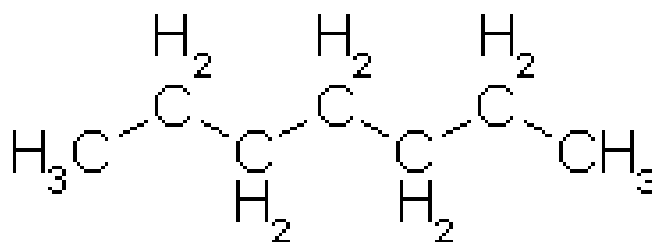


Figure 1.6: Molecular structure of *n*-heptane [19]

N-heptane which is used in RON and MON tests must be minimum 99.75% purity [4, 5]. The basic properties of *n*-heptane are given in table 1.6.

Table 1.6: Basic properties of *n*-heptane [19]

Molecular Formula	C <sub>7</sub> H <sub>16</sub>
Molar Mass	100.2 g/mol <sup>-1</sup>
Appearance	Colorless liquid
Density	684.0 kg/m <sup>3</sup> , liquid
Melting point	-90.6°C, 182.5 K
Boiling point	98.4°C, 371.6 K

### 1.3.3.3. Tetra Ethyl Lead (TEL)

Tetraethyl lead is an organometallic compound containing toxic metal lead and has been used in gasoline as an octane booster, since it is known as most effective antiknock element. Lead is stable and fuel-soluble in the form of lead alkyls [7]. Addition of 0.8 grams of tetraethyl lead to modern gasoline results in approximately 10 octane numbers increase in gasolines antiknock property. The use of leads as an antiknock agent has been prohibited in most countries due to its toxicity.

For octane number determination of fuel samples above 100 octane number, TEL is added to iso-octane according to a pre-defined empirical formula given in equation 1.4;

$$O.N._{(above\ 100)} = 100 + \frac{28.28(T)}{1.0 + 0.736(T) + [1.0 + 1.472(T) - 0.035216(T)^2]^{0.5}} \quad (1.4)$$

where, T = mL TEL per U.S. gal. in iso-octane, in addition, table 1.7 expresses the octane numbers for blends of TEL in iso-octane.

*Table 1.7: Octane numbers for blends of tetraethyl lead in iso-octane [4, 5]*

mL TEL per U.S. gal	Octane Number	mL TEL per U.S. gal	Octane Number
0.0	100.0	1.2	109.6
0.05	100.7	1.4	110.5
0.1	101.3	1.5	111.0
0.2	102.5	2.0	112.8
0.3	103.5	2.5	114.3
0.4	104.4	3.0	115.5
0.5	105.3	3.5	116.6
0.6	106.0	4.0	117.5
0.7	106.8	4.5	118.3
0.8	107.4	5.0	119.1
0.9	108.0	5.5	119.7
1.0	108.6	6.0	120.3

#### **1.4. Liquified Petroleum Gas (LPG) as a Fuel in Internal Combustion Engines**

LPG is mainly produced by gas extraction and liquefaction from the separator gas in a processing plant and consists of propane, propylene, butane, butylene, and small amounts of pentane, pentylene, as well as impurities such as unsaturated hydrocarbons (olefins) and possible contamination such as ammonia, acidic gases and sulfur.

The ratio of propane to butane and methyl-propane determines the fuel's gauge vapor pressure and minimum vaporization temperature which is particularly important in cold climates. LPG fuel is commonly used in heating appliances, cooking equipment and is a clean, non-toxic, high calorific value fuel.

The first attempt of LPG use as an SI engine fuel dates back to as early as 1930s at USA. However, the commercializing of LPG as an alternative fuel did not happen in that time due to lack of sufficient technology [15]. Nowadays, LPG is one of the most well-known alternative SI engine fuel because of its environmental and economic benefits.

##### **1.4.1. Liquified Petroleum Gas**

LPG, which can also be produced from natural gas, is a mixture of gases produced in petroleum refineries. After production, LPG is stored in liquid state, under critical pressure conditions for convenience and ease of handling [16]. LPG is at gaseous state at room temperature, but tends to condense when moderate pressure is applied. Since

LPG can evaporate to about 250 times its volume, large amount of energy can be packed, stored, transported and used in small containers. The volumetric ratios of components of LPG and their higher heating values are given in table 1.8.

*Table 1.8: Composition of LPG components and their higher heating values [16]*

Component	% by volume	HHV (MJ/kg)
Propane (C <sub>3</sub> H <sub>8</sub> )	60–85	50.4
Butane (C <sub>4</sub> H <sub>10</sub> )	14–38	49.6
Pentane (C <sub>5</sub> H <sub>12</sub> )	0–6	49.1
Isopentane (C <sub>5</sub> H <sub>12</sub> )	0–0.2	49.0
Cyclopentane (C <sub>5</sub> H <sub>12</sub> )	0–0.1	45.5
Ethylene (C <sub>2</sub> H <sub>4</sub> )	0–1.5	49.6
Others	0–2	—

LPG is denser than air and tends to settle down if released into air. In natural state, it is a non-toxic fuel, but an odorant called ethyl mercaptan [17] is added, for detecting any leakage in the tank or at any appliance utilizing it. The odor concentration varies according to the volume of LPG remained in the tank, since the container/tank contains both liquid and gaseous states of LPG.

LPG is mainly produced from Wet Natural Gas/Associated Gas or refinery operations. The ingredients of LPG differs according to production method. In the first phase, the LPG produced from wet natural gas fully consists of propane and butane which are saturated hydrocarbons. LPG which is derived from straight distillation process consists of saturated hydrocarbons (propane, n-butane and iso-butane).

Finally, LPG which is produced using both cracking and reforming processes includes some quantities of unsaturated carbons which are propylene and butylene in addition to saturated hydrocarbons.

#### **1.4.1.1. LPG Use as an Alternative Fuel**

As mentioned before, LPG is used as a fuel in cooking and heating appliances, and for lighting in rural areas [16]. On the other hand, LPG is a desirable source of fuel for SI engines because of its low air pollution and residue with high octane rating.

It was first utilized in an SI engine in 1930's. Since the environmental concerns and fuel crisis were not as viable as they are nowadays, LPG did not develop as an automobile fuel.

Another reason for LPG for becoming more popular than other alternative fuels is its unit price [18]. In addition, having high octane number, ability to store easily, lower emissions of CO, HC and CO<sub>2</sub> are the other advantages of LPG for being preferred as an alternative fuel for SI engines.

Nowadays, engines are either produced with LPG use compatibility or can be modified to utilize LPG such as dual fuel systems which are carburetor LPG systems, sequential LPG system and direct injection LPG systems. Such dual fuel systems require additional engine parts in order to store, inject or vaporize LPG. These additional parts can be listed as

- ⇒ LPG storage tank
- ⇒ Electronic cut-off valves
- ⇒ Regulator/vaporizer
- ⇒ Mainline flow adjuster
- ⇒ Mixer
- ⇒ Petrol delivery shut-off system
- ⇒ LPG/gasoline switch

In many countries, vehicles with LPG fuel are imposed less tax than the vehicles working with petrol or fuel-oil which enhances LPG consumption. On the other hand, in many European countries, high annual road taxes for automobiles using LPG fuel compensates lower taxes applied. Given these circumstances, propane becomes the third most widely used motor fuel, where more than 13 million vehicles were fueled with propane at 2008 and approximately 20 million tons of propane is used as vehicle fuel annually.

#### 1.4.1.2. Composition of LPG

LPG mainly consists of propane and butane but also can contain propylene, butylene and trace amount of other olefins. Table 1.9 shows the main properties of propane and butane.

*Table 1.9: Typical properties of commercial LPG gas components [16]*

Property	Propane	Butane
Relative density of gas (air = 1) at 288.8 K and 1 atm	1.90–2.10	1.40–1.55
Relative density at 288.8 K (water = 1)	0.57–0.58	0.50–0.51
Ratio of gas volume to liquid volume at 288.8 K and 1 atm	233	274
Boiling point at 273.2 K and 1 atm (K)	271	228
Flammable limits (% by volume in air)	1.8 to 9.0	2.2 to 10.0
Air required (m <sup>3</sup> ) for combustion to burn 1 m <sup>3</sup> of gas	30	24
Ignition temperature in air (K)	560	705
Maximum flame temperature in air (K)	2263.8	2251.5
Freezing point (K)	84.5	134.8
Critical temperature (K)	369.9	425.3
Critical press (bar)	42.5	38.0
Latent heat vaporization (kJ/kg)	358	372
Flammability limit (%)	2.2–9.5	1.8–8.5
Vapor pressure at specified maximum pressure (bars)		
Temperature (K)	243.2	—
	255.4	—
	273.2	1.93
	311.0	5.86
	318.2	6.89
	338.2	9.70

The composition of commercial LPG differs according to the region it is used and also manufacturers change the volumetric ratios of ingredient gases according to weather conditions.

#### 1.4.1.3. The Pros and Cons of LPG

In commercial use, LPG is preferred as an alternative fuel in SI engines due to its low unit price which make fuel costs per kilometer decrease. As well as its unit price advantage, more benefits of LPG be listed as;

- ⇒ LPG causes less air pollution, since CO, HC and CO<sub>2</sub> emissions are reduced [16, 20].

- ⇒ LPG does not dilute the engine lubricants since less solid residue occurs during combustion [16].
- ⇒ LPG has high octane rating, higher compression ratios are available. As the compression ratio increases, pressure and temperature of compression and combustion increases, thus mean effective pressure and efficiency increases. Increased compression ratio also allows LPG to work under lean conditions [20].
- ⇒ Since LPG burns with lower carbon build up and oil contamination, there occurs less wear at engine parts such as rings and bearings. In addition, having higher octane rating makes know originated engine wear decrease [16].
- ⇒ Engine runs smoother with LPG, due to its gaseous state [17].

On the other hand, there also exists some deficiencies of LPG usage on SI engine. Such disadvantages can be listed as;

- ⇒ LPG does not contain lead or any fuel additive like gasoline, thus wear rate of valves increases at some early LPG conversion engines. However, newer engines are designed with hardened valve seat materials [16].
- ⇒ LPG has a high octane and low cetane rating, thus LPG is unsuitable for CR engines [16].
- ⇒ LPG has higher ignition temperature than gasoline. If an engines ignition system is working properly, improper combustion may occur resulting stepping run of engine [16].
- ⇒ When LPG fuel system applied to a SI engine that normally designed for gasoline, the power output decreases since LPG needs higher compression ratios [20].
- ⇒ NO<sub>x</sub> formation increases [20].
- ⇒ Combustion stability decreases when A/F ratio is too lean [20].
- ⇒ Spark timing has to be advanced since LPG has a lower flame speed in contrast with gasoline [17].

In summary, LPG application to gasoline engines without increasing their compression ratio results in lower CO and HC emissions and fuel consumption with a slight decrease at power output. When compression ratio is increased for LPG



combustion, power output increases when compared with gasoline combustion and the fuel consumption and CO emission show further decrease.

### **1.5. Octane Testing of LPG**

Octane testing of SI engine fuels are conducted on Cooperative Fuel Research – CFR engines according to ASTM 2699 and ASTM 2700 standards which identify the research octane number and motor octane number methods, respectively. On the other hand, octane testing of LPG is carried out by *Near Infrared Spectroscopy* and *Gas Chromatography* methods. However, RON and MON ratings measured by NIR and GC methods are generally higher than the RON and MON ratings measured with CFR engines, since factors like temperature, load, etc. are not taken into consideration.

#### **1.5.1. Near Infrared Regression (NIR) Spectroscopy Method**

Infrared energy is defined as the electromagnetic energy molecular vibration. In addition, near, mid or far terms define the energy band where, near infrared defines a band between 0.78 to 2.50 microns, mid infrared defines a band between 2.50 to 40.0 microns and far infrared defines a band between 40.0 to 1000 microns [21].

In near IR spectroscopy, the information about the overtone and combination bands of C-H, O-H and NH fundamentals are provided from the NIR region of the electromagnetic spectrum. The given information refers to the chemical composition of the sample and both quantitative and qualitative analyses can be conducted according to this information.

Experimental results in literature proves that the quality control of LPG products can be handled with infrared system in a robust and cost effective way [22].

#### **1.5.2. Gas Chromatography (GC) Method**

Gas chromatography is an analytical separation technique for analyzing volatile substances in gas phase, and depends on the differential distribution of components of a mixture between a “*mobile bulk phase and a thin film stationary phase*” [22, 23]. In gas chromatography, the vaporized sample is the mobile phase, usually with a carrier gas such as nitrogen, which carries the molecules of the analyte through the heated column; and stationary phase is the liquid retained as a surface layer on a supporting medium.

The components of a LPG sample can be quantified with an accuracy of minimum of 1% with a modern chromatograph in a few minutes. On the other hand, gas chromatographs are large, expensive and fragile instruments that are not suitable for field usage [22].

## **CHAPTER 2**

### **LITERATURE SURVEY**

#### **2.1. LPG Combustion**

The design and analysis of industrial combustion devices is largely dependent on the level of understanding of the reacting flow field, chemical kinetics and chemistry-turbulence interaction. Problems such as engine knock, fuel auto ignition and pollutants in internal combustion engine sector or blow out, flashback and combustion instabilities for industrial combustors such as gas turbines have increased demand for better understanding of the combustion phenomena [24].

Besides conventional fuels such as natural gas or gasoline, some of these combustor designs need to be capable of utilizing coal derived gas (syngas), liquefied petroleum gas (LPG), liquefied natural gas (LNG) and other fuels such as biomass, etc. [25]. Among these alternative fuels, LPG serves as a clean fuel in heating appliances [26], automotive and vehicles (as auto-gas) [27, 28] as well as petrochemical feedstock for ethylene production (used in plastic and fabric materials) through hydrocarbon cracking process or for syngas production [29].

It is one of the most important alternative fossil fuel in the world having a considerable advantage in terms of combustion pollution, easier transportation and maintenance [30]. Nowadays, LPG is known to be used in over 17 million vehicles in many countries [1] including Turkey, where its application was legalized in 1995 [2].

### **2.1.1. Effects of Higher Hydrocarbons on LPG Combustion**

LPG is mainly produced by gas extraction and liquefaction from the separator gas in a processing plant and consists of propane, propylene, butane, butylene, small amounts of pentane, pentylene, as well as impurities such as unsaturated hydrocarbons (olefins) and possible contamination such as ammonia, acidic gases and sulfur [31]. The ratio of propane to butane and methyl-propane determines the fuel's gauge vapor pressure and minimum vaporization temperature which is particularly important in cold climates.

Even though study of the effect of LPG composition and impurities on its combustion characteristics and emission performance has attracted attention in the research community, there are quantitatively a limited number of works reported in the literature in this regard. The level of olefins (i.e. propene, 1-butene and isobutene) present in LPG is important in industrial applications where a particularly clean and soot-free flame is required [32].

The presence of these olefins in the LPG is believed to have an undesirable effect on the combustion mainly due to production of smoke, which is proportional to the mole percent of olefin content [33]. There are, therefore, several manufacturing processes in the chemical industry which are used to saturate or separate these olefins to achieve the LPG quality pertaining to the legislations for environmental aspects.

In the study by Gurulakshmanan and his colleagues [33], the saturation of the LPG olefin content is numerically simulated using the modeling software HYSYS. The method described in this paper was hydrogenation of LPG streams in a hydrogenation reactor to convert unsaturated hydrocarbons to saturated ones. It was shown that approx. 15 % decrease in the olefin content was possible by hydrogenation reaction and hydrogen regeneration.

LPG is the major energy source for cooking and heating in urban households in Mexico City. In a study by Gamas et al [34] on hydrocarbon emissions caused by consumption of LPG in Mexico City; a number of commercial LPG samples available to consumers were analyzed with average olefin concentrations as high as 5%. It was found that a high olefin content in the LPG mixture results in ozone-forming caused by photo-chemically reactive combustion exhaust gases.

The olefinic hydrocarbons present in LPG, contribute to the production of aldehydes in a reactive atmosphere by means of chemical chain reactions. On the basis of the results presented in this paper, an official environmental standard was issued limiting the concentration of olefins in the formulation of LPG in Mexico City. Some reports in the literature claim that higher olefins in LPG used as auto-gas tend to increase combustion chamber deposits which can lead to clogging of the engine [35].

There are very few studies in the literature and further investigations are required in order to better understand the effect of such impurities on LPG combustion. One way to do this is to develop an experimental combustion setup to study the effect of different fuel compositions and additive content on the combustion and emission characteristics of the fuel.

#### **2.1.2. Experimental Studies on LPG Flame Characteristics**

One of the most important aspects in studying the combustion characteristics of fuels is the burning velocity of the flame. Accurate determination of the laminar burning velocity of combustible mixtures has received particular attention as being:

- a) A fundamental property of a fuel/air mixture,
- b) Having important role in studying flame stabilization,
- c) Use in determination of the rate of energy released during combustion and
- d) As a main parameter that influences the performance of the combustor device and emissions.

It is also considered as a property that affects the ignition delay, ignition energy and flame quenching of the combustible mixture. Calibration and validation of the chemical reaction mechanisms for use in wide ranges in different combustion simulations and modeling is also highly related to the study of laminar flame velocity of the fuel [36, 37].

There are different methods used in the literature to determine the laminar burning velocity which can be classified into two main categories:

- The stationary methods, such as the Bunsen burners and stagnation plates
- The propagating methods such as spherical or cylindrical combustion bombs

Utilization of a constant volume combustion chamber such as a combustion bombs for laminar flame speed calculation is often the selected method in the combustion

research community since it requires smaller amounts of fuel compared to other methods and also allows best control over the initial conditions and mixture composition.

Combustion bomb also enables the possibility of investigating combustion of fuel under elevated pressures, typical of internal combustion engines and industrial combustors [37].

In the bomb method, the quiescent combustible mixture is normally ignited at the center of a rigid volume. Simultaneous records of the rising pressure and photography of the growing spheres of flame are obtained via optical access to the chamber. The expansion of the burned gases in a rigid volume causes both pressure and temperature of the unburned gas to increase.

This progressive change in the initial conditions of the mixture makes it very difficult to propose a single equation for the calculation of burning velocity. Therefore, it is necessary to establish accurate relations between burning velocity and the pressure rise inside the bomb.

Huzayyin and coworkers at Benha University in Egypt performed an extensive study to map the variations of the laminar burning velocity of LPG/air and propane/air mixtures over wide ranges of equivalence ratios, initial temperatures and pressures [37]. The combustion bomb used was a closed cylindrical chamber that could withstand an internal pressure up to 90 MPa, had an internal diameter of 144.5 mm and length of 150 mm. Figure 2.1 shows the layout of the experimental setup in this work.

To fulfill greater filling accuracy and repeatability, the combustible mixture preparation was performed in a separate cylindrical vessel. An external electrical heating circuit was incorporated at the outside surface of the bomb to facilitate uniform heating of the mixture within the bomb to the desired initial temperature of the test. The mixture was ignited at the center of the bomb by electrodes. The ignition energy was supplied from a capacitive circuit with precise adjustment of the minimum ignition energy.

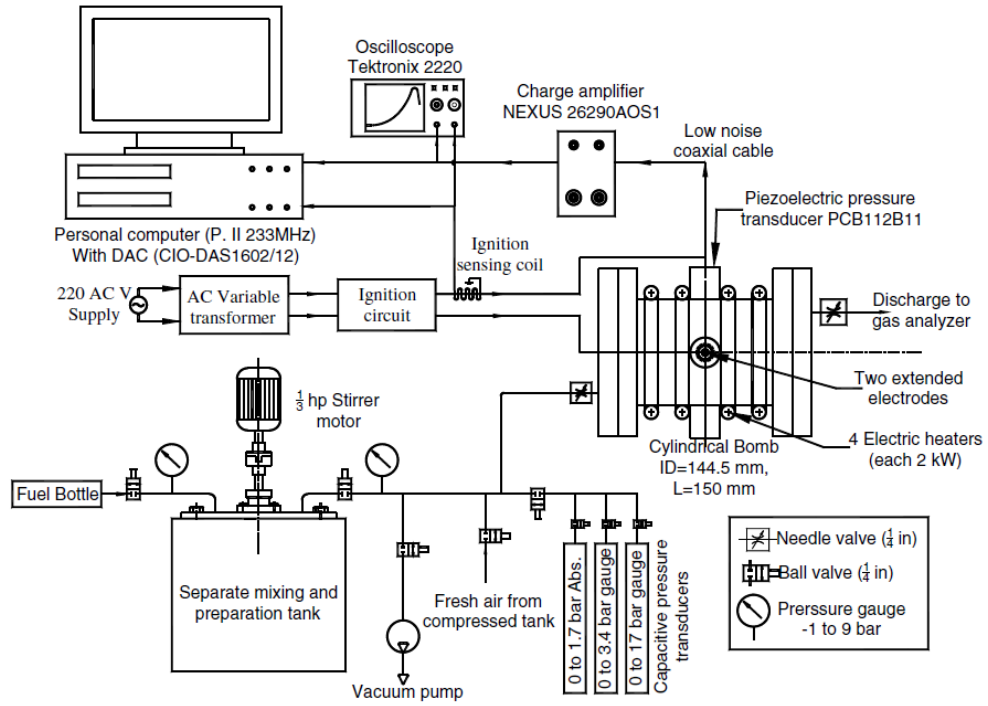


Figure 2.1: Experimental setup of Huzayyin et al [37]

Modified thermodynamic models were used to determine the laminar burning velocity of LPG fuel using acquired experimental data. They concluded that modified model of Rallis with the assumption of uniform gas distribution and ignoring the pressure gradient through the unburned mixture, give the best estimate for the determination of the laminar burning velocity under their experimental conditions.

At lower initial pressures, the maximum combustion pressure was higher for propane than that for LPG, while at elevated pressures, this value was higher for LPG. Maximum laminar flame velocity for propane was nearly 455 mm/s at equivalence ratio of 1.1, which was slightly higher than that for LPG of approximate 432 mm/s at equivalence ratio of 1.4. This was attributed to the differences in the chain-branching and the recombination reaction mechanisms in the LPG and propane combustion.

Figure 2.2 shows the effect of mixture preheating on the pressure record and pressure rise rate for LPG–air mixtures at the specified conditions. It could be seen that an increase in initial temperature decreased the ignition delay while also decreasing the maximum pressure owing to lower density of the unburned mixture.

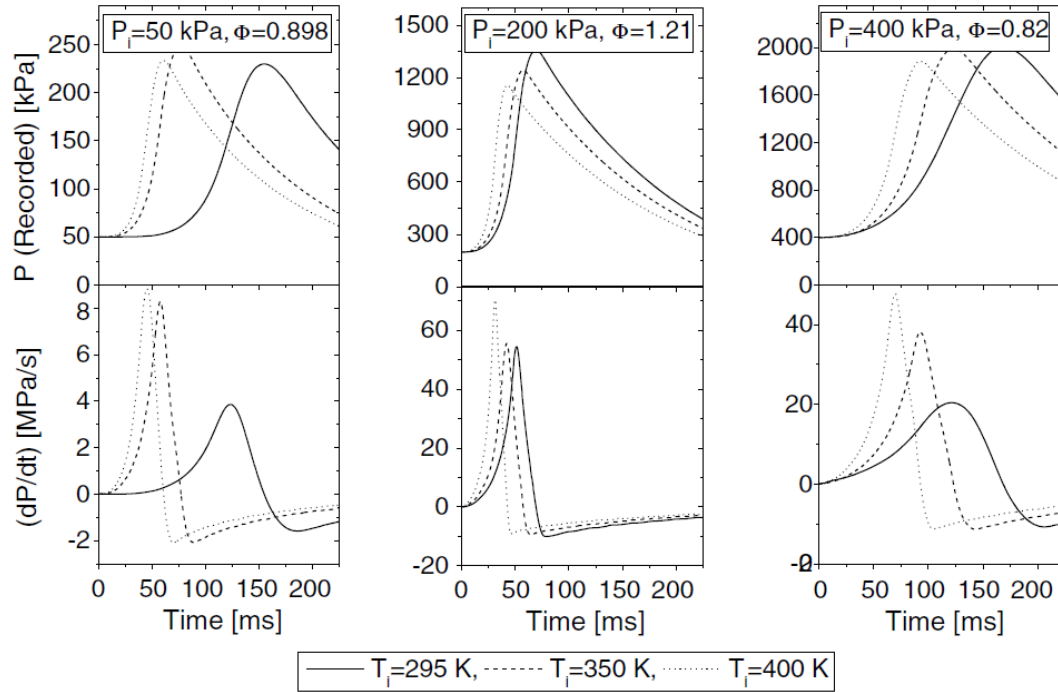


Figure 2.2: Samples of the preheat temperature effect on the pressure record and pressure rise rate for LPG–air mixtures at the specified conditions in [37]

It was also concluded that as initial mixture pressure increases, laminar burning velocity decrease. The authors also introduced equations for maximum pressure and laminar flame speed based on equivalence ratio, initial pressure and temperature.

In a joint study with Texas A&M University, Yash et al from Georgia Institute of Technology investigated the laminar flame speed of pure methane, methane/propane and methane/ethane mixtures at elevated pressures (up to 10 bars) using both Bunsen burner method and spherical propagating flame method [38]. They used helium as diluent to increase the stability of the experimental flames at high pressure. For the spherical flame speed approach, they employed a constant volume combustion bomb provided by Texas A&M University (TAMU facility). A Schlieren system was used to monitor the expansion of the flame in the experiments as shown in figure 2.3. The images were recorded using a high-speed camera.



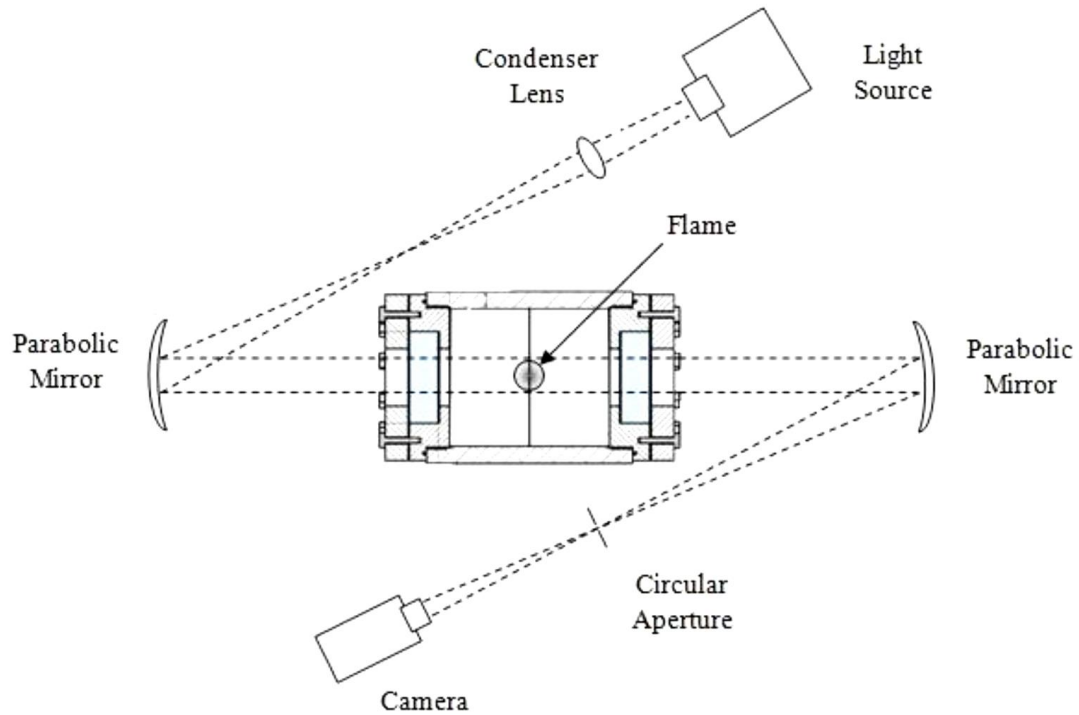


Figure 2.3: Optical setup for Schlieren system in [38]

In the Bunsen burner method, they utilized a laminar jet flame and measured the burned flame area using imaging of the chemiluminescence emissions (GT facility). This approach was said to provide access to higher temperatures than typically attainable in the spherical flame approach. The axisymmetric jet flames were produced using contoured laminar nozzle. Optical access for flame imaging was provided by quartz windows.

Broadband chemiluminescence images of the Bunsen flame were acquired using a 16-bit intensified CCD camera attached with UV lens. The camera was sensitive in the visible and ultraviolet range and capable of capturing  $\text{CH}^*$ ,  $\text{OH}^*$  and  $\text{CO}_2^*$  chemiluminescence from the flame. The schematics of the experimental Bunsen burner setup can be seen in figure 2.4. The chemiluminescence images were analyzed to determine the reaction zone location with a gradient-based edge detection algorithm.

In this algorithm, the inner edge of the reaction zone for both the left and right half images are found from which the reaction zone area are averaged after 50 realizations to determine the flame area at each operating condition. The flame speed is then calculated based on flame area and volumetric flow rate of the reactants.

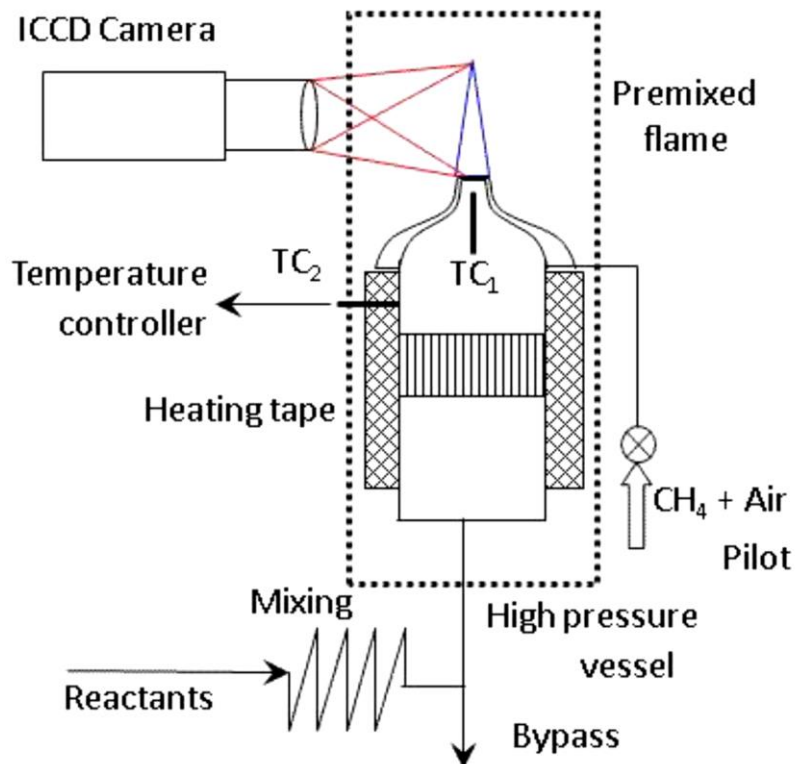


Figure 2.4: Bunsen burner experimental setup in [38]

A significant result of this study was that the effect of mixture composition on flame speed was well captured by the author's previously developed chemical kinetics mechanism over wide ranges of initial pressure and temperature. The results also showed that even small increases in initial temperature could produce measurably higher flame speeds.

Figure 2.5 indicates the effect of blending ratio for the helium-diluted flames by showing the effect of decreasing the methane concentration on flame speed for mixtures of both methane-ethane and methane-propane. The data from both facilities show a decrease in flame speed with increasing methane concentration from 60–80% at both low and high temperatures and at 5 and 10 atm.

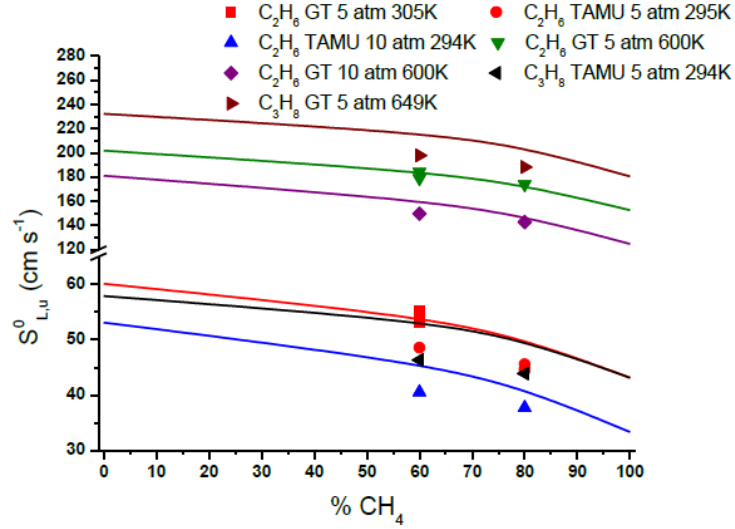


Figure 2.5: Effect of mixture composition on laminar flame speed results for methane-ethane and methane-propane mixtures with  $O_2 / He$  (1:6) diluent,  $P = 5$  and 10 atm, unburned mixture temperature  $\approx 300$  and 600 K, equivalence ratio at 1.0 taken in the two facilities. Points are experimental results, lines are model predictions [38]

Laminar flame speed of propane-air mixtures was also experimentally investigated by Zhao et al at Princeton University [39] over an extensive range of equivalence ratios at atmospheric pressure. They accounted for the effects of exhaust gas dilution on the flame characteristic by addition of  $N_2$ .

The experiments employed the stagnation jet-wall flame configuration in which the flow velocity was obtained by using Particle Image Velocimetry (PIV) as shown in figure 2.6. The experimental setup used a stagnation plate under which a premixed flame burner is located. The premixed reactant flowed upward from a nozzle situated at the center of the burner surface and impinging vertically onto a ceramic flat plate. The airflow first goes into a seeder to pick up particles for the PIV, and then the flow was preheated by using an inline heater. Finally the flow is mixed with gaseous fuel in a turbulent mixer. The entire burner system was housed within a cylindrical chamber to contain exhaust gases. Three optical windows in the chamber wall are purged with preheated  $N_2$  to keep the windows clear of pollutants and condensation.

The PIV laser beam was shaped into a thin light sheet using cylindrical and spherical lenses. The images at two different times were recorded and analyzed using an autocorrelation code.

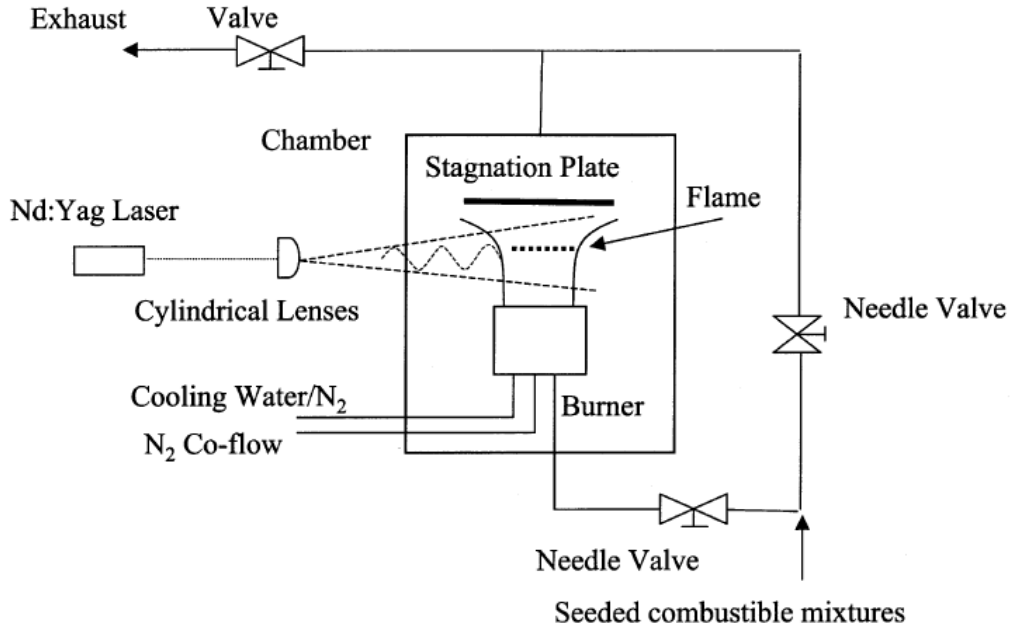


Figure 2.6: Schematic diagram of experimental setup in [39]

The results showed that a quasi-linear relationship exists between the laminar flame speed and the dilution ratio, contrary to the nonlinear correlations suggested elsewhere as shown in figure 2.7.

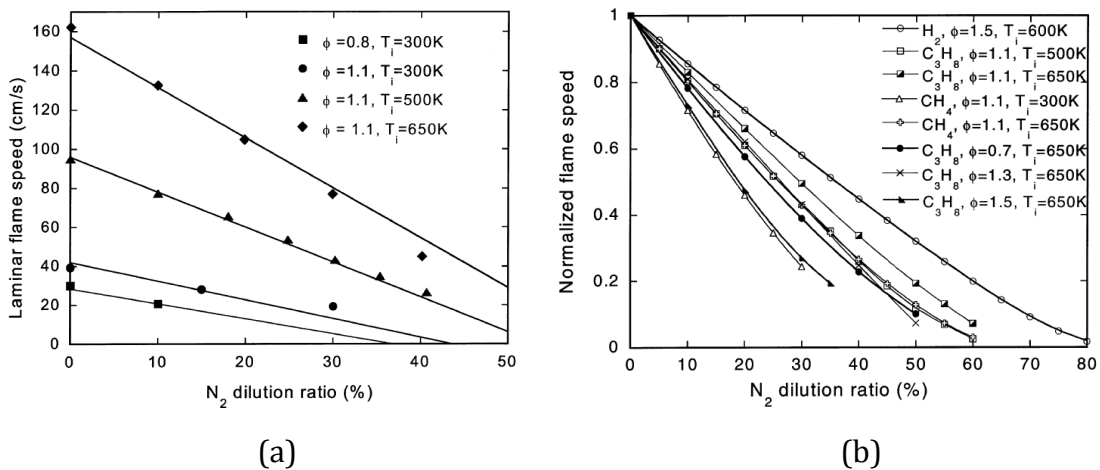


Figure 2.7: Variation of laminar flame speed with N<sub>2</sub> dilution at different conditions [39] (a) Propane (b) Various Fuels

Lee and Ryu [40] from Hunyang University South Korea investigated the flame propagation and combustion characteristics of LPG using a constant volume combustion chamber (CVCC) with a port injection as in a heavy duty engine. For this purpose, they used a single cylinder engine with a displacement volume of 1858.2 cm<sup>3</sup>.

Propane was used as a suitable surrogate to LPG fuel. The air/fuel mixture was prepared at a pre-mixer as shown in figure 2.8. Both the laser deflection method (LDM) and the high-speed Schlieren photography method were employed to measure the flame propagation speed of LPG fuel.

Figure 2.9 shows the optical system used in this work to investigate the flame propagation in the CVCC. The system was comprised of a He–Ne laser, a beam splitter and photodiodes. The beam splitter, composed of a full reflection mirror and two half-reflection mirrors, divides the single laser beam into three beams. Each beam then passes horizontally through an optical window installed at the CVCC, where it is accurately focused on the control volume by a beam translator.

The objective of using the LDM method in this work was to evaluate its potential as an alternative to a cost-prohibitive high speed camera. Figure 2.10 shows the positions of the said photodiode and an example of signals detected by the photodiodes in the paper. The LDM method uses the time as the flame front passes each laser beam to measure the flame propagation speed between two beams.

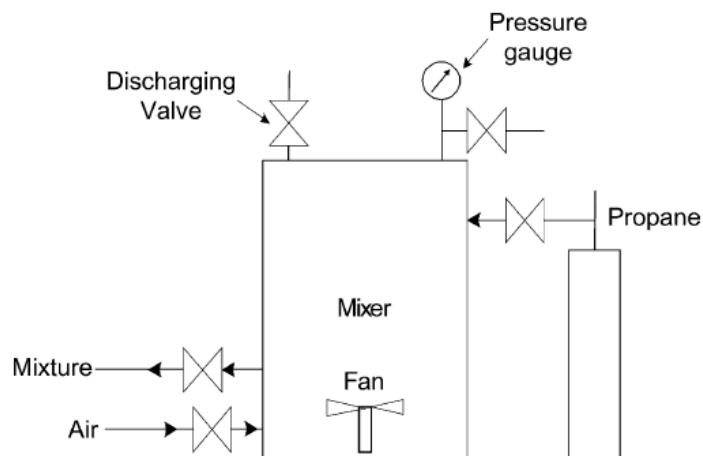


*Figure 2.8: Air/fuel pre-mixer in [40]*

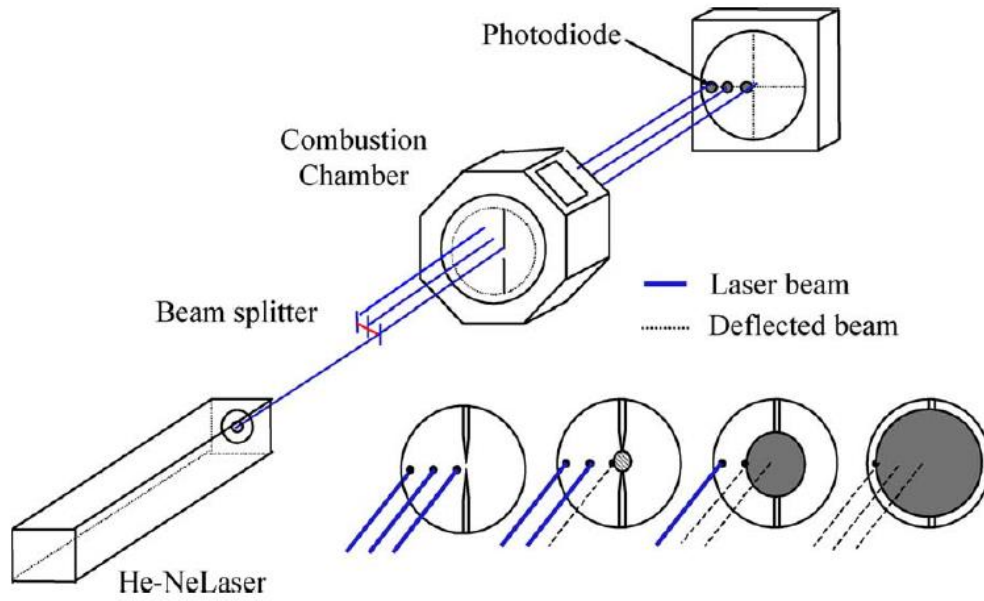


Figure 2.9: Schematic diagram of flame propagation speed detection system in [40]

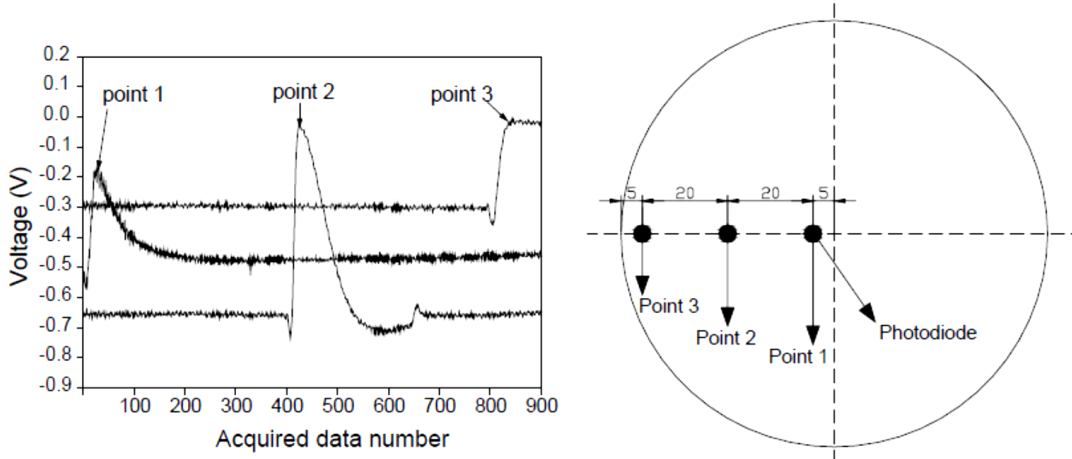


Figure 2.10: Position and signal of photodiode [40]

To compare the LPG combustion characteristics in the CVCC with that of a real engine, a single cylinder liquid injection type heavy duty LPLi engine was specially manufactured with the same displacement volume as in the CVCC and a compression ratio of 10.

The experimental results indicated that the laser deflection method showed the measuring accuracy of this method to be less than 5% when compared with the result of the high-speed camera as shown in figure 2.11. It was shown that the flame propagation reached a maximum speed at the stoichiometric equivalence ratio, regardless of operating conditions.

In addition, both the combustion duration of a laminar flame in the CVCC and the combustion duration of a turbulent flame in a real LPLi engine were proportional to the initial unburned mixture pressure.

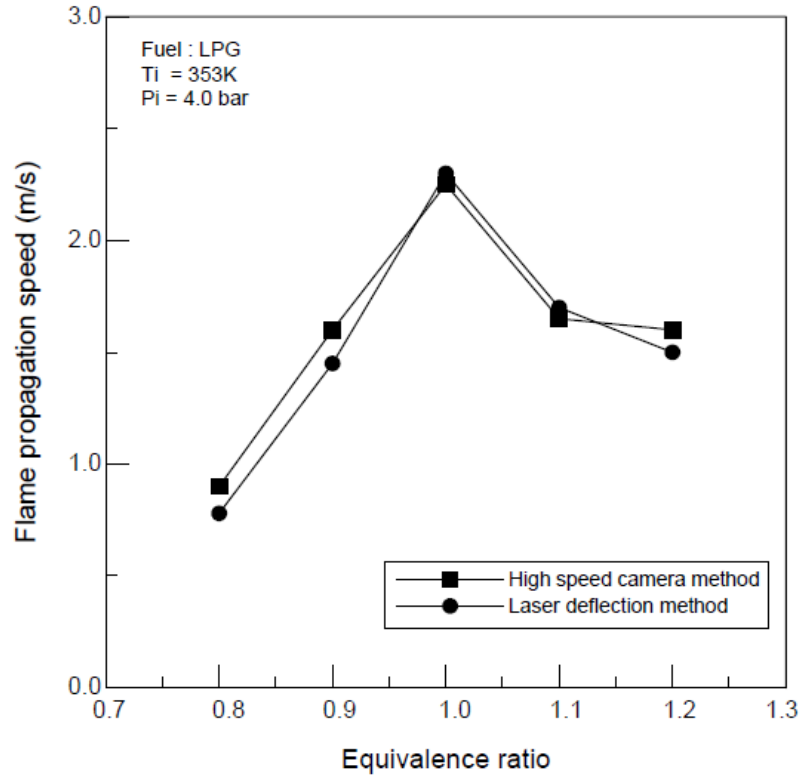


Figure 2.11: Comparison of flame propagation speed obtained by LDM method and the high speed camera method [40]

In other studies, Hochgreb, et al [41] investigated the effect of fire suppressant addition as inhibitors to laminar flame speed of a fuel in terms of pressure and temperature of unburned mixture using a laminar combustion bomb. In order to do so, the addition of  $CF_3H$  and  $C_2F_6$  on propane/air mixture was studied and the preliminary results showed little reduction in the burning rate of propane by adding 1%  $CF_3H$ , however, an increase to 2% resulted in a 25% reduction in the burning rate of the fuel.

### **2.1.3. Experimental Studies on Syngas Flame Characteristics**

The effect of cylindrical bomb geometry on the evolution of outwardly propagating flames and the determination of laminar flame speeds was investigated experimentally and theoretically by Burke et al [42] at Princeton University. The idea for this study was to show if the cylindrical chamber boundary modifies the propagation rate of the flame through the interaction of the wall with the flow induced by thermal expansion across the flame.

It is believed that such confinements can result in nonzero burned gas velocities, which in turn may lead to significant errors in flame speeds calculated using the conventional assumptions, especially for large flame radii. To remedy this, a methodology was proposed in this study to estimate the effect of nonzero burned gas velocities on the measured flame speed in cylindrical chambers.

Experiments were conducted on hydrogen-air, syngas-air and methane-air mixtures in a dual-chambered high-pressure combustion apparatus as shown in figure 2.12. The chamber consisted of two concentric cylindrical vessels of inner diameters 10cm and 28 cm. The iron plates provided a seal between chambers for pressure differences between outer and inner chambers greater than 0.3 atm. The inner vessel volume was smaller than that the outer vessel which resulted in small total pressure increase after combustion.

This ensured a nearly constant-pressure experiment and also operational safety for experiments conducted at high initial unburned gas pressures. Schlieren photography method was also utilized for imaging the flame propagation. A high-speed digital video camera with  $4\ \mu\text{s}$  shutter speed and frame rates of 8000 to 24,000 fps was used to record images of the propagating flames.



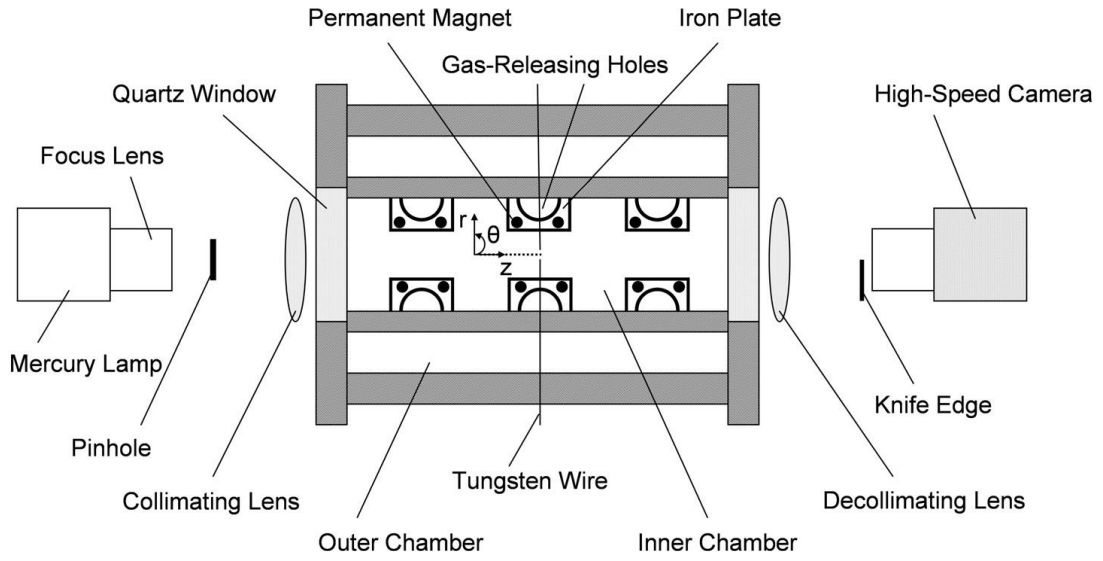


Figure 2.12: Diagram of experimental apparatus for [42]

Experiments indicated that the effect of confinement can be neglected for flame radii less than 0.3 times the wall radius while still achieving acceptable accuracy (within 3%) as can be seen in figure 2.13. The methodology was applied to correct the flame speed calculations for nonzero burned gas speeds.

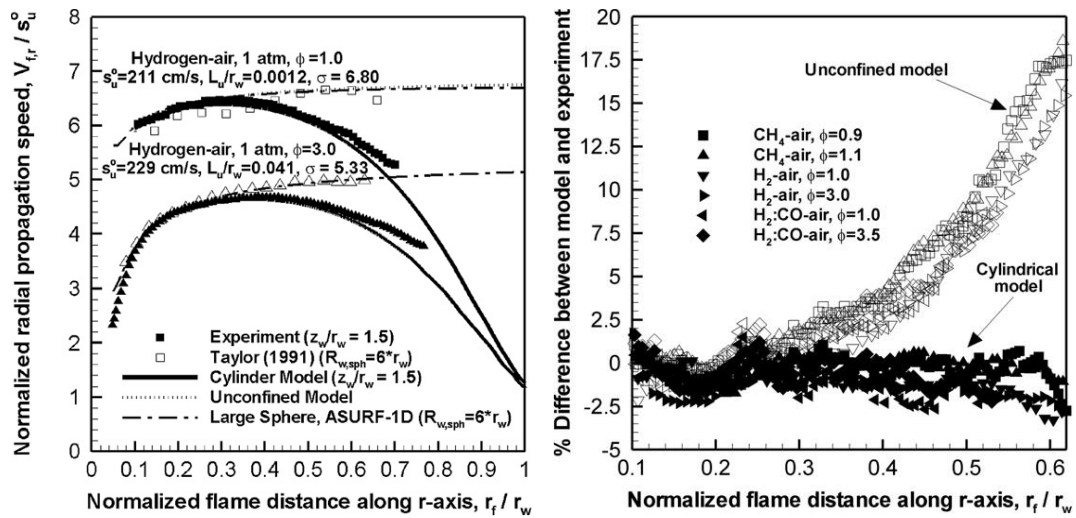


Figure 2.13: Comparison of experimental traces with model results for flames in a small cylindrical chamber and a large spherical chamber (left) and percent difference between models and experiment for a variety of mixtures for confined and un-confined models (right) [42]

It was shown that under a proposed scaling, the burned gas speed could be well approximated as a function of only flame radius for a given chamber geometry meaning that the correction function need only be determined once for an apparatus and then it can be used for any mixture.

It was observed that calculation of flame speed neglecting the confinement on could lead to 15-20% lower measurements. It was also recommended that for cylindrical chambers, data analysis should be restricted to flame radii less than 0.3 times the wall radius or a flow correction should be employed to account for the burned gas motions. Santner et al [43] studied the effect of water vapor addition on the burning rates of hydrogen-air and syngas-air and ethylene-air mixtures at equivalence ratio of 0.85, within pressure range of 1 atm to 10 atm and at flame temperatures between 1600 K and 1800 K using spherical flames in a nearly constant pressure combustion bomb. Experiments were conducted in a high pressure constant volume heated spherical bomb as shown in figure 2.14. The chamber had an inner diameter of 20 cm which allowed for a relatively large range of data that is minimally affected by the confinement induced fluid motion described in the previous study by Burke et al [39]. A magnetically assisted passive pressure release system was used to release the high pressure generated after ignition and quench the flame. The chamber was connected to a nitrogen tank to maintain the pressure within safe limits once it rises above a specific limit. For photography, a high speed Schlieren system was again utilized in this study to image the flame propagation.

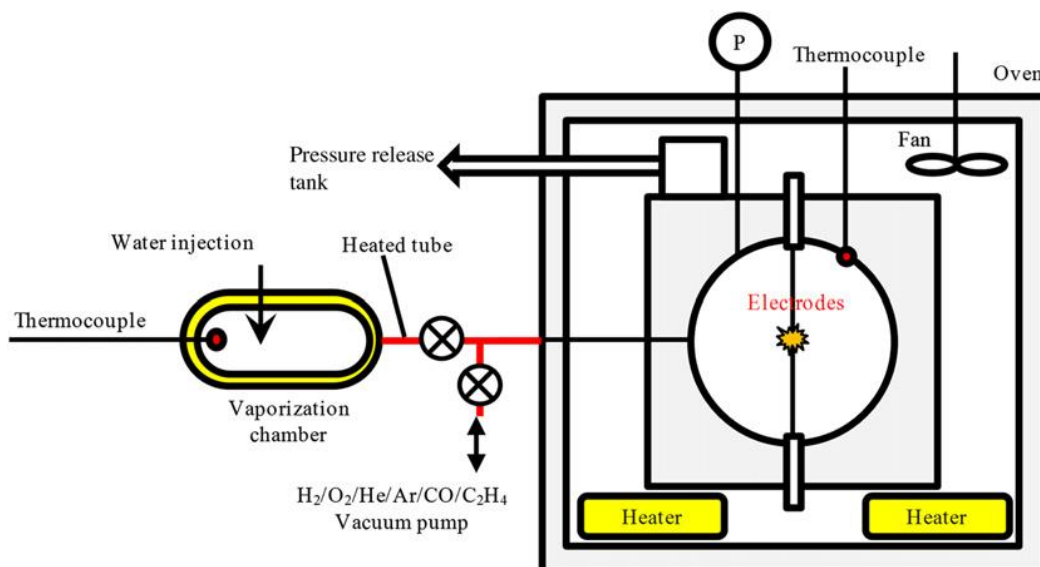


Figure 2.14: Experimental setup [43]

Before filling the combustion chamber, deionized liquid water was vaporized in a separate vaporization chamber. Results showed that water vapor addition causes a monotonic decrease in mass burning rate and the inhibitory effect increases with pressure.

Also, water vapor dilution was found to reduce the total radical pool and shift the reaction zone of hydrogen flames to a narrow high temperature region; however these effects were not observed for ethylene flames. These results can also be seen in figure 2.15 below.

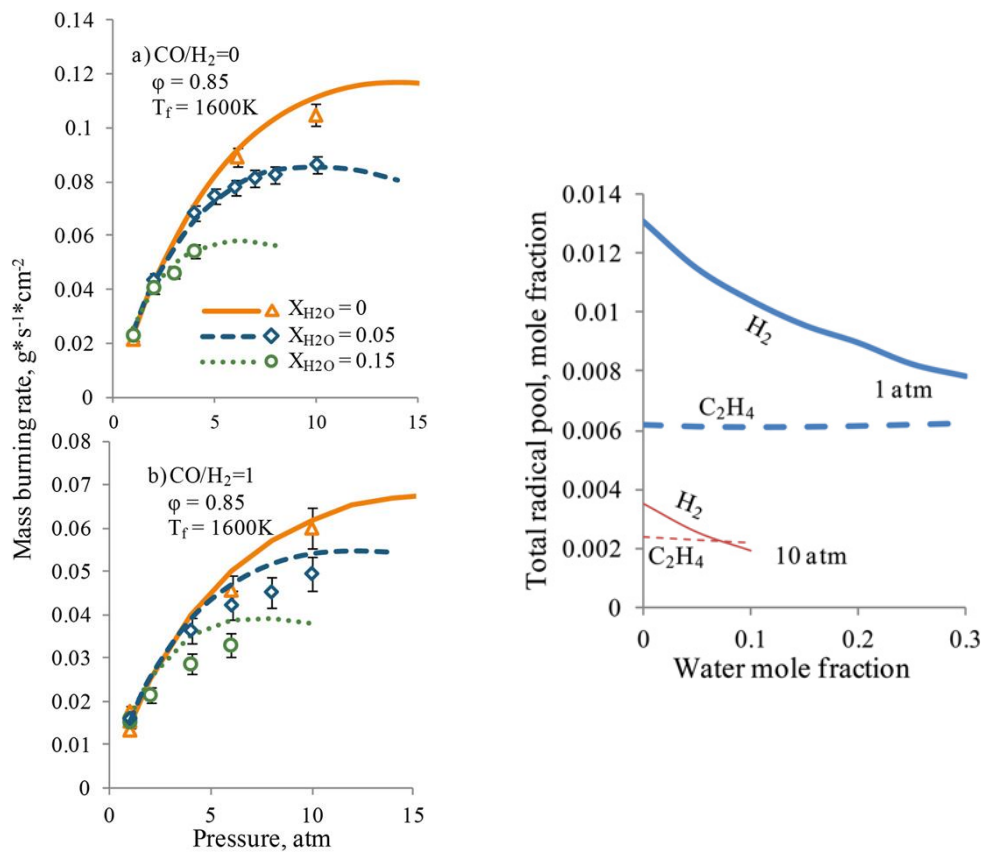


Figure 2.15: Pressure dependence of the mass burning rate for (a) hydrogen flame and (b) syngas flame (left) and effect of water mole fraction on radical pool formation in hydrogen and ethylene flames (right) [43]

Premixed laminar flame speeds of syngas mixtures have also been studied by Bouvet et al [44, 45] using straight Bunsen type and nuzzle burner at Centre National de la Recherche Scientifique (CNRS) combustion group. The experimental apparatus is shown in figures 2.16 and 2.17 and the burners are magnified in figure 2.18.

A wide range of equivalence ratios and mixture compositions were considered and flame speed correlation scheme was established for lean syngas flames. As it can be seen on the figure, the  $H_2/CO/Air$  gases were initially stored in separated tanks. A mixing section allowed a rapid mixing of the reactants prior to injection into the burner.

A nominal burner length of 900mm was chosen to ensure a fully developed laminar flow at the burner rim. A Z-type two-mirror Schlieren system was arranged as shown in figure 2.8 as the diagnostic system in the study. The top of the burner was placed in the middle of the test region defined by the parallel beam formed between two spherical mirrors.  $OH^*$  chemiluminescence images were recorded with an intensified ICCD camera.

A horizontal knife edge was used to reduce the intensity from the base of the flame and make its tip more visible. This method substantially improved the trace of the flame reaction zone boundaries and thus the laminar flame speed computations. Two methodologies were used in their studies in calculation of flame speed, namely, the flame surface area and flame cone angle approach which are respectively based on  $OH^*$  chemiluminescence and Schlieren imaging techniques.

In the flame surface area averaging method, a FORTRAN program was used to process the recorded images to provide the 2-D boundaries of the flames, based on the maximum emission of  $OH^*$  for area calculation.

The second measurement approach adopted was the flame cone angle methodology applied to Schlieren images of the studied flames. This approach was particularly convenient for flames displaying straight-sided cones and required the use of aerodynamically contoured nozzles.

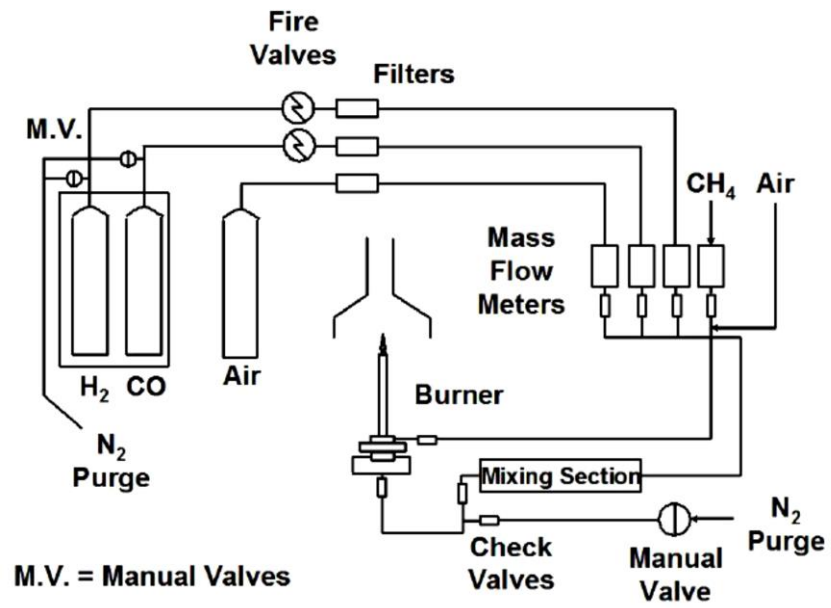


Figure 2.16: Experimental setup [44, 45]

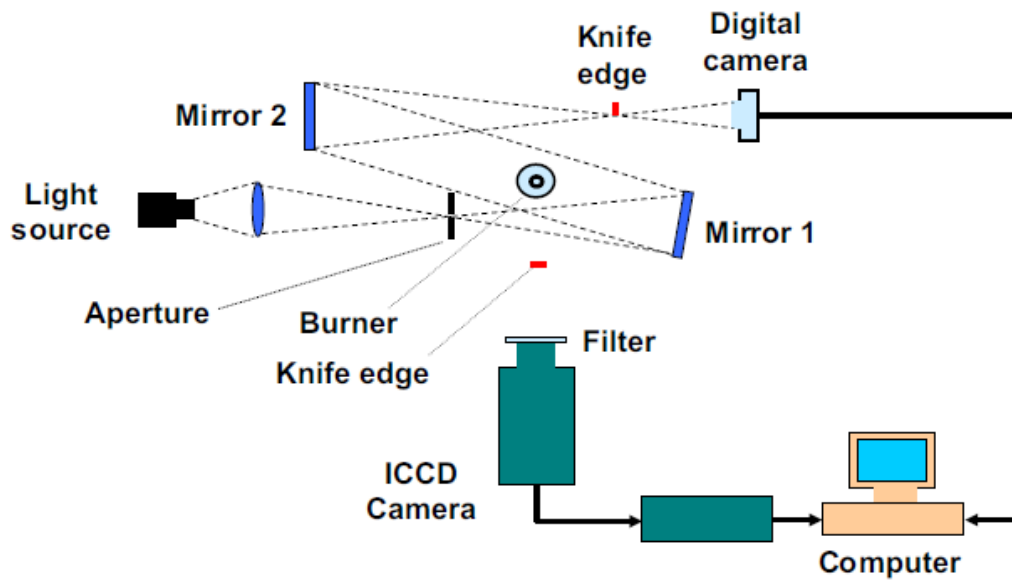
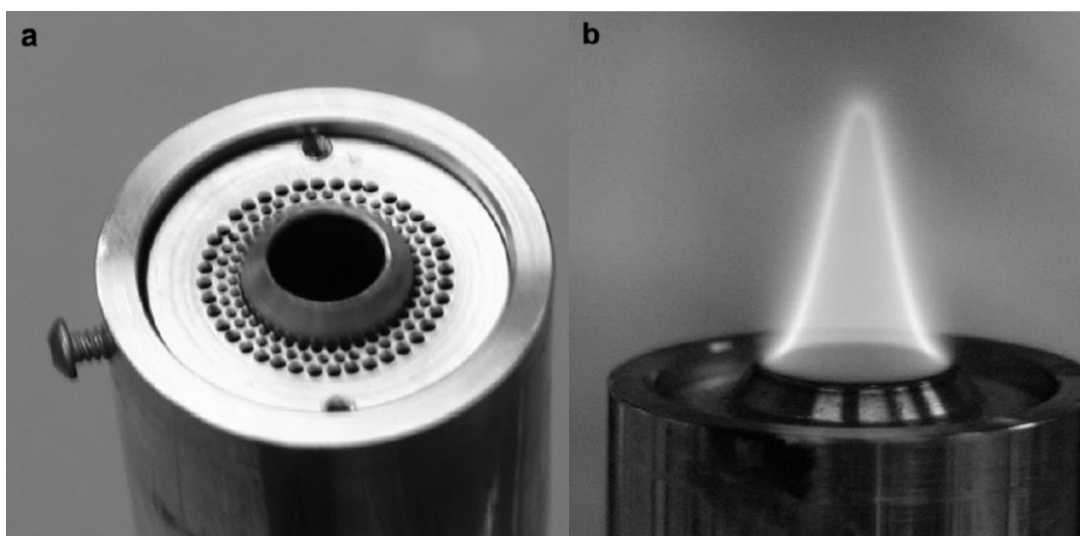


Figure 2.17: Diagnostics setup [44, 45]



*Figure 2.18: The straight burner setup [44, 45]: (a) Burner exit with sharp edge and perforated plate for the pilot flame tests, (b) Syngas conical flame stabilized with methane/air pilot flame*

Results showed a very good agreement with predictions calculated with recent  $H_2/CO$  chemical kinetic mechanisms. The flame surface area methodology based on the maximum  $OH^*$  chemiluminescence emission showed to yield to an overall good accuracy when compared to the available experimental data for  $H_2$ /air mixtures.

The flame cone angle methodology performed on Schlieren images was found to give systematically higher results. A correlation for the syngas flame was also proposed. Also, large burner diameters were recommended for laminar flame speed studies using the flame surface area methodology.

Later in 2011, Bouvet and coworkers at CRNS carried out the laminar flame speed measurements of various syngas blends at atmospheric pressure and ambient temperature [46]. In their study, they used spherically expanding flame configurations and both linear and non-linear processing methodologies.

The combustion vessel used was a stainless steel cylindrical chamber at 160 mm inner diameter and 300 mm height. Figure 2.19 depicts the experimental setup used in this study. Two sharpened-edge tungsten electrodes linked to a capacitive discharge ignition system were used to provide the ignition energy.

The volumes of each mixture component of the syngas were injected in the combustion. The pressure and the temperature inside the chamber were measured using a piezoelectric transducer and a type K thermocouple. The optical access to the chamber was provided through two opposite portholes. An argon ion laser with two planoconvex lenses was used to create the parallel light beam that crosses the combustion chamber. Images were recorded using a high speed camera.

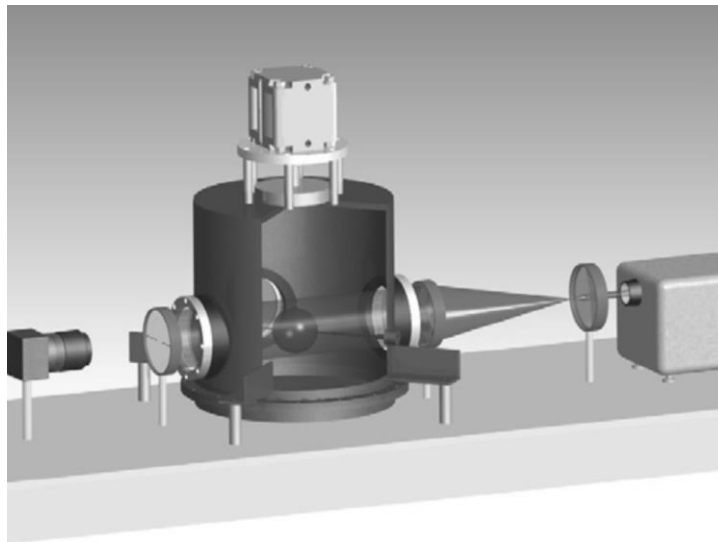


*Figure 2.19: Experimental setup [46]*

As can be seen in figure 2.23, there was a very good agreement between model predictions using chemical kinetic mechanisms and measurements at a wide range of equivalence ratios. However, it is shown that the measurements are best predicted by the mechanism by Li et al from Princeton University [47].

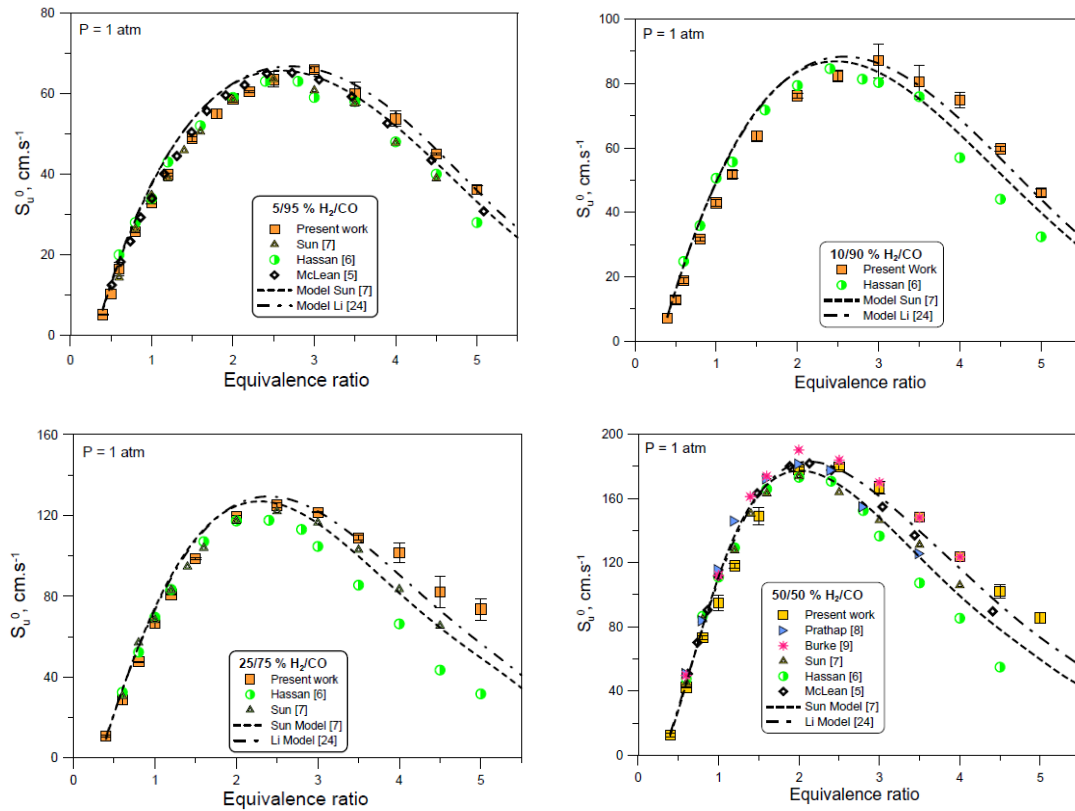


Figure 2.20: Experimental and predicted laminar flame speed variation with equivalence ratio at different syngas composition [46]

## 2.2. LPG Octane Number Measurement

At the present time, LPG is considered as one of the most important alternative fuel due its low unit price and lower emissions in contrast to gasoline. Due to this increase in demand for a viable alternative fuel, there are numerous studies regarding combustion, emissions, flame propagation, etc. of LPG in the literature, however, the octane number verification of LPG using CFR engine has received very little attention as is a new field of study and there exists only a few studies about this issue.

Morganti et al. presented an experimental study for measuring the research (RON) and motor (MON) octane numbers of LPG [48]. A method which is consistent to active research and motor octane number measuring methods, which are ASTM 2699 and ASTM 2700 respectively, was used during experiments, and a large set of RON and MON data for pure propane, propylene, iso-butane, n-butane and; binary, ternary and their quaternary mixtures were obtained.



For predicting octane number of gaseous fuel compositions, regression models for RON and MON were developed as follows [24],

$$RON = 109.4 X_1 + 100.2X_2 + 93.5X_3 + 100.1X_4 - 5.55X_1X_2 - 4.31X_1X_3 + 2.64X_2X_3 + 4.94X_2X_4 + 59.48X_1X_2^2X_3 + 44.15X_1X_2^2X_4 \quad (2.1)$$

$$MON = 96.3 X_1 + 83.3X_2 + 89.0X_3 + 96.8X_4 - 2.79X_1X_4 - 3.53X_2X_3 + 6.26X_2X_4 \quad (2.2)$$

Where,

$X_1$ : mole fraction of propane in mixture,

$X_2$ : mole fraction of propylene in mixture,

$X_3$  mole fraction of n-butane in mixture,

$X_4$ : mole fraction of iso-butane in mixture, and the sum of  $X_1$ ,  $X_2$ ,  $X_3$  and  $X_4$  are supposed to be unity.

The standard error (SE) between the predicted and experimented octane numbers were calculated according to the formula below,

$$SE = \sqrt{\sum \frac{(ON_{measured} - ON_{predicted})^2}{N}} \quad (2.3)$$

The calculated octane numbers according to regression models were both used for predicting the octane number of the sample fuel, and also for comparing with the experimental results [48]. In addition, the results were first compared with the RON and MON values of fuels with the equivalent data found in literature and then an empirical model was validated for the RON and MON value of LPG according to its composition [48]. In other works, the auto ignition of  $C_3/C_4$  hydrocarbon mixtures in a CFR octane rating engine were investigated and the gaseous fuel octane ratings measured using a CFR engine [18]. Morganti et al. acquired the in-cylinder pressure data for both autoigniting and non-autoigniting conditions.

### **2.3. Aim of the Study**

By reference to the literature survey carried out in the previous section, it can be concluded that there are a limited number of studies in the combustion research database regarding the effect of LPG impurities and composition on the combustion and emissions.

The importance of LPG as an alternative, low cost, clean fuel used in combustion systems and internal combustion engines is thoroughly demonstrated which means that further investigations are required in better understanding of the LPG combustion characteristics, control of combustion and emissions and also its utilization in different applications.

As the usage of LPG fuel is getting wider for automobile industry, the octane rating of LPG is getting more important. However unlike liquid fuels, LPG octane number used to be measured with chemical methods, i.e. gas chromatography and near infrared regression methods due to its gaseous state.

The chemical methods however, do not simulate the fuels characteristics for road conditions, for instance parameters like engine speed, ambient temperature, load etc. are not taken into consideration. For this reason knocking characteristics of LPG needs to be reviewed using CFR engines, when the potential and economic benefits of LPG are taken into consideration.

The aim of this thesis is to modify a variable compression ratio CFR engine in order to measure the octane number of LPG fuel and determine the effects of olefin compounds on knock characteristics of LPG.

## **CHAPTER 3**

### **EXPERIMENTAL SETUP**

#### **3.1. Octane Testing System**

##### **3.1.1. Cooperative Fuel Research (CFR) Engine**

The Cooperative Fuel Research engine is a specific engine that is developed for determination of octane numbers of fuels for spark ignition internal combustion engines. This engine has a special design that allows the user to control and change the compression ratio, ignition timing and intake air and air-fuel mixture temperatures. CFR engines normally have 3 fuel trays which let user to measure the knocking characteristics of the desired fuel by comparing the knock intensity of the fuel with two primary reference fuels. The reference fuels are usually iso-octane and n-heptane which have octane ratings of 100 and 0 respectively. The unknown octane number of the specific fuel is determined through interpolation of the knocking tendencies of reference fuels.

*Table 3.1: Diameters of pulleys for RON and MON tests*

Test Type	Pulley Diameter
Research ON	100 mm
Motor ON	150 mm

CFR engines are capable of determining Research Octane Number-RON and Motor Octane Number-MON. For this purpose, CFR engines can run at constant speeds for RON (600rpm) and MON (900 rpm) tests, by the help of electric motor connected to the flywheel of CFR engine by V-belts. The electric motor has two purposes in the whole system; starting the CFR engine, and keeping the engine speed constant for both octane measuring tests. In addition, while the electric motor is running at

constant speed for all processes, the differing CFR engine speeds are provided by the help of the pulleys having different diameters.

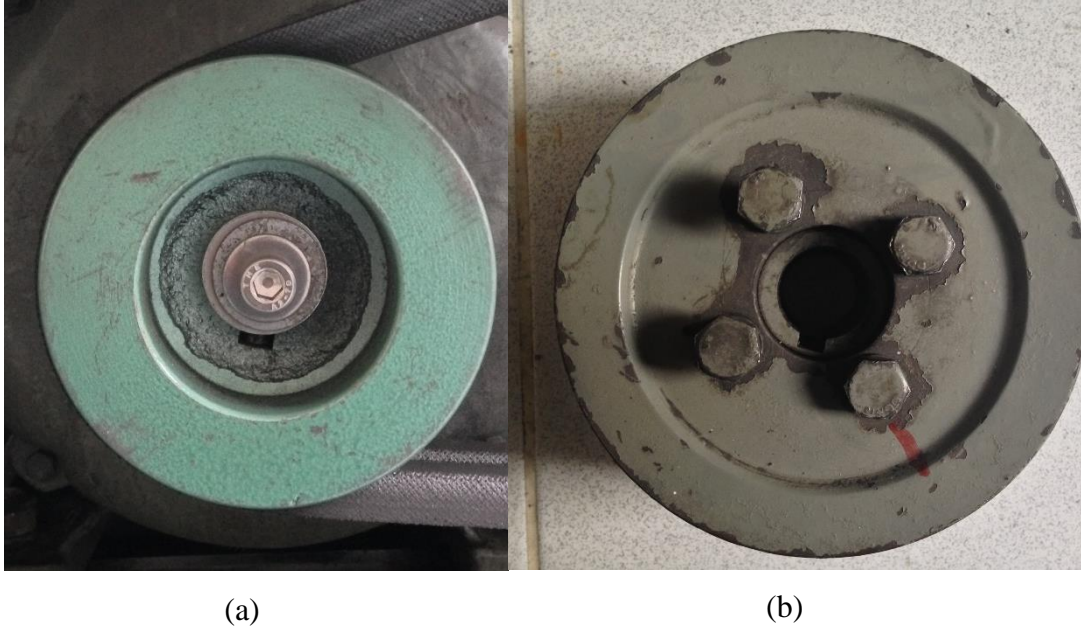


*Figure 3.1: Pulleys for RON setup (a) and MON setup (b)*

CFR engines that are manufactured as a complete unit by Waukesha Engine Division, Dresser Industries, Inc. are accepted as standard testing unit for determination of octane number of fuels [4, 5]. The specifications of standard Waukesha engine are given in table 3.2 [4, 5].

Table 3.2 : Specifications of a standard Waukesha CFR engine [4, 5]

Manufacturer	Waukesha Engine Division, Dresser Industries, Inc.
Test Engine	CFR F1 Research Method Octane Rating Method / F2 Motor Method Octane Rating Unit, with cast iron, box type crankcase with flywheel connected by V-belts to power absorption electrical motor for constant speed operation.
Cylinder Type	Cast iron with flat combustion surface and integral coolant jacket
Compression Ratio	Adjustable 4:1 to 18:1 by cranked worm shaft and worm wheel drive assembly in cylinder clamping sleeve
Cylinder Bore	3,250 in. (standard)
Stroke	4.50 in.
Displacement	37,33 cu in.
Valve Mechanism	Open rocker assembly with linkage for constant valve clearance as C.R. changes
Intake Valve	Stellite faced, with 180° shroud
Exhaust Valve	Stellite faced, plain type without shroud
Piston	Cast iron, flat top
Piston Rings	
Top Compression Ring	1 chrome plated or ferrous, straight sided
Other Compression Rings	3 ferrous, straight sided
Oil Control	1 cast iron, one piece, slotted (Type 85)
Camshaft overlap, deg.	5
Fuel System	
Carburetor	Single vertical jet and fuel flow control to permit adjustment of fuel-air ratio
Venturi Throat Diameter, in. (RON)	9/16 for all altitudes
Venturi Throat Diameter, in. (MON)	Dependent on installation altitude 9/16; sea level to 500 m (1600 ft) 19/32; 500 m to 1000 m (3300 ft) 3/4; over 1000 m (3300 ft)
Ignition	Electronically triggered condenser discharge through coil to spark plug
Ignition Timing (RON)	Constant 13 BTC
Ignition Timing (MON)	Variable as cylinder height (C.R.) is changed
Intake Air Humidity	Controlled within the specified limited range

In this thesis, however, the octane number determination experiments are performed on Knock Testing Unit – BASF. The engine is a vertical type single cylinder 4 stroke gasoline engine manufactured by BASF. The specifications of the stock BASF CFR engine are given in table 3.3.

*Table 3.3: Specifications of a standard BASF CFR engine*

Manufacturer	Hermann Ruf Mannheim Elektrotechnische Spezialfabrik
Engine Type	4 stroke, variable compression ratio, naturally aspirated
Displacement	332 cc
Bore	65 mm
Stroke	100 mm
Cylinder Head	Removable
Wet Liner	Removable
Piston	Light Alloy, fitted with 3 sealing rings and 1 oil scraper ring
Crankshaft	Hardened sliding surfaces, double bearing
Connecting Rod	Copper-Lead bearings
Gudgeon Pin	Hardened
Valves and Valve Seats	Hard-faced
Low Voltage Ignition	12 V
Spark Plug	Bosch W145 T1
Lubrication	Forced lubrication of crankshaft, connecting-rod, bearing and control wheel; splash lubrication of piston and gudgeon pins
Cooling	Thermosiphon type (automatic circulation by evaporative cooling) with water-cooled condenser, fresh water cooling and coolant level indication

The engine was subjected to reconditioning before octane number determination experiments. Before reconditioning, the head gasket was out of condition. Due to this reason there were compression, oil and coolant leakages caused by the head gasket. The cooling system was damaged, preventing coolant water to circulate easily, and the signal measurement system was not working properly. There was oil leakage from the oil pipe circulating the engine from oil pump to oil pressure gauge.

During reconditioning, the cylinder head was milled 0.5 mm for fixing the deformations caused by the heat produced by engine. In addition; this operation was done in order to achieve higher compression ratio. A new piston was designed and manufactured in order to achieve higher compression ratio by increasing the distance between the piston head and the gudgeon pin by 2.5 mm.



*Figure 3.2: Comparison of piston height before (on the right hand side) and after reconditioning (on the left hand side)*

Furthermore, two blind holes were drilled on top surface of the piston to avoid valve and piston head contact at TDC. On the other hand, the diameter of the piston remained the same as the stock size.



*Figure 3.3: New designed piston head*

A new designed head gasket was installed, which is durable in high temperatures. New wet liner produced and installed according to stock engine size, to prevent compression leakages caused by over-sized hole diameter. The rust accumulated in the cooling system was cleaned completely. Leaking oil pipes were replaced with suitable oil hoses, in order to prevent loss of oil.



*Figure 3.4: New head gasket*



The drum type scale disc which was indicating compression ratio of engine and approximate octane number of the unknown fuel blend was removed, since the engine size was changed. Instead of this scale disc, a dial indicator was installed on the engine to measure the cylinder height.

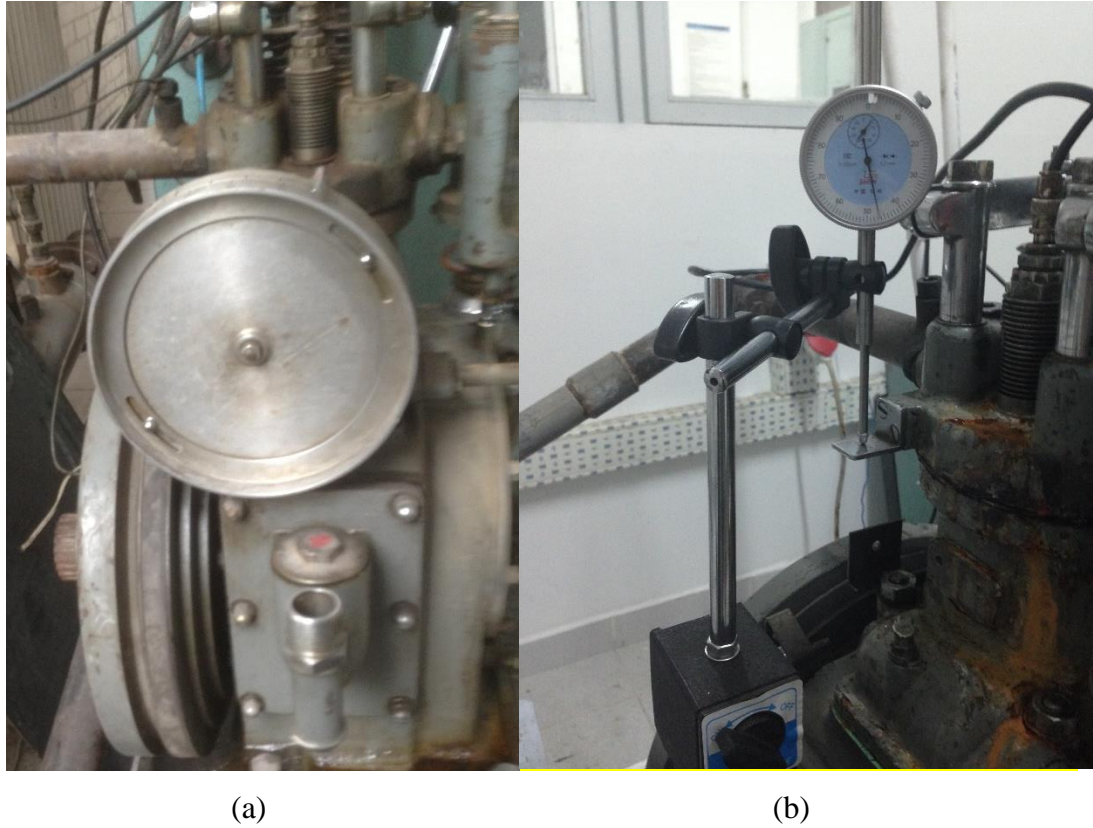


*Figure 3.5: Scale Disc (a), Dial Indicator (b)*

Finally after all reconditioning operations were carried out; the engine underwent pressure test by means of mounting a pressure gauge to spark plug hole in order to measure the maximum compression pressure and cylinder height-pressure matchings. The pressure values with respect to cylinder heights are given in figure 3.7.



*Figure 3.6: Pressure gauge*

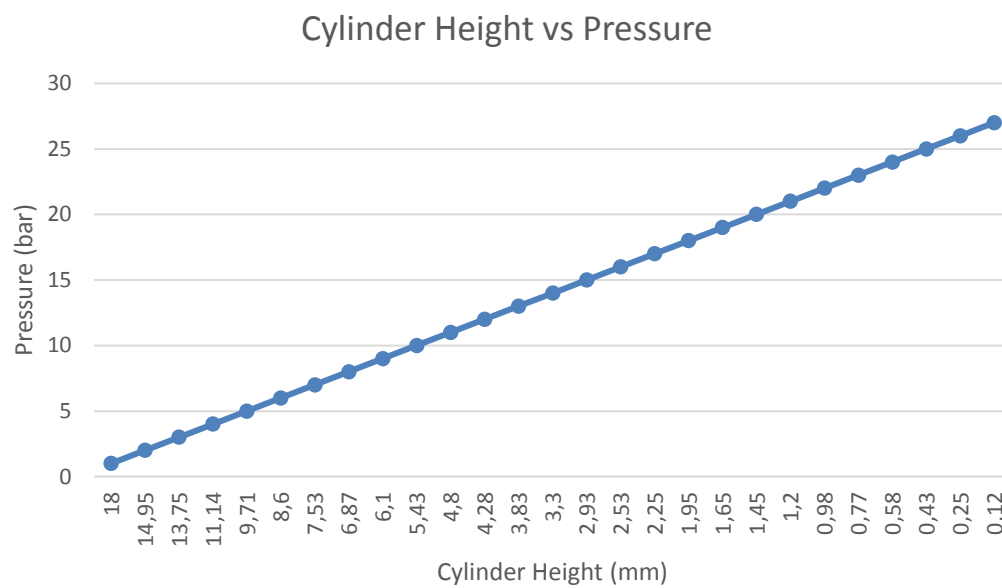


*Figure 3.7: Graphical representation of cylinder height vs. in-cylinder pressure*

These pressure values were used as reference data for checking the engine condition whenever any modification or repair was done on the CFR engine, in case of any pressure leakages.

### 3.1.2. Detonation Pick-up

Detonation pickup is a magnetostrictive type transducer that provides an electrical signal that is proportional to the rate of change of cylinder pressure [4, 5]. Inside the pickup, there is a longitudinally magnetized rod in a constant magnetic field. When pressure is applied to the pickup, the magnetic field changes its permeance as well as the magnitude of the magnetic flux. The change of the flux is proportional to the rate of change of pressure, so the voltage delivered by the pickup is also proportional to the rate of change of pressure and changes between 200 to 500 millivolts.

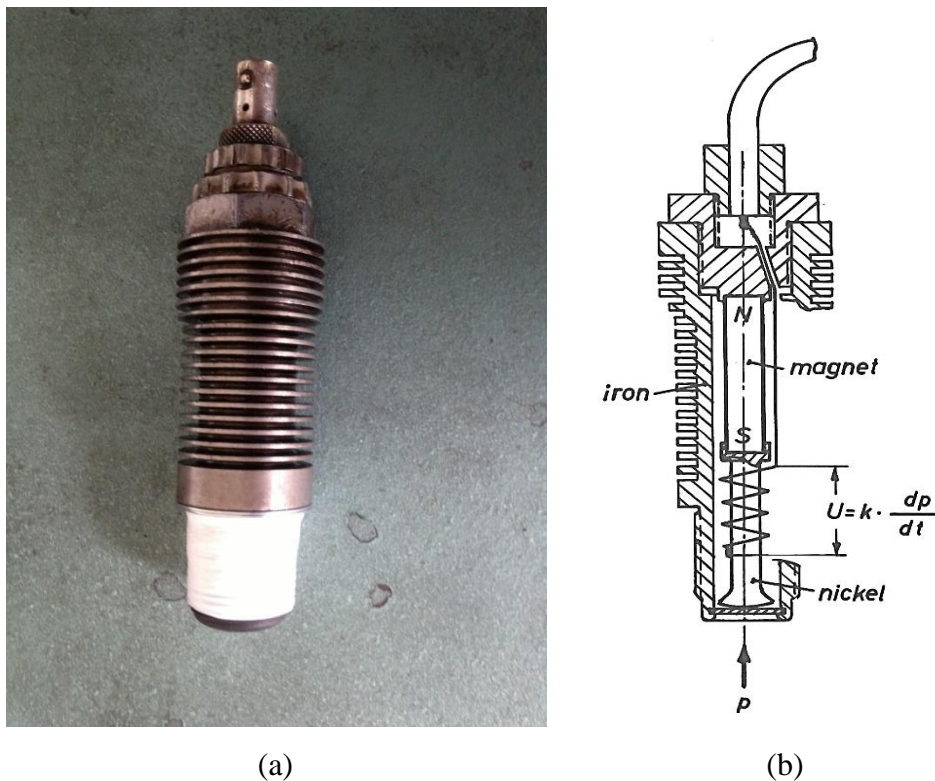
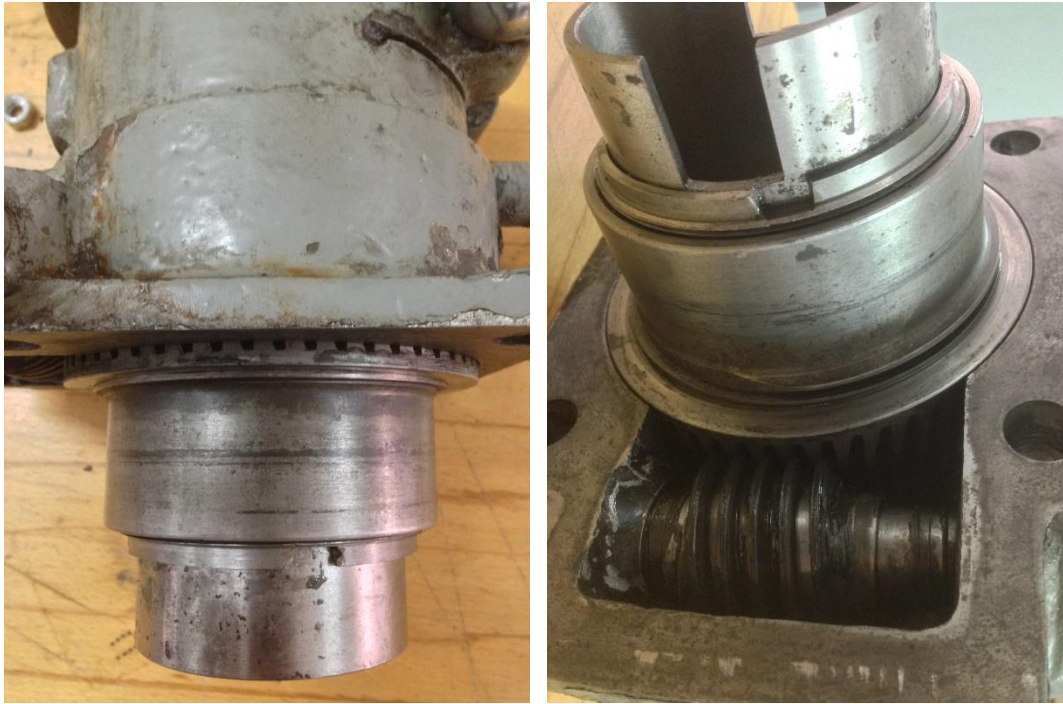


Figure 3.8: Detonation pickup (a), Cross section of detonation pickup (b) [6]

### 3.1.3. Compression Ratio Control Mechanism

The stock BASF engine had a variable compression ratio ranging from 4:1 to 12:1. Since the sizes of the piston and cylinder head depth were changed during reconditioning for current experiments, the operating compression ratio range was changed to 4.36:1 and 17.27:1.

The compression ratio of the engine is controlled with a worm gear fitted to the cylinder support. The worm gear is actuated by a hand crank, and at every cylinder height, it can be locked by a clamp lever.



*Figure 3.9: Worm gear*

#### **3.1.4. Fuel Tanks and Fuel Selector**

The BASF engine includes 3 containers for 3 different fuels having different octane numbers that are used in octane tests. Each of the fuel containers may be connected to the carburetor by a three-way selector valve, which lets the user to switch between the sample fuel and the reference fuels quickly.

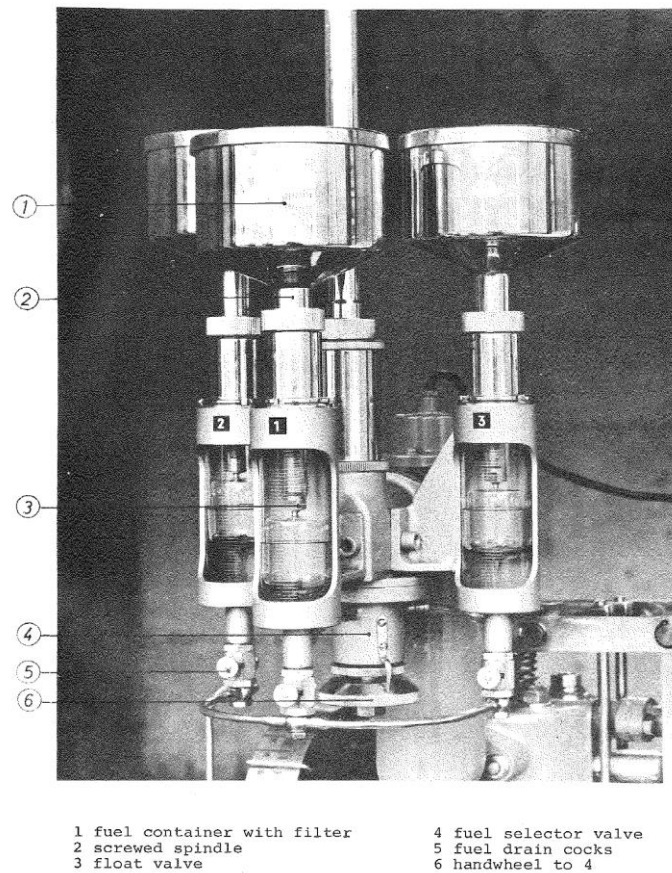


*Figure 3.10: Fuel tanks and fuel selector [6]*

### **3.1.5. Air – Fuel Ratio Control Mechanism**

Each container may be raised or lowered by means of a screwed spindle (fig. 3.11) to adjust the air fuel ratio by changing the level of the fuel inside graduated glass bowl (fig. 3.10). The level of the fluid inside the graduated glass bowl is kept constant by a glass float and float valve.





*Figure 3.11: Fuel tank and screw spindle*

### **3.1.6. Air Heating System**

The CFR engine is equipped with additional heating elements to preheat the air for research method that is placed before the carburetor or the air-fuel mixture for motor method which is placed between the carburetor and the engine.

During octane tests, 120 W heater is used which is connected to a NTC type temperature transmitter and fed from the control panel of the BASF test unit. The NTC type temperature transmitter is fitted into the heating element and is also connected to the BASF test unit.

The air heater is controlled automatically by an electronic phase shift controller, placed in the control unit. The NTC controls automatically thyristors through a transistorized amplifier by means of variable phase shift [6]. The fine adjustment is done using a rheostat, which is mounted to the control panel of the test unit.

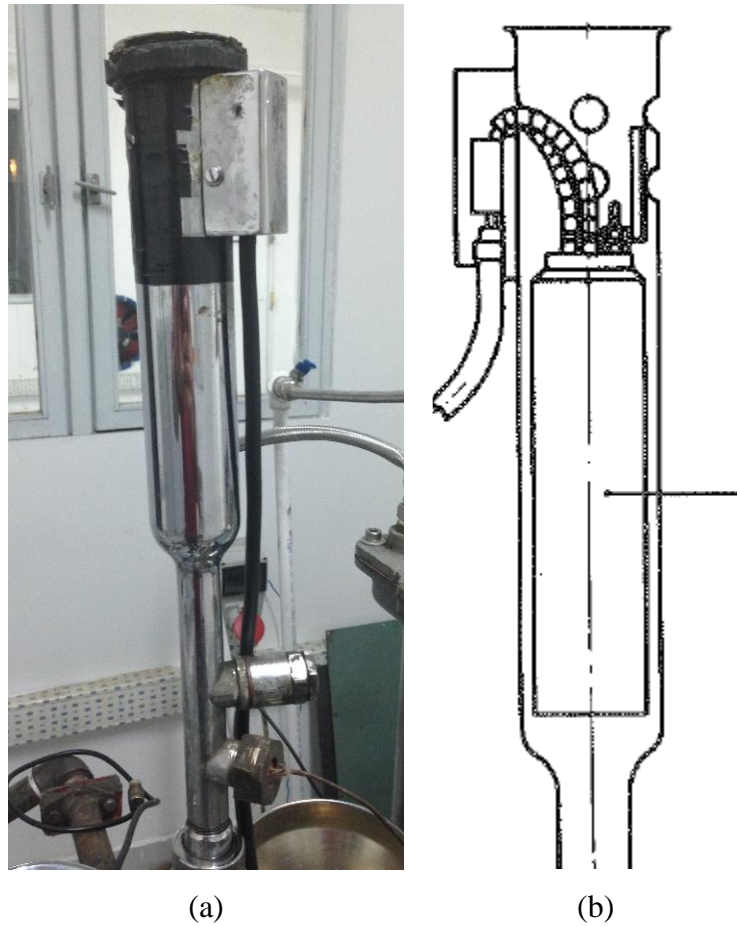


*Figure 3.12: Air heater (a), Cross section of air heater (b) [6]*

The temperature of the air or air-fuel mixture was used to be indicated by thermometers in the original BASF setup on the other hand, during experiments, the temperature of air was measured by hot wire anemometer.

### **3.2. Gaseous Fuel System**

Since the original octane testing unit is capable of measuring the knock intensities of liquid fuels, some adaptations had been applied on the unit to enable octane measurement experiments on LPG. Those adaptations are similar to the ones applied on personal automobiles; on the other hand, the sizes and forms of the parts may differ from the commercial parts.

### 3.2.1. Fuel Tanks

Fuel tanks, shown in figure 3.13, filled with differing volumetric compositions of LPG fuel, are sent by AYGAZ Company.



Figure 3.13: LPG tank

For safety concerns, the tanks are placed outside of the test room, away from the test unit and electricity wiring for the possibility of any unwanted leakage of LPG. The tanks are placed in a well-ventilated atmosphere, close to the windows of the laboratory.

### 3.2.2. LPG Evaporator

LPG stored in fuel tanks is in liquid state, so it has to be vaporized before entering directly into engine or fuel mixer. LPG evaporator is the part where LPG fuel is converted from liquid state to gaseous state.

The evaporators use engine coolant as heat source to warm up and evaporate the fuel. For this purpose, the evaporator has 2 entry ports and 2 exit ports; 1 entry and 1 exit for engine coolant, 1 entry and 1 exit for LPG fuel. In addition, the evaporator has a solenoid valve on LPG entry port, to let or prevent LPG fuel from entering.





*Figure 3.14: LPG evaporator*

The evaporator used in LPG conversion of test engine, has coolant entry and exit ports, but they were not used. This is because, the flow rate of LPG is very low and the ambient temperature where evaporator located was enough to warm up LPG and change its state from liquid to gas. In addition, a switch was inserted on the control panel of the CFR engine, which controls the solenoid valve on the fuel entry port of the evaporator.

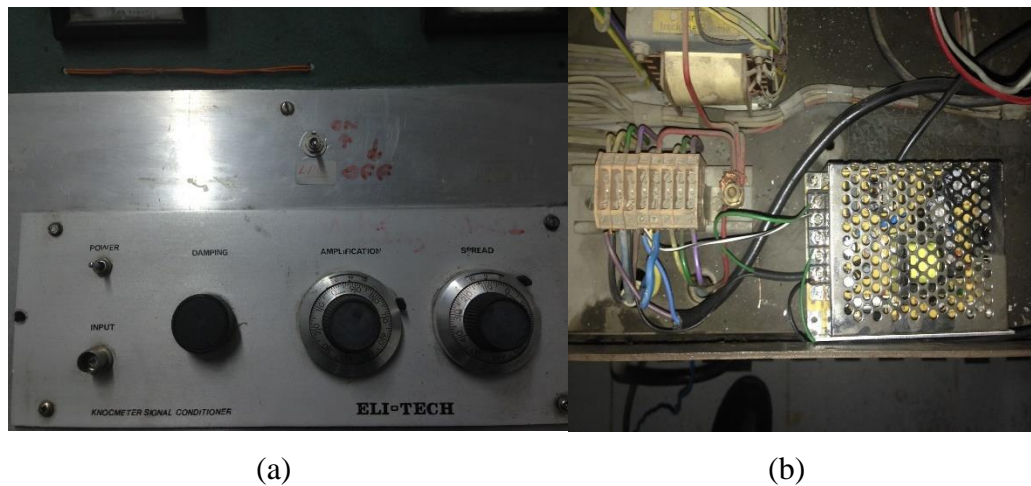


*Figure 3.15: LPG on-off switch (a), Solenoid control unit (b)*

### 3.2.3. Air-Fuel Ratio Control Mechanism

The air-fuel ratio of the LPG fuel is adjusted with a small valve between the LPG evaporator and the fuel mixer. Since the amount of air passing through the air entry of the engine is constant, the air-fuel ratio is controlled by the amount of fuel passing through the valve.



*Figure 3.16: LPG fuel flow control valve*

### 3.2.4. Gaseous Fuel Mixer

During LPG conversion, an additional tubular part inserted to the system between the air heater and intake manifold. By this means, LPG fuel is routed to the intake manifold.



*Figure 3.17: LPG Mixer*

LPG fuel coming from the evaporator, is directed into the tubular part by the help of a handmade nozzle. The nozzle is designed to spray the fuel in the same direction with the air flow.



*Figure 3.18: LPG nozzle*

Since the air inducted into air heater is turbulent, LPG and air are mixed automatically before entering the combustion chamber.

### **3.3. Data Acquisition System**

Since the data acquisition or, in other words, the knock measuring system of BASF test unit was out of use, the octane tests were completed using an up-to-date data acquisition system. In order to use the new data acquisition system, the testing procedure had been changed; which will be given in chapter 4.

### **3.3.1. Oscilloscope**

During octane tests, an oscilloscope was used for adjusting the suitable compression ratio for the specified fuel sample. In addition; during adjusting the air-fuel ratio for the maximum knock intensity, voltage signals created by the detonation pickup were observed on the oscilloscope.

### **3.3.2. Data Acquisition Card**

The signal created by the detonation pickup were collected by a data BNC type data acquisition card and then sent to the computer for converting to meaningful voltage values created by the detonation pickup at each knock.

### **3.3.3. Software**

The voltage values that created by the detonation pickup and collected by the data acquisition card, were monitored using National Instruments LabView SignalExpress software. Then the list of signal values were exported to MS Excel for processing.

## **CHAPTER 4**

### **EXPERIMENTAL METHOD**

The experiments were conducted on BASF engine, which is not approved as a standard engine by American Society for Testing and Materials – ASTM. In addition, since some of the parts of BASF engine were replaced and modified during reconditioning as explained in chapter 2, a new experimental method was designed. The testing procedure of LPG and liquid fluids are the same as bracketing method of ASTM D2699 standard. Since standard knockmeter was not used, the new method differs from the ASTM standard in terms of calculations done on unknown fuel blends octane number.

The details and steps of this new experimental method will be given in section 4.3.

#### **4.1.Composition of Test Fuels**

LPG samples that were used in octane testing experiments had been provided by AYGAZ. The samples had a wide variety of compositions including propane, iso-butane, n-butane and trace amount of olefins.

The compositions of LPG fuels were arranged in order to observe the knock characteristics of LPG fuel, when the amount of one of ingredient fuel was kept constant while the amount of the other two were more or less the same. In addition, composition variations were used in order to observe the effect of each fuel on the knock intensity and prediction of the unknown fuels octane number.

Table 4.1: Compositions of test fuels provided by AYGaz Company

METU PAL No:	METU Mec. No:	Composition						
		Propane %	iso- butane %	n- butane %	Olefin C3 %	Olefin C4 %	Ethane %	Total
652	643	16,70%	2,00%	78,10%	0,20%	2,70%	0,30%	100%
647	656	19,40%	20,10%	57,00%	0,10%	3,40%	0,10%	100%
638	654	17,90%	30,70%	48,10%	0,10%	3,20%	0,10%	100%
305	289	26,50%	1,90%	68,50%	0,20%	2,50%	0,40%	100%
671	635	23,70%	9,40%	63,70%	0,10%	2,90%	0,30%	100%
675	655	23,00%	19,40%	53,70%	0,10%	3,70%	0,10%	100%
291	297	26,70%	2,00%	68,10%	0,20%	2,70%	0,20%	99,90%
299	300	31,60%	11,10%	54,20%	0,10%	2,80%	0,30%	100%
634	677	37,50%	3,40%	55,60%	0,10%	3,10%	0,40%	100%
658	669	41,30%	3,10%	52,60%	0,10%	2,60%	0,40%	100%
648	672	49,00%	3,00%	44,50%	0,10%	3,10%	0,40%	100%
668	651	48,60%	13,30%	33,70%	0,10%	4,00%	0,30%	100%
644	645	60,30%	2,90%	32,60%	0,10%	3,70%	0,40%	100%
676	673	65,90%	2,70%	27,80%	0,10%	3,10%	0,50%	100%
649	639	66,30%	11,90%	18,30%	0,10%	3,10%	0,30%	100%

Prior to experiments, LPG tanks with the same specified compositions as shown in table (a pair of each compositions), had been prepared by AYGaz, for instance Tank 652 and Tank 643 store LPG fuel with exactly same composition. Moreover, all tanks were sealed under control of notary. After sealing, one of each pair was sent to METU PAL and the other to internal combustion engines laboratory for the purpose of this research.

In the second group of experiments, the effects volumetric ratios of olefins on octane rating of LPG were inspected. For this purpose, 33 samples of LPG with different olefin compositions were prepared by AYGaz.

5 different 99.9% pure C3 and C4 olefins which are propylene, i-butene, 1-butene, t2-butene and c2-butene were procured from BOC Ltd., UK. Then the olefins were mixed with standard LPG in differing compositions (1%, 3%, 5%, 10%, 15%, and 50%) and were filled in 24 kg. tanks at AYGaz Yarımca terminal. The composition of sample tanks are given in table 4.2.



*Figure 4.1: 99.9% pure olefins: propylene, i-butene, 1-butene, t2-butene and c2-butene*

While preparing the samples, the olefinic gases were first transferred into tanks and then standard LPG was filled into tanks using standard LPG pump. While preparing the samples, a high precision scale was used for having accurate olefin and LPG ratios.



*Figure 4.2: Transfer of LPG and olefins into tanks*

Table 4.2: Compositions of Olefins Samples Provided by AYGaz Company

Tank Number	Composition									
	Propane	i-butane	n-butane	Ethane	Propylene	1-butene	i-butene	t2-butene	C2-butene	Total
297	22,71%	10,86%	64,83%	0,58%	1,00%	0,00%	0,00%	0,00%	0,00%	100%
676	22,25%	10,64%	63,52%	0,57%	3,00%	0,00%	0,00%	0,00%	0,00%	100%
677	21,79%	10,42%	62,21%	0,56%	5,00%	0,00%	0,00%	0,00%	0,00%	100%
672	20,64%	9,87%	58,94%	0,53%	10,00%	0,00%	0,00%	0,00%	0,00%	100%
306	19,50%	9,33%	55,66%	0,50%	15,00%	0,00%	0,00%	0,00%	0,00%	100%
852	22,71%	10,86%	64,83%	0,58%	0,00%	1,00%	0,00%	0,00%	0,00%	100%
635	22,25%	10,64%	63,52%	0,57%	0,00%	3,00%	0,00%	0,00%	0,00%	100%
669	21,79%	10,42%	62,21%	0,56%	0,00%	5,00%	0,00%	0,00%	0,00%	100%
295	20,64%	9,87%	58,94%	0,53%	0,00%	10,00%	0,00%	0,00%	0,00%	100%
302	19,50%	9,33%	55,66%	0,50%	0,00%	15,00%	0,00%	0,00%	0,00%	100%
848	22,71%	10,86%	64,83%	0,58%	0,00%	0,00%	1,00%	0,00%	0,00%	100%
651	22,25%	10,64%	63,52%	0,57%	0,00%	0,00%	3,00%	0,00%	0,00%	100%
673	21,79%	10,42%	62,21%	0,56%	0,00%	0,00%	5,00%	0,00%	0,00%	100%
654	20,64%	9,87%	58,94%	0,53%	0,00%	0,00%	10,00%	0,00%	0,00%	100%
839	19,50%	9,33%	55,66%	0,50%	0,00%	0,00%	15,00%	0,00%	0,00%	100%
856	22,71%	10,86%	64,83%	0,58%	0,00%	0,00%	0,00%	1,00%	0,00%	100%
853	22,25%	10,64%	63,52%	0,57%	0,00%	0,00%	0,00%	3,00%	0,00%	100%
857	21,79%	10,42%	62,21%	0,56%	0,00%	0,00%	0,00%	5,00%	0,00%	100%
855	20,64%	9,87%	58,94%	0,53%	0,00%	0,00%	0,00%	10,00%	0,00%	100%
844	19,50%	9,33%	55,66%	0,50%	0,00%	0,00%	0,00%	15,00%	0,00%	100%
851	22,71%	10,86%	64,83%	0,58%	0,00%	0,00%	0,00%	0,00%	1,00%	100%
849	22,25%	10,64%	63,52%	0,57%	0,00%	0,00%	0,00%	0,00%	3,00%	100%
854	21,79%	10,42%	62,21%	0,56%	0,00%	0,00%	0,00%	0,00%	5,00%	100%
850	20,64%	9,87%	58,94%	0,53%	0,00%	0,00%	0,00%	0,00%	10,00%	100%
A03	19,50%	9,33%	55,66%	0,50%	0,00%	0,00%	0,00%	0,00%	15,00%	100%
845	0%	0%	0%	0%	0,00%	0,00%	0,00%	0,00%	100,00%	100%
842	11,47%	5,49%	32,74%	0,29%	50,00%	0,00%	0,00%	0,00%	0,00%	100%
305	0,00%	0,00%	0,00%	0,00%	100,00%	0,00%	0,00%	0,00%	0,00%	100%
308	11,47%	5,49%	32,74%	0,29%	0,00%	50,00%	0,00%	0,00%	0,00%	100%
304	0,00%	0,00%	0,00%	0,00%	0,00%	100,00%	0,00%	0,00%	0,00%	100%
843	11,47%	5,49%	32,74%	0,29%	0,00%	0,00%	50,00%	0,00%	0,00%	100%
841	0,00%	0,00%	0,00%	0,00%	0,00%	0,00%	100,00%	0,00%	0,00%	100%
838	22,94%	10,97%	65,49%	0,59%	0,00%	0,00%	0,00%	0,01%	0,00%	100%



The prepared mixtures were waited for 24 hours in order to have homogeneous mixture. Then 500 mL samples were taken from the tanks and sent to GC laboratory for checking the composition of LPG using EN 15470:2007, Liquefied petroleum gases – Determination of dissolved residues - High temperature Gas chromatographic method.

After checking the mixture compositions, 2 lt of sample tanks were sent to METU Internal Combustion Engines laboratory for octane rating experiments. EN ISO 4257:2001, Liquefied petroleum gases - Method of sampling (ISO 4257:2001) standard was used for sampling the LPG mixtures.

#### 4.2. Reference Fuels

For octane testing of unknown fuel samples with 0-100 octane number, iso-octane and n-heptane were used as primary reference fuels. Furthermore, tetra ethyl lead was added to iso-octane within a pre-defined empirical formula for fuels having octane number higher than 100.

For octane tests performed for this study, reference fuels were supplied by AYGAZ Company. Reference fuels were prepared by Tübitak MAM – Marmara Research Center, and before sending to METU, their RON-research octane numbers were verified using a standard CFR engine.



*Figure 4.3: Reference fuels prepared by Tübitak MAM*

During preparation of reference fuels, octane number range was determined for octane test in order to cover all predicted octane numbers of LPG samples. The octane number range of reference fuels differ from 94 to 120. Moreover, the octane number

difference between two reference fuels was kept constant for maximum 2-3 octanes, in order to determine the unknown octane number more precisely for each LPG sample.

#### **4.3. Test Procedure**

During octane test, standard bracketing method was used for calculation of octane number of unknown fuel sample. However, testing procedure was somewhat changed since the CFR engine used for tests was different from the standard CFR engine. In addition, the absence of knockmeter and the change in compression ratio of standard BASF engine, required a new methodology for LPG octane tests.

The main steps of octane test remained the same while, the procedure for determination of suitable compression ratio and data acquisition for created signal values for each fuel sample were modified according to new experimental setup.

The steps of new experimental procedure is as below,

1. Reference fuels are selected according to the predicted octane number of unknown fuel sample. While selecting the reference fuels, it is important to check that, the difference between unknown sample octane number and reference fuel octane number should not be very high.
2. Engine coolant water is turned on.
3. The amount of water inside the coolant condenser of CFR engine is checked. Water is added if the level is too low.
4. Electrical switch of the CFR engine is turned on.
5. The engine is checked if any wire-hose etc. is in contact with the belt and pulley mechanism of engine.
6. CFR engine is started.
7. The engine is checked for any undesired noise to make sure it is running properly.
8. Spark ignition and air heater switches are turned on.
9. One of the fuel tanks is filled with ordinary gasoline for warming up the engine, since the octane tests could be started after engine coolant temperature reaches 95° C.

10. The needle valve controlling the fuel entry to intake manifold is opened, and fuel is fed to the CFR engine.
11. The compression ratio of the CFR engine is adjusted by loosening the compression clamp lever in order to run the engine under normal conditions without knock for 30 minutes. Then the compression ratio of the engine is increased to force slight knocking. CFR engine is run under slight knocking condition for another 15 minutes.
12. The coolant temperature is checked occasionally during engine run to check any overheating risk. In addition, the coolant temperature should be 95° C in order to start experiments. After reaching the specified temperature, experimenter has to be sure if the temperature remains stable at that value.
13. The computer is turned on and the oscilloscope and the data acquisition card are placed near to computer for ease of use.
14. The drain cock of one of the carburetor is opened and 20-30 mL of reference fuel with higher octane number is poured in to container in order to flush the container chamber completely. Then the fuel container is filled with reference fuel with higher octane number.
15. The detonation pickup cable is connected to the oscilloscope.
16. The compression ratio of the CFR engine is adjusted by loosening the clamp lever to have a voltage reading of 0.1-0.2 V on oscilloscope screen at each knock. The air-fuel ratio of the CFR engine is adjusted to have maximum knock intensity at that compression ratio for the first reference fuel. If the reading value is higher than 0.2 V, the compression ratio should be decreased. This operation is repeated until the maximum knock reading on oscilloscope is between 0.1-0.2 V for the first reference fuel, with higher octane number. Then the clamp lever is tightened. The compression ratio of the engine will remain constant during the rest of test.
17. The data acquisition card is connected to the computer via one of the USB ports and NI LabView Signal Xpress program is run.
18. “Add Step – Data Acquisition – Analog Input – Voltage” are selected on Signal Xpress respectively.
19. Input port of data acquisition card is selected on pop-up window. (i.e. a0)

20. The reading frequency is set to 10 kHz.
21. The detonation pickup is connected to data acquisition card, and then “RUN” button on program window is clicked.
22. After being sure that the program is working properly, “RECORD” button is clicked and “VOLTAGE” is selected on pop-up window. Then “OKAY” is clicked so storage of knock data is started.
23. After collecting data for 45 seconds, recording process is stopped and the knock data is exported to Microsoft Excel.
24. The experimenter shall repeat steps 22 and 23 for 5 more times to have 6 sets of knock data for the reference fuel with high octane number.
25. After collecting 6 sets of data for reference fuel with higher octane number, without changing the compression ratio, steps 16-24 are repeated for reference fuel with lower octane number and unknown fuel sample.
26. After data acquisition process ends, the needle valve controlling fuel inlet to intake manifold is closed and spark ignition and air heating are turned off.
27. Engine is run under no fuel and no heating condition, in order to cool down the CFR engine. Then the engine is turned off.
28. Engine coolant water is turned off.
29. Electricity is switched off.

While conducting an octane test for any gaseous fuel, the experimental procedure has to be changed slightly. Above procedure is applicable for reference fuels compared with gaseous fuels since, reference fuels are in liquid state. On the other hand for gaseous fuels, the procedure differences can be listed as;

- ⇒ Before sending the gaseous fuel to intake manifold, first the needle valve has to be closed in order to prevent liquid fuel to enter intake manifold.
- ⇒ The switch controlling the solenoid valve on entrance port of evaporator has to be opened, so gaseous fuel can flow through evaporator from fuel tank to intake manifold.
- ⇒ The air fuel ratio of gaseous fuel is adjusted by means of the fuel valve which restricts the gaseous fuel flow.

⇒ When data acquisition for gaseous fuel ends, the switch has to be turned off to end the fuel flow.

After data acquisition process ends, the raw knock data has to be processed to have meaningful knock peak values. After determining peak values, bracketing method can be conducted for calculating the octane number of unknown fuel sample, which will be explained in section 4.4.4.

#### **4.4.Calculation Procedure**

Standard BASF engine has a knockmeter gauge, which allows user to compare the knock intensities of different fuels for same compression ratio. Since the knockmeter of standard BASF engine was out of use, the knock intensities of fuels were measured by data acquisition card. National Instruments LabView SignalExpress program was used for gathering pressure changes inside the combustion chamber by means of voltage values. In addition, these values were had to be processed in order to determine the peak value of each detonation.

##### **4.4.1. Data Processing**

During octane measurement tests for each fuel, 2 reference fuels and 1 unknown fuel sample, were tested to obtain 6 sets of knock data. In other words, in the end of each octane test, there were 18 sets of knock data.

To gather a meaningful voltage value of each knock, the maximum voltage value of each cycle had to be found. In order to do this, the each data set of each fuel was exported to Microsoft Excel, for processing the raw detonation voltage values.

##### **4.4.2. Peak Value Selection-Elimination**

Since the data exported to Microsoft Excel includes all voltage values per each cycle, the maximum voltage value was found for each revolution of CFR engine. The maximum voltage value indicates the peak pressure point of each detonation.

For each fuel, 120 peak values were determined for each data set. Then, the maximum 10 and the minimum 10 peak values were eliminated in order to eliminate any possible abnormalities occurred during data acquisition.

In the end, the average of 100 peak points were taken so, that value was named as the average knock intensity of that data set.

#### 4.4.3. Detonation Voltage Determination

The process identified in section 4.3 was repeated for each data set. Furthermore, the average of 6 average knock intensities were taken in order to have the knock voltage value of corresponding fuel.

The same procedure was repeated for each fuel, and in the end there were 3 average voltage values in total, defining the knock intensities of reference fuels and the sample fuel.

#### 4.4.4. Octane Value Calculation

During calculations for unknown fuel sample's octane value, bracketing method was used as explained in BASF catalogue. The steps of this method can be given as [4];

1. Sensitivity per octane number, which represents the voltage value variation per 1 octane number, is calculated as below;

$$S = \frac{V_1 - V_2}{n} \quad (4.1)$$

In which;

*S: sensitivity*

*V<sub>1</sub>: knock intensity of lower octane number reference fuel*

*V<sub>2</sub>: knock intensity of higher octane number reference fuel*

*V<sub>3</sub>: knock intensity of petrol fuel*

*n: octane number difference of reference fuels*

2. Minimum voltage difference between the sample and the reference fuel (d) is calculated
3. The value  $\frac{d}{S}$  is calculated which represents the octane number difference between the LPG fuel and the reference fuel (considered in step 2) with closest knock intensity

## **CHAPTER 5**

### **RESULTS and CONCLUSION**

The knock characteristics of sample fuels supplied by AYGAZ Company were determined according to new experimental procedure as described in chapter 4. After determining the maximum detonation voltages of each fuel, the octane numbers of regarding fuels were calculated according to bracketing method which is also discussed in detail in chapter 4.

Octane number determination of LPG samples consisting of different compositions using a variable compression ratio engine with a modified experimental methodology was performed and reported for the first time. The compositions and octane numbers which were determined according to experiment results of regarding fuels are given in the table 5.1.

From results shown in table 5.1, the octane number increases mainly with the increase of propane compound found in the sample composition. For the samples having nearly same propane percentage, then it is seen that the sample having higher percentage of iso-butane, has the higher octane number, if the olefin percentages are also more or less the same.

To explore the relationship between octane number and exogenous variables, propane, iso-butane, n-butane, olefin C3, olefin C4 and ethane, the stepwise regression method was used. Stepwise regression is an automated implementation to identify the most significant subset of predictors.

*Table 5.1: Research octane numbers (RON) for the fuel samples prepared by AYGaz Company*

Research Octane Number									
Sample No.	METU Mec. No:	Propane %	iso-butane %	n-butane %	Olefin C3 %	Olefin C4 %	Ethane %	Total	Octane #
1	643	16.7%	2.0%	78.1%	0.2%	2.7%	0.3%	100%	97.7
2	656	19.4%	20.1%	57.0%	0.1%	3.4%	0.1%	100%	98.8
3	654	17.9%	30.7%	48.1%	0.1%	3.2%	0.1%	100%	99.5
4	289	26.5%	1.9%	68.5%	0.2%	2.5%	0.4%	100%	97
5	635	23.7%	9.4%	63.7%	0.1%	2.9%	0.3%	100%	98.6
6	655	23.0%	19.4%	53.7%	0.1%	3.7%	0.1%	100%	99.7
7	297	26.7%	2.0%	68.1%	0.2%	2.7%	0.2%	99.9%	97.8
8	300	31.6%	11.1%	54.2%	0.1%	2.8%	0.3%	100%	98.9
9	677	37.5%	3.4%	55.6%	0.1%	3.1%	0.4%	100%	99.2
10	669	41.3%	3.1%	52.6%	0.1%	2.6%	0.4%	100%	100.7
11	672	49.0%	3.0%	44.5%	0.1%	3.1%	0.4%	100%	101.6
12	651	48.6%	13.3%	33.7%	0.1%	4.0%	0.3%	100%	101.6
13	645	60.3%	2.9%	32.6%	0.1%	3.7%	0.4%	100%	102.9
14	673	65.9%	2.7%	27.8%	0.1%	3.1%	0.5%	100%	104
15	639	66.3%	11.9%	18.3%	0.1%	3.1%	0.3%	100%	104.9

From results shown in table 5.1, the octane number increases mainly with the increase of propane compound found in the sample composition. For the samples having nearly same propane percentage, then it is seen that the sample having higher percentage of iso-butane, has the higher octane number, if the olefin percentages are also more or less the same.

To explore the relationship between octane number and exogenous variables, propane, iso-butane, n-butane, olefin C3, olefin C4 and ethane, the stepwise regression method was used. Stepwise regression is an automated implementation to identify the most significant subset of predictors.

The scatter plot between the octane number and propane suggests a curvature relation, therefore the square of the propane is also implemented into the model. To overcome the multi-collinearity problem (linear relationship between exogenous variables), each predictor is standardized by subtracting its mean and dividing by its standard



deviation (i.e.,  $\left( \frac{X_{j,i} - \bar{x}_j}{s_j} \right)$ , where  $\bar{x}_j$  is the mean of j-th predictor and  $s_j$  is its

standard deviation,  $j = 1, 2, \dots, 6$ ,  $i = 1, 2, \dots, 15$ .

The stepwise regression recommends a statistically significant effect of propane and its square, n-butane and olefin C3 variables on octane number at 5% significance level.

There are positive relations between Propane and its square but negative ones between n-butanenes and olefin C3. The variability in all these four predictors explains the 96% of the variation in octane number (Adjusted  $R^2 = 0.96$ ). The final model satisfies all assumptions of multiple regression. The standardized residuals are normally distributed. There is no autocorrelation among residuals and the variance of residuals are constant.

*Table 5.2: Descriptive statistics of all variables*

VARIABLE	N	MEAN	STDEV	MINIMUM	MAXIMUM
<b>X<sub>1</sub>=PROPANE</b>	15	36.960	17.40	16.70	66.30
<b>X<sub>2</sub>=ISO-BUTANE</b>	15	9.130	8.71	1.90	30.70
<b>X<sub>3</sub>=N-BUTANE</b>	15	50.430	16.61	18.30	78.10
<b>X<sub>4</sub>=OLEFIN C3</b>	15	0.120	0.04	0.10	0.20
<b>X<sub>5</sub>=OLEFIN C4</b>	15	3.107	0.44	2.50	4.00
<b>X<sub>6</sub>=ETHANE</b>	15	0.300	0.13	0.10	0.50
<b>Y=OCTANE</b>	15	100.200	2.37	97.00	104.90

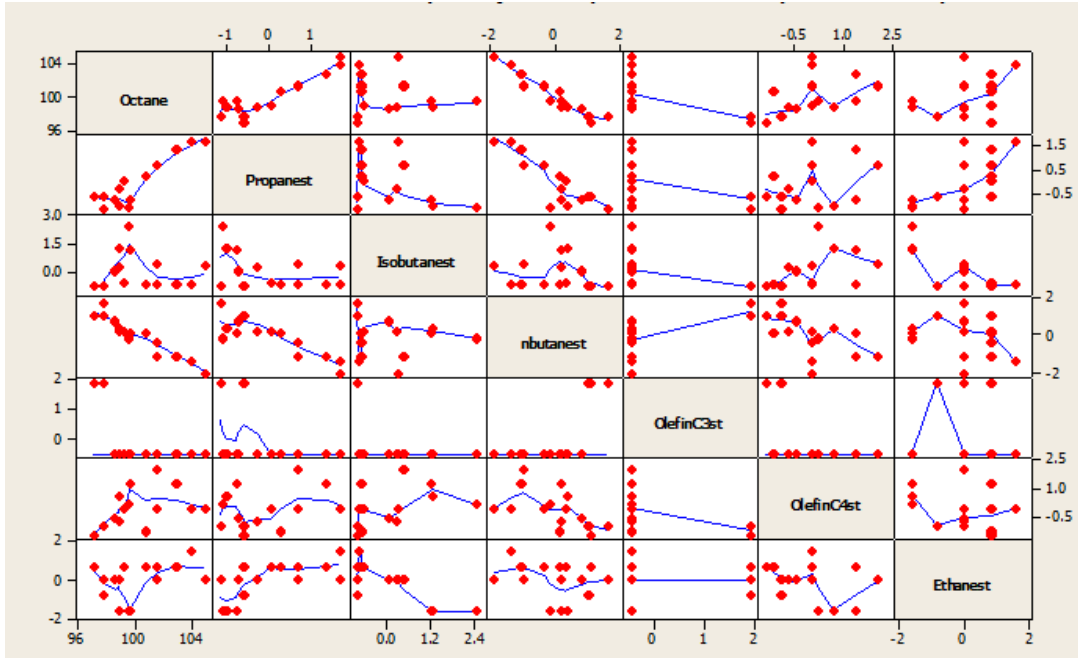


Figure 5.1: Matrix Plot of octane number, propanst, iso-butanest, n-butanest, olefinC3st, olefinC4st and ethanest

### 5.1 Regression Analysis: Octane Number vs. Propanst, P2, nbutanest, OlefinC3st

The regression equation is;

$$Y_i = 99.6 + 1.068 \left( \frac{X_{1,i} - \bar{x}_1}{s_1} \right) + 0.609 \left( \frac{X_{1,i} - \bar{x}_1}{s_1} \right)^2 - 0.727 \left( \frac{X_{3,i} - \bar{x}_3}{s_3} \right) - 0.407 \left( \frac{X_{4,i} - \bar{x}_4}{s_4} \right), i = 1, 2, \dots, 15 \quad (5.1)$$

where  $\bar{x}_j$  is the mean of j-th predictor and  $s_j$  is its standard deviation,  $j = 1, 2, \dots, 6$ . When the standardized propane increases 1 unit, Octane increases  $1.677 + 1.218 * \text{propane}^{\text{st}}$  where propane<sup>st</sup> represents the standardized propane variable. When the standardized n-butanes increases 1 unit, octane number decreases 0.727 unit. When the standardized olefin C3 increases 1 unit, octane number decreases 0.407 unit.

Table 5.3: Calculation parameters

PREDICTOR	COEF	SE COEF	T	P	VIF
CONSTANT	99.6311	0.2248	443.29	0.000	*
PROPANEST	1.0678	0.2882	3.70	0.004	5.231
P2	0.6088	0.2024	3.01	0.013	2.149
NBUTANEST	-0.7273	0.4148	-1.75	0.110	10.883
OLEFINC3ST	-0.4071	0.2140	-1.90	0.086	2.884

S = 0.471565 R-Sq = 97.2% R-Sq(adj) = 96.0%

PRESS = 4.93980 R-Sq(pred) = 93.72%

The comparative plot of the actual Octane values and predicted ones obtained by the regression model, given in figure 5.2 shows pretty good fit.

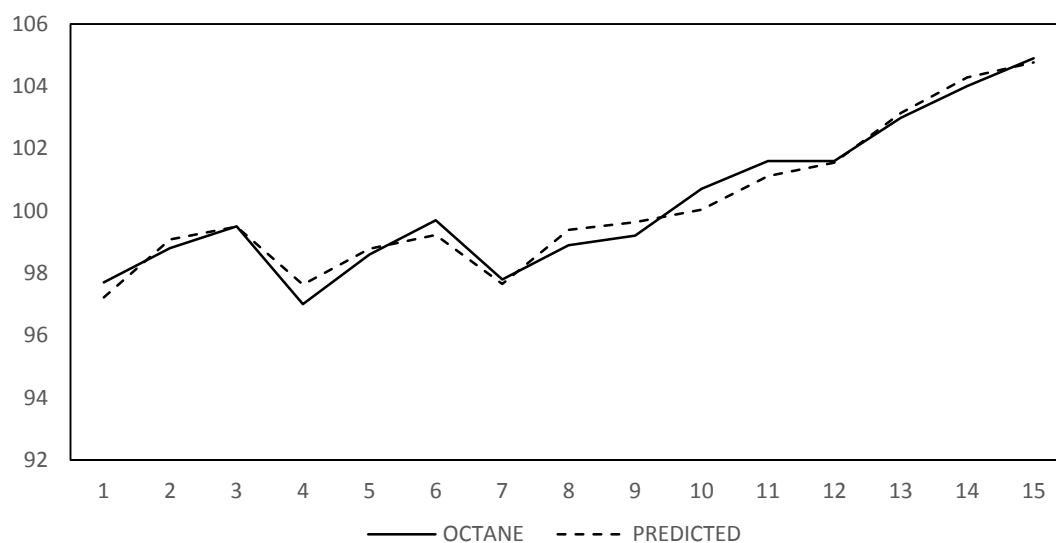


Figure 5.2: Comparison of actual octane numbers vs. predicted octane numbers for each experiment

Additional experiments were conducted for inspecting the effect of olefin compounds found in LPG to the octane number. Octane numbers for LPG samples including various compositions of olefin compounds are given in table 5.4.

Among all 4 olefins, which are 1-butene, c2-butene, i-butene and propylene, i-butene has the highest octane number. Figure 5.2 shows the octane numbers of pure olefins.

Table 5.4: Research octane numbers (RON) for LPG samples including various amounts of olefins prepared by AYGAZ Company

Research Octane Number											
Tank Number	Propane	i-butane	n-butane	Ethane	Propylene	1-butene	i-butene	t2-butene	C2-butene	Total	Octane #
297	22.71%	10.86%	64.83%	0.58%	1.00%	0.00%	0.00%	0.00%	0.00%	100%	102.7
676	22.25%	10.64%	63.52%	0.57%	3.00%	0.00%	0.00%	0.00%	0.00%	100%	102.6
677	21.79%	10.42%	62.21%	0.56%	5.00%	0.00%	0.00%	0.00%	0.00%	100%	102.6
672	20.64%	9.87%	58.94%	0.53%	10.00%	0.00%	0.00%	0.00%	0.00%	100%	102.6
306	19.50%	9.33%	55.66%	0.50%	15.00%	0.00%	0.00%	0.00%	0.00%	100%	102.2
852	22.71%	10.86%	64.83%	0.58%	0.00%	1.00%	0.00%	0.00%	0.00%	100%	102.5
635	22.25%	10.64%	63.52%	0.57%	0.00%	3.00%	0.00%	0.00%	0.00%	100%	102.0
669	21.79%	10.42%	62.21%	0.56%	0.00%	5.00%	0.00%	0.00%	0.00%	100%	102.6
295	20.64%	9.87%	58.94%	0.53%	0.00%	10.00%	0.00%	0.00%	0.00%	100%	102.3
302	19.50%	9.33%	55.66%	0.50%	0.00%	15.00%	0.00%	0.00%	0.00%	100%	100.3
848	22.71%	10.86%	64.83%	0.58%	0.00%	0.00%	1.00%	0.00%	0.00%	100%	102.7
651	22.25%	10.64%	63.52%	0.57%	0.00%	0.00%	3.00%	0.00%	0.00%	100%	102.8
673	21.79%	10.42%	62.21%	0.56%	0.00%	0.00%	5.00%	0.00%	0.00%	100%	102.8
654	20.64%	9.87%	58.94%	0.53%	0.00%	0.00%	10.00%	0.00%	0.00%	100%	102.5
839	19.50%	9.33%	55.66%	0.50%	0.00%	0.00%	15.00%	0.00%	0.00%	100%	101.4
856	22.71%	10.86%	64.83%	0.58%	0.00%	0.00%	0.00%	1.00%	0.00%	100%	102.9
853	22.25%	10.64%	63.52%	0.57%	0.00%	0.00%	0.00%	3.00%	0.00%	100%	103.1
857	21.79%	10.42%	62.21%	0.56%	0.00%	0.00%	0.00%	5.00%	0.00%	100%	102.8
855	20.64%	9.87%	58.94%	0.53%	0.00%	0.00%	0.00%	10.00%	0.00%	100%	103.0
844	19.50%	9.33%	55.66%	0.50%	0.00%	0.00%	0.00%	15.00%	0.00%	100%	99.6
851	22.71%	10.86%	64.83%	0.58%	0.00%	0.00%	0.00%	0.00%	1.00%	100%	102.5
849	22.25%	10.64%	63.52%	0.57%	0.00%	0.00%	0.00%	0.00%	3.00%	100%	102.8
854	21.79%	10.42%	62.21%	0.56%	0.00%	0.00%	0.00%	0.00%	5.00%	100%	103.0
850	20.64%	9.87%	58.94%	0.53%	0.00%	0.00%	0.00%	0.00%	10.00%	100%	103.0
A03	19.50%	9.33%	55.66%	0.50%	0.00%	0.00%	0.00%	0.00%	15.00%	100%	101.7
845	0%	0%	0%	0%	0.00%	0.00%	0.00%	0.00%	100.00%	100%	96.6
842	11.47%	5.49%	32.74%	0.29%	50.00%	0.00%	0.00%	0.00%	0.00%	100%	100.8
305	0.00%	0.00%	0.00%	0.00%	100.00%	0.00%	0.00%	0.00%	0.00%	100%	99.9
308	11.47%	5.49%	32.74%	0.29%	0.00%	50.00%	0.00%	0.00%	0.00%	100%	96.6
304	0.00%	0.00%	0.00%	0.00%	0.00%	100.00%	0.00%	0.00%	0.00%	100%	96.4
843	11.47%	5.49%	32.74%	0.29%	0.00%	0.00%	50.00%	0.00%	0.00%	100%	99.0
841	0.00%	0.00%	0.00%	0.00%	0.00%	0.00%	100.00%	0.00%	0.00%	100%	100.0
838	22.94%	10.97%	65.49%	0.59%	0.00%	0.00%	0.00%	0.01%	0.00%	100%	103.1

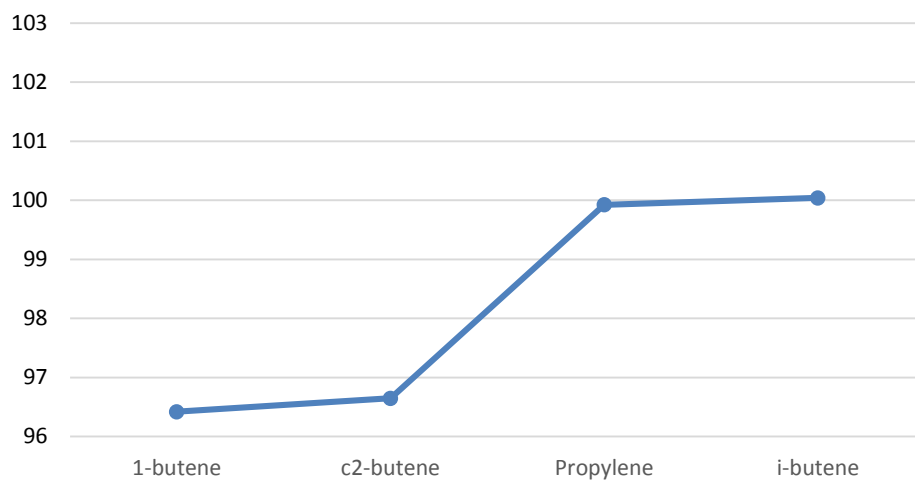


*Figure 5.3: Octane numbers of pure olefins*

When samples containing fixed volumetric ratio of propane 19.5%, i-butane %9.33, n-butane 55.66% and ethane 0.50%, and including 15% of only 1 kind of olefin are compared, it can be easily seen that, the sample having highest octane number is the one containing 15% of propylene; however the sample with least octane number is the one containing t2-butene which can be seen in Figure 5.4.

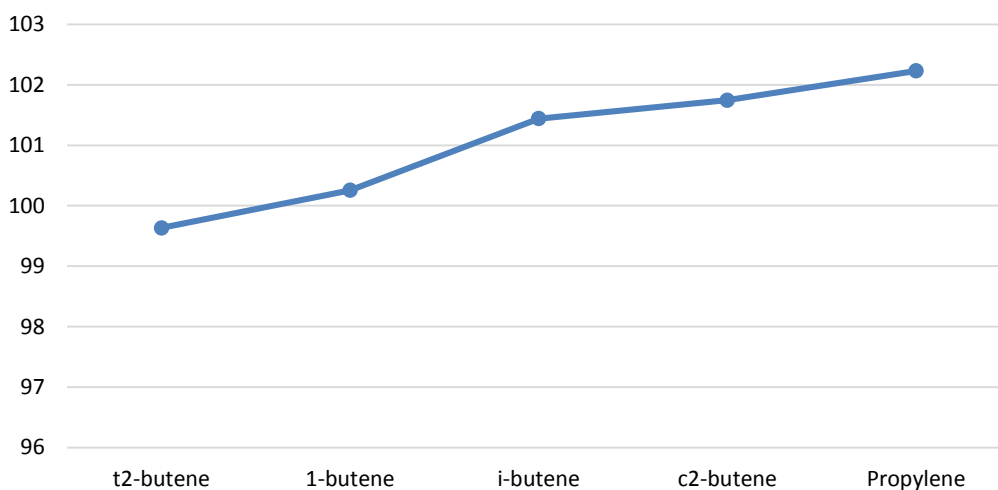


*Figure 5.4: Octane number comparison of samples containing 15% of each olefins*

In figure 5.5, octane numbers of samples which have equal volumetric ratios of each olefins which are propylene, i-butene and 1-butene are compared. For instance, olefin 1% compares the octane numbers of 3 samples which each of them only include %1 of 1 kind of olefin.

The general trend shows us, samples containing propylene and i-butene have nearly same octane number which are higher than the samples containing 1-butene. For the samples containing 1%, 3%, 5% and 100% of olefins, samples containing i-butene have higher octane number than samples having propylene. However, the difference between the octane numbers of samples with i-butene and propylene are less than 0.2 octane number.

On the other hand, for the samples containing 10%, 15% and 50% of olefins, samples containing propylene have higher octane number than samples containing i-butene and the difference between octane numbers of these samples are nearly 1-2 octanes.

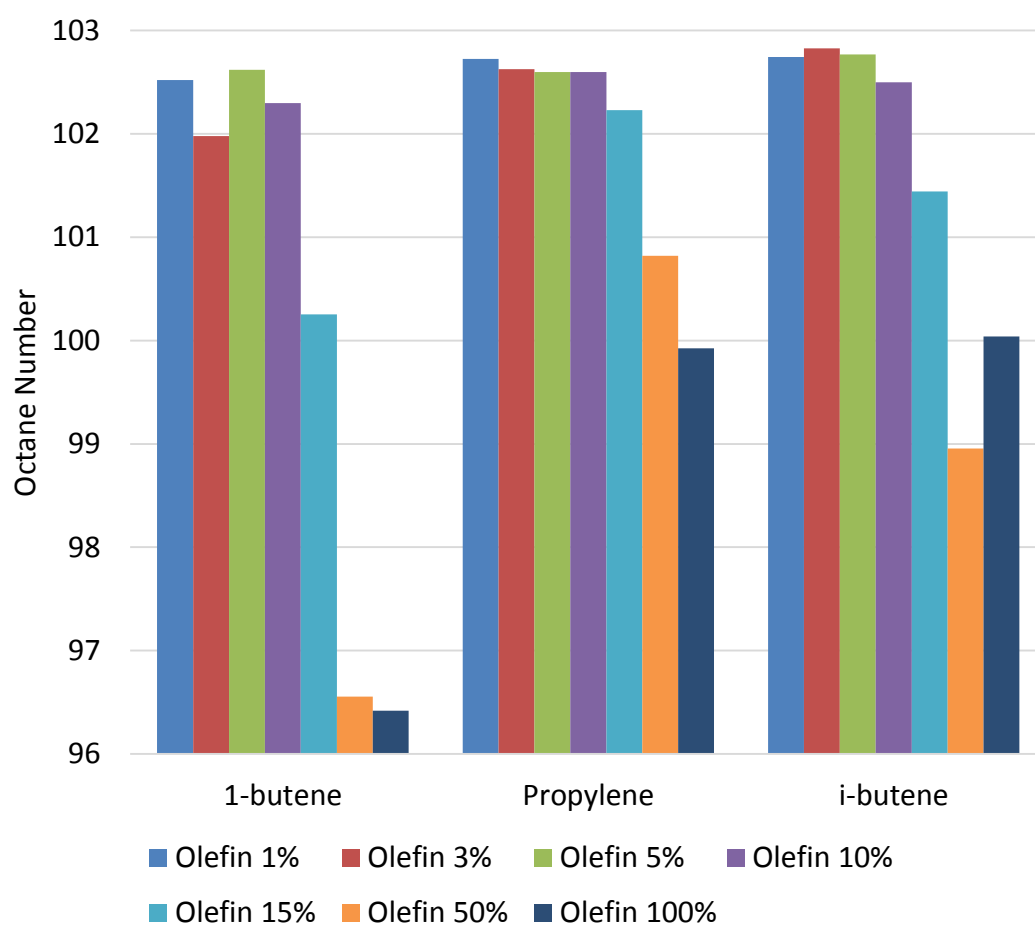


Figure 5.5: Octane number comparison of samples having equal amount of olefins

To explore the relationship between olefin and exogenous variables, propane, iso-butane, n-butane, 1-butene, i-butene, c2-butene, t-butene, and ethane, the stepwise regression method is used. To satisfy the normality assumption of the dependent variable, olefin, the square root of the series is taken.

The scatter plot between the transformed olefin and ethane suggests a curvature relation, therefore the square of the ethane is also into the model. To overcome the multicollinearity problem (linear relationship between exogenous variables), each predictor is standardized by subtracting its mean and dividing by its standard deviation.

The stepwise regression recommends a statistically significant effect of propane, 1-butene, c2-butene, t-butene, ethane and its square variables on olefin at 5% significance level. There are positive relations between propane and squared ethane but negative ones between the others.

The variability in all these four predictors explains the 88.3% of the variation in octane (Adjusted  $R^2 = 0.883$ ). The final model satisfies all assumptions of multiple regression. The standardized residuals are normally distributed. There is no autocorrelation among residuals and the variance of residuals are constant.

*Table 5.5: Descriptive statistics of all variables*

VARIABLE	N	MEAN	STDEV	MINIMUM	MAXIMUM
<b>X<sub>1</sub>=PROPANE</b>	33	0.1793	0.0743	0.0000	0.2294
<b>X<sub>2</sub>=ISO-BUTANES</b>	33	0.0858	0.0355	0.0000	0.1097
<b>X<sub>3</sub>=N-BUTANES</b>	33	0.5120	0.2122	0.0000	0.6549
<b>X<sub>4</sub>=ETHANE</b>	33	0.0046	0.0019	0.0000	0.0059
<b>X<sub>5</sub>=PROPILEN</b>	33	0.0558	0.1923	0.0000	1.0000
<b>X<sub>6</sub>=1- BUTENES</b>	33	0.0558	0.1923	0.0000	1.0000
<b>X<sub>7</sub>=I- BUTENES</b>	33	0.0558	0.1923	0.0000	1.0000
<b>X<sub>8</sub>=T2- BUTENES</b>	33	0.0103	0.0319	0.0000	0.1500
<b>X<sub>9</sub>=C2- BUTANES</b>	33	0.0406	0.1751	0.0000	1.0000
<b>Y=RON</b>	33	101.5700	1.9700	96.42	103.1500

The regression equation is

$$\sqrt{Y_i} = 10.041 + 3.298 \left( \frac{X_{1,i} - \bar{x}_1}{s_1} \right) - 3.182 \left( \frac{X_{4,i} - \bar{x}_4}{s_4} \right) + 0.038 \left( \frac{X_{4,i} - \bar{x}_4}{s_4} \right)^2 - 0.042 \left( \frac{X_{6,i} - \bar{x}_6}{s_6} \right) - 0.010 \left( \frac{X_{8,i} - \bar{x}_8}{s_8} \right) - 0.29 \left( \frac{X_{9,i} - \bar{x}_9}{s_9} \right), i = 1, 2, \dots, 33 \quad (5.2)$$

Where,  $\bar{x}_j$  is the mean of  $j$ -th predictor and  $s_j$  is its standard deviation,  $j = 1, 2, \dots, 9$

When the standardized propane increases 1 unit, olefin increases  $3.298^2 = 10.877$  unit.

When the standardized ethane increases 1 unit, olefin decreases  $3.144 - 0.076 \times \text{ethane}^{\text{st}}$  unit where  $\text{ethane}^{\text{st}}$  represents the standardized ethane variable. When the standardized 1-buthane increases 1 unit, olefin decreases 0.002 unit. When the standardized t2-butane increases 1 unit, olefin decreases 0.001 unit. When the standardized c2-butane increases 1 unit, olefin decreases 0.0008 unit.

Table 5.6: Calculation parameters

PREDICTOR	COEF	SE COEF	T	P	VIF
CONSTANT	10.0413	0.0113	886.03	0.000	
PROPANEST	3.298	4.629	0.71	0.483	606850.728
IBUTANEST	-0.041605	0.006981	-5.96	0.000	1.380
TBUTENEST	-0.010407	0.006053	-1.72	0.097	1.038
CBUTENST	-0.028952	0.006953	-4.16	0.000	1.373
ETANST	-3.182	4.637	-0.69	0.499	609005.196
E2	0.03752	0.01001	3.75	0.001	9.627

S = 0.0336131 R-Sq = 90.5% R-Sq(adj) = 88.3%

PRESS = 0.211998 R-Sq(pred) = 31.46%

Analysis of Variance

SOURCE	DF	SS	MS	F	P
REGRESSION	6	0.279942	0.046657	41.30	0.000
RESIDUAL ERROR	26	0.029376	0.001130		
LACK OF FIT	19	0.024144	0.001271	1.70	0.243
PURE ERROR	7	0.005232	0.000747		
TOTAL	32	0.309318			

Durbin-Watson statistic = 1.96047



The comparative plot of the actual olefin values and predicted ones obtained by the regression model, given in figure 5.6, shows very close fit.

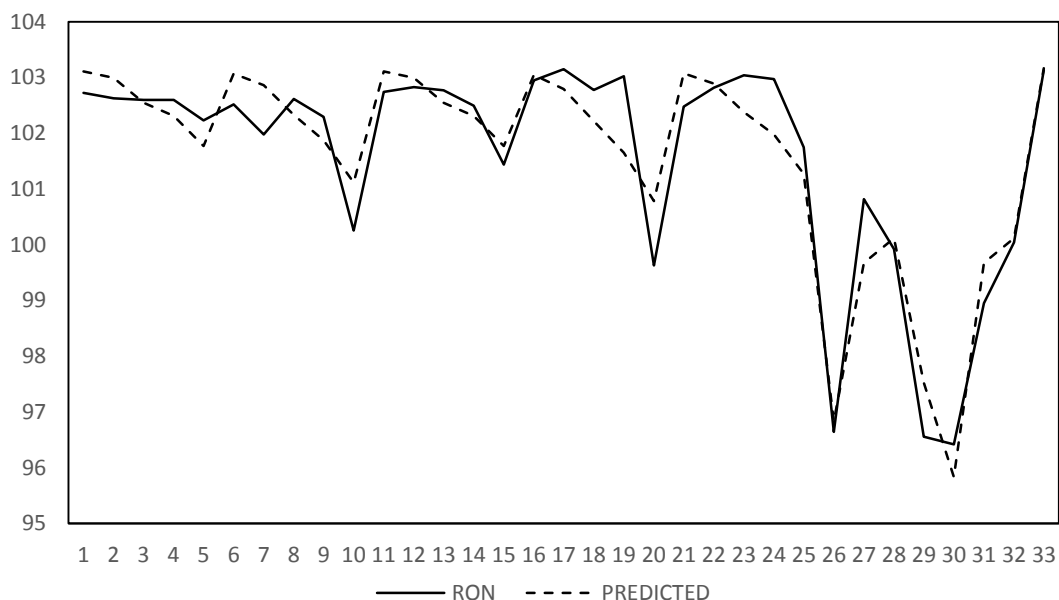


*Figure 5.6: The plot of actual olefin and predicted olefin for each experiment*

This study introduces a method for measuring the octane number of LPG in a CFR engine. 2 sets of data were analyzed. A mathematical method was developed to understand the effect of various compounds in LPG like olefins on the octane number of the fuel.



## **BIBLIOGRAPHY**

- [1] <http://www.sustainablebusinessoregon.com>
- [2] Karamangil, M. I., 2007, “Development of the auto gas and LPG - Powered Vehicle Sector in Turkey: A Statistical Case Study of the Sector for Bursa” Energy Policy, Vol. 35, 640–649, DOI:10.1016/j.enpol.2006.01.004.
- [3] Brock, C., Stanley, D. L., 2012, “The Cooperative Fuels Research Engine: Applications for Education and Research”, Journal of Aviation Technology and Engineering, Vol. 2, 130–135 DOI: 10.5703/1288284314865
- [4] ASTM D2699 Standard Test Method for Research Octane Number of Spark-Ignition Engine
- [5] ASTM D2700 Standard Test Method for Motor Octane Number of Spark-Ignition Engine Fuel
- [6] Lauer, W., “Knock Testing Engine BASF – Fuel Rating and Operation “, Issue H
- [7] Heywood, J.B., “Internal Combustion Engine Fundamentals”, McGraw-Hill International Editions Automotive Technology Series.
- [8] Ettetfagh, M. M., Sadeghi, M. H., Pirouzpanah, V., Arjmandi Tash, H., 2008, “Knock Detection in Spark Ignition Engines by Vibration Analysis of Cylinder Block: A Parametric Modeling Approach”, Mechanical Systems and Signal Processing, Vol. 22, 1495-1514
- [9] Jagadeesha, T., “ME 667: Internal Combustion Engines” Lecture Notes, National Institute of Technology Calicut, Retrieved from [http://www.nitc.ac.in/dept/me/jagadeesha/Internal\\_Combustion\\_Engines/Chapter1.pdf](http://www.nitc.ac.in/dept/me/jagadeesha/Internal_Combustion_Engines/Chapter1.pdf)
- [10] Sigel, A., Sigel, H., Sigel, R. K O, “Organometallics in Environment and Toxicology: Metal Ions in Life Science”, RSC Publishing
- [11] <http://zhome.com/ZCMnL/PICS/detonation/detonation.html>

- [12] Ghosh, P., Hickey, K. J., Jaffe, S. B., 2006, "Development of a Detailed Gasoline Composition-Based Octane Model", *Industrial & Engineering Chemistry Research*, Vol 45, 337-345
- [13] ISO/FDIS 5164 International Standard, Petroleum Products – Determination of Knock Characteristics of Motor Fuels – Research Method
- [14] ISO/FDIS 5163 International Standard, Petroleum Products – Determination of Knock Characteristics of Motor and Aviation Fuels – Motor Method
- [15] Ozcan, H., Yamin, J. A. A., 2008, "Performance and Emission Characteristics of LPG Powered Four Stroke SI Engine under Variable Stroke Length and Compression Ratio", *Energy Conversion and Management*, Vol. 49, 1193-1201
- [16] Balat, M., "The Significance of LPG in Turkish Vehicular Transportation: Liquefied Petroleum Gases (LPG) in Fueled Systems". Taylor & Francis, *Energy Sources*, 27 (2005) 485-488, DOI: 10.1080/00908310490449216.
- [17] Sulaiman, M. Y., Ayob, M. R., Meran, I., 2013, "Performance of Single Cylinder Spark Ignition Engine Fueled by LPG", *Procedia Engineering*, Vol. 53, 579-585
- [18] Morganti, K. J., Brear, M. J., Da Silva, G., Yang, Y., Dryer, F. L., 2015, "The Auto Ignition of Liquefied Petroleum Gas (LPG) in Spark-Ignition Engines, *Proceedings of the Combustion Institute*, Vol. 35, 2933-2940
- [19] Bhasin, A., 2010, "Method for Determination of Octane Rating by Flame Quenching Experiments" (Master's Thesis, The University of Iowa, Iowa City, Iowa) Retrieved from <http://ir.uiowa.edu/cgi/viewcontent.cgi?article=1967&context=etd>
- [20] Çelik, M. B., Balki, M.K., "The Effect of LPG Usage on Performance and Emissions at Various Compression Ratios in a Small Engine", 2006, *Gazi Üniv. Müh. Mim. Fak. Der. vol:22, no:1*, 82-86, 2007
- [21] Workman, J. Jr., 2014, "An Introduction to Near Infrared Spectroscopy", *Education Article*, Retrieved from <http://www.spectroscopynow.com/details/education/sepspec1881education/An-Introduction-to-Near-Infrared-Spectroscopy.html?&tzcheck=1&tzcheck=1>

- [22] Ryan, J. D., Russel, P.C., Jones, G. R., Gerrard, C.A., Strachan, D., “Near Infrared Spectroscopy for LPG Quality Control”
- [23] [http://chemwiki.ucdavis.edu/Analytical\\_Chemistry/Instrumental\\_Analysis/Chromatography/Gas\\_Chromatography](http://chemwiki.ucdavis.edu/Analytical_Chemistry/Instrumental_Analysis/Chromatography/Gas_Chromatography)
- [24] Lieuwen, T., et al., Fuel Flexibility Influences on Premixed Combustor Blowout, Flashback, Autoignition, and Stability, *Journal of Engineering for Gas Turbines and Power*.
- [25] Molière, M., Stationary gas turbines and primary energies: A review of fuel influence on energy and combustion performances, *Int. J. Therm. Sci.* (2000) 39, 141–172
- [26] Pantagi, V.K., et al. Studies on porous radiant burners for LPG (liquefied petroleum gas) cooking applications. *Energy* 36 (2011) 6074-6080, DOI:10.1016/j.energy.2011.08.008.
- [27] Massi, M., Experimental analysis on a spark ignition petrol engine fuelled with LPG (liquefied petroleum gas). *Energy* 41 (2012) 252-260, DOI:10.1016/j.energy.2011.05.029.
- [28] Miller Johthi, N.K., et al. LPG fueled diesel engine using diethyl ether with exhaust gas recirculation. *International Journal of Thermal Sciences* 47 (2008) 450–457, DOI:10.1016/j.ijthermalsci.2006.06.012.
- [29] Lucadamo, G.A., et al. Improved ethylene and LPG recovery through dephlegmator technology. *Gas Separation & Purification* 1 (1987) 94–102.
- [30] Liguang, L., et al. Combustion and Emissions Characteristics of a Small Spark-Ignited LPG Engine. *SAE Paper* 2002-01-1738.
- [31] Baosheng, L., et al. LPG characterization and production quantification for oil and gas reservoirs. *Journal of Natural Gas Science and Engineering* 2 (2010) 244-252, DOI:10.1016/j.jngse.2010.08.002.
- [32] Ryan, J.D., et al., Near infrared spectroscopy for LPG quality control, Part of the SPIE Conference on Chemical, Biochemical, and Environmental Fiber Sensors X 58 Boston. Massachusetts, November 1998 SPIE Vol. 3540
- [33] Gurulakshmanan, G., et al. Conversion of Olefins in LPG through hydrogenation. *International Petroleum Technology Conference* held in Bangkok, Thailand, 15–17 November 2011, IPTC 14454.

- [34] Gamas, E.D., et al. Contribution of Liquefied Petroleum Gas to Air Pollution in the Metropolitan Area of Mexico City. *Journal of the Air & Waste Management Association* 50 (2000) 188-198.
- [35] Review of LPG (auto-gas) Fuel Quality Standard. The Department of Environment, Water, Heritage and Arts (Australia), January 2010.
- [36] Law C K, *Combustion Physics*.
- [37] Huzayyin, A.S., et al., Laminar burning velocity and explosion index of LPG–air and propane–air mixtures, *Fuel* 87 (2008) 39–57
- [38] Yash, K., et al. Laminar flame speed measurements and modeling of alkane blends at elevated pressures with various diluents, *Proceedings of ASME Turbo Expo 2011 GT2011 June 6-10, 2011, Vancouver, British Columbia, Canada*.
- [39] Zhao, et al. the initial temperature and n2 dilution effect on the laminar flame speed of propane/air, *Combust. Sci. and Tech.*, DOI: 10.1080= 001022004 90487553
- [40] Lee, K., Ryu, J., An experimental study of the flame propagation and combustion characteristics of LPG fuel, *Fuel* 84 (2005) 1116–1127
- [41] Hochgreb, S., et al. Laminar Flame Speeds of CF<sub>3</sub>H-Propane-Air Mixtures at Elevated Pressures. , NISTIR 5499; September 1994.
- [42] Burke, et al. Effect of cylindrical confinement on the determination of laminar flame speeds using outwardly propagating flames, *Combustion and Flame* 156 (2009) 771–779
- [43] Stanter et al. The effects of water dilution on hydrogen, syngas, and ethylene flames at elevated pressure. *Proc. Combust. Inst.* (2012), <http://dx.doi.org/10.1016/j.proci.2012.06.065>
- [44] Bouvet, et al. Flame Speed Characteristics of Syngas (H<sub>2</sub>-CO) with Straight Burners for Laminar Premixed Flames. *Third European Combustion Meeting ECM 2007*.
- [45] Bouvet, et al. Characterization of syngas laminar flames using the Bunsen burner configuration. *Intl. journal of hydrogen energy* 36(2011)992e1005

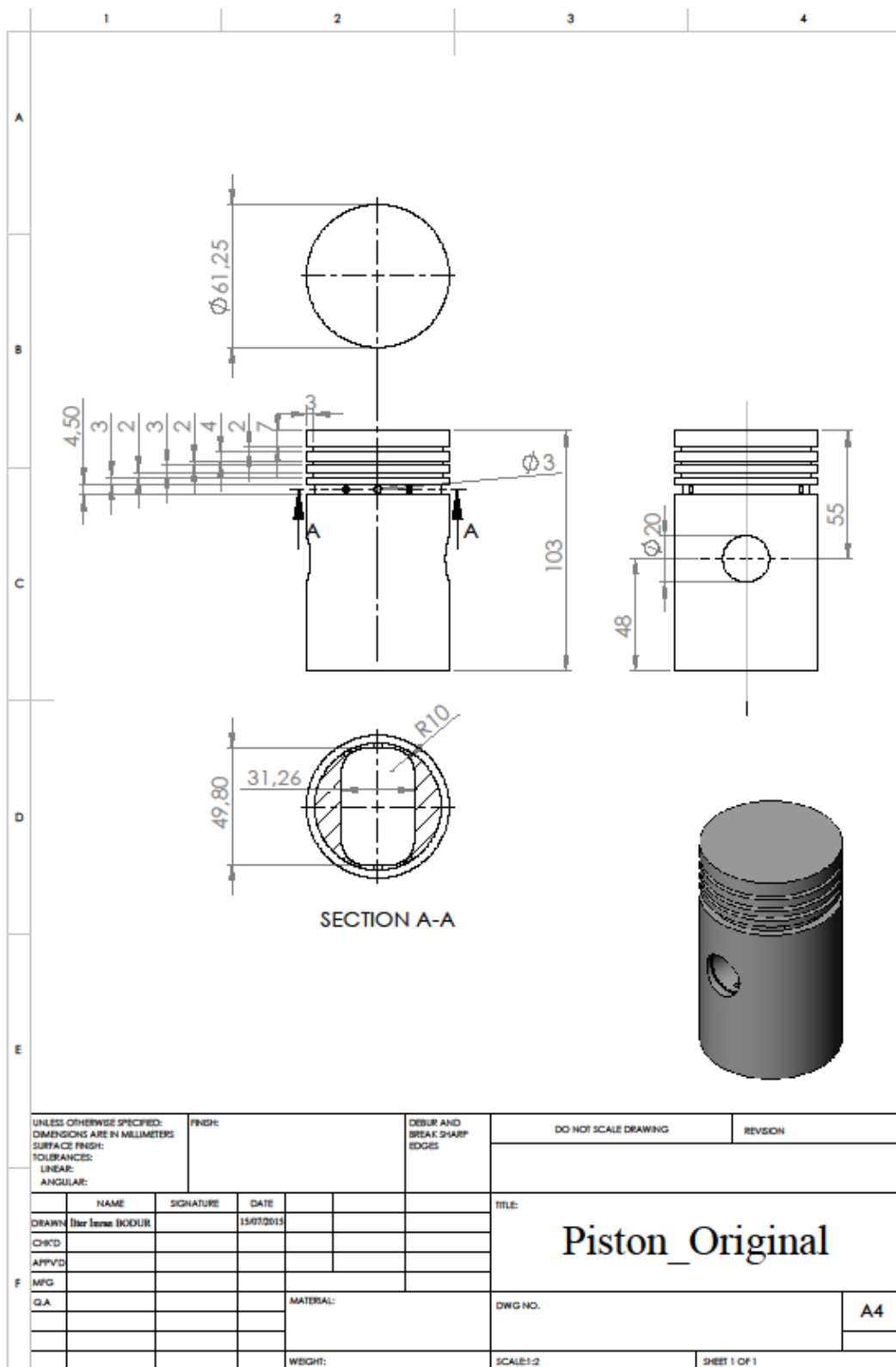
- [46] Bouvet et al. Experimental studies of the fundamental flame speeds of syngas (H<sub>2</sub>/CO)/air mixtures. *Proceedings of the Combustion Institute* 33 (2011) 913–920
- [47] Li et al, A Comprehensive Kinetic Mechanism for CO, CH<sub>2</sub>O, and CH<sub>3</sub>OH Combustion, *Int. J. Chem. Kinet.* 39 (3) (2007) 109–136
- [48] Morganti, K. J., Foong, T. M., Brear, M. J., Da Silva, G., Yang, Y., Dryer, F. L., 2013, “ The Research and Motor Octane Numbers of Liquefied Petroleum Gas (LPG) “, *Fuel*, Vol. 108, 797-811





## **APPENDICES**

### A-1 Technical Drawing of Original Piston



# A-2 Technical Drawing of Modified Piston

